

**AUTOTHERMAL REFORMING (ATR) FOR FUEL CELLS IN AUTOMOTIVE
APPLICATIONS**

by

Ritsdeliz Pérez Rodríguez

A thesis submitted in partial fulfillment of the requirements for the degree of

MASTER OF SCIENCE

in

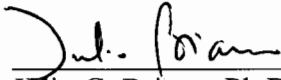
CHEMICAL ENGINEERING

UNIVERSITY OF PUERTO RICO

MAYAGÜEZ CAMPUS

2004

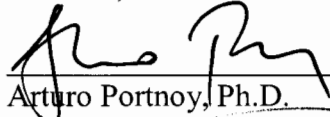
Approved by



Julio G. Briano, Ph.D.
Member, Graduate Committee

13 Mayo 2004

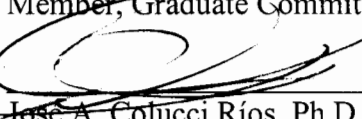
Date



Arturo Portnoy, Ph.D.
Member, Graduate Committee

13/Mayo/2004

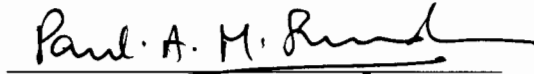
Date



José A. Colucci Ríos, Ph.D.
President, Graduate Committee

MAY 13/04

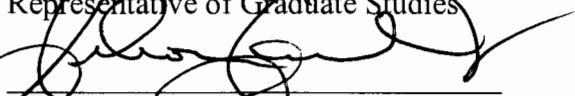
Date



Paul Sundaram, Ph.D.
Representative of Graduate Studies

5/13/04

Date



Nelson Cardona Martínez, Ph.D.
Chairperson of the Department

5/13/04

Date

ABSTRACT

Autothermal reforming of liquid fuels had been demonstrated to be feasible for use in fuel cell vehicles. One of the main problems with reforming systems is that the concentration product of carbon monoxide has to be less than 20ppm to avoid the contamination of the PEM Fuel Cell. The University of Puerto Rico in collaboration with Argonne National Laboratory (ANL) is developing and implementing a Reforming Catalyst Characterization Program to help in the development of a better performance of the fuel processor. The specific objectives of this study were to establish the feasibility of using a Pt-based catalyst to: 1) convert methanol and isooctane to a hydrogen-rich product gas; 2) study the effects of O_2/fuel and H_2O/C ratios, and reactor temperature that maximize the selectivity to H_2 ; 3) compare experimental gas product concentrations with simulation equilibrium results. A bench-scale basket stirred tank reactor (BSTR) was used to perform the reforming experiments; and a gas chromatograph with a thermal conductivity detector was used to perform the exit gas analyses. The best condition ($O_2/\text{fuel}=0.39$ and $H_2O/C=0.76$, 900°F) of the reforming process in the range studied was observed when a higher H_2 (59.8%) and minimal CO_2 (14.6%) and CO (12.6%) concentrations were obtained. At an $O_2/\text{fuel}=0.5$ and $H_2O/C=1.12$ (dry basis) ratios and 900°F , the maximum H_2 concentration found was nearly 60%, which is the maximum theoretically concentration that can be reached at equilibrium. No methane or coke formation was observed. The Pt- catalyst used promoted methanol decomposition rather than reforming because the $H_2/(CO+CO_2)$ ratios calculated at each level and temperature were frequently between 1 and 2 (decomposition ratio).

RESUMEN

La reformación autotermal de combustibles líquidos ha demostrado ser viable para aplicaciones en los vehículos que utilizarán celdas de combustible. Uno de los problemas que tienen los sistemas de reformación, es que la concentración de CO en el producto tiene que ser menor de 20ppm para no contaminar la celda de combustible que utiliza como electrolito una membrana (PEMFC, por sus siglas en inglés). La Universidad de Puerto Rico, en colaboración con el Laboratorio Nacional Argonne está desarrollando e implementando un programa de caracterización de catalizadores capaces de reformar. Los objetivos específicos de este estudio fueron establecer la viabilidad de usar un catalizador de platino para: 1) convertir metanol e isooctano a un producto rico en hidrógeno; 2) estudiar los efectos de diferentes razones de O_2/fuel y H_2O/C , junto con la temperatura de reacción que maximicen la selectividad de H_2 ; 3) comparar las concentraciones experimentales obtenidas del gas con los resultados obtenidos de la simulación hecha para los productos en equilibrio. Para hacer este proceso se utilizó un reactor de flujo continuo. Un cromatógrafo de gases con un detector de conductividad termal fue utilizado para llevar a cabo el análisis de los gases que salían del reactor. La mejor condición ($O_2/\text{fuel}=0.39$ y $H_2O/C=0.76$) del proceso estudiado, fue observado cuando se produjo la mayor concentración de H_2 (59.8%), junto con las mínimas concentraciones producidas de CO (14.6%) y CO_2 (12.6%). No se observó formación de metano ni de carbón. El catalizador utilizado no reformó el metanol y sólo promovió la descomposición del alcohol, ya que la razones de $H_2/(CO+CO_2)$ calculadas para cada nivel y temperatura fueron valores entre 1 y 2.

Copyright © 2004 by Ritsdeliz Pérez Rodríguez. All rights reserved. Printed in the United States of America. Except as permitted under the United States Copyright Act of 1976, no part of this publication may be reproduced or distributed in any form or by any means, or stored in a data base or retrieved system, without the prior written permission of the publisher.

*To my most loved ones,
God
My Family
And to you, my love, Ernesto*

ACKNOWLEDGMENTS

First of all, I would like to thank God for giving me the courage and strength to make this dream come true. My strength and faith comes from Him and without Him this important goal for me wouldn't have been achieved. To the University of Puerto Rico at Mayagüez, the Chemical Engineering Department, and Argonne National Laboratory for sponsoring this research project which allowed me to pursue my MS studies. I would like to thank Dr. José A. Colucci, my advisor, for being my guide during this process and for his effort of teaching me all that I have learned during these two years. Thanks for your personal and academic advises.

I have no words to say thanks to mom and dad, for being always my economical and moral support. For just giving me the gift of life and the tools to be a better person every day. To Michelle, Yasmin, and Landy for being my family in the whole sense of the word. To my little nephew, Derek, since his birth day I am the happiest aunt in this world. His childhood and always-shiny smile shows me the beauty of being alive. To my dear love, Ernesto, for his patience with me and his help in completing this work. I really enjoyed the intellectual discussions (sorry!). To my best friends Yaritza, Madeline, and Marisel for being there when I needed the most. I will really miss all the moments that we shared together. Thanks to Mónica for her every-day little touch of “happiness” in the laboratory. Good luck in your coming work! Finally, and not less important, to undergraduate students for their best effort in helping me with the performance of the experiments.

Table of Contents

List of Tables	ix
List of Figures	x
List of Appendixes	xiv
1. INTRODUCTION	1
1.1 Justification	2
1.2 Objectives	5
1.3 Theory	6
1.3.1. Reforming Technology	6
1.3.2. Fuel Choices.....	10
1.3.3. Reformer Systems	14
1.3.4. Reformer efficiency	16
1.3.5. Reforming Catalysts.....	17
1.3.6. Coke Formation	18
1.3.7. Effect of Steam to Carbon Ratio(ψ) and Oxygen to Fuel Ratio(x)	19
1.3.8. Carbon Monoxide and Sulfur Removal	20
2. LITERATURE REVIEW	22
2.1 Fuel Cells Systems.....	22
2.2 Reformer Systems.....	25
2.2.1 Steam Reforming	26
2.2.1.1. Microchannel Reactors.....	29
2.2.1.2. Plasma Reactors.....	32
2.2.2. Autothermal Reforming.....	33
2.3 Argonne National Laboratory (ANL).....	38
2.3.1 Polymer Electrolyte Membrane (PEM) Fuel Cells.....	41
2.3.2 Water-Gas Shift (WGS) Catalysis (6).....	50
3. EXPERIMENTAL METHODS AND APPARATUS	52
3.1 Materials and equipment.....	53
3.1.1 Materials and reagents	53
3.1.2 Equipment	53
3.2 Analytical analysis.....	56
3.2.1 Gas chromatography analysis	56
3.3 Procedure	58
3.4 Experimental Design.....	59
4. RESULTS AND DISCUSSION.....	62

4.1. Experimental Design.....	62
4.2. Reactor Exit Gas Composition, Methanol	68
4.3. Hydrogen to (CO + CO ₂) ratio.....	77
4.4. Hydrogen Selectivity	79
4.5. Gas Hourly Space Velocity (GHSV).....	84
4.6. Reforming of isooctane (2,2,4-trimethylpentane).....	86
4.6.1. Coke Formation.....	86
4.7. Methanol and isooctane reforming without catalyst.....	92
5. CONCLUSIONS.....	94
6. RECOMMENDATIONS FOR FUTURE WORK	100
7. BIBLIOGRAPHY	102
8. APPENDIX.....	107

List of Tables

Table 2.1. Comparison of the Ida Tech Fuel Processor.....	27
Table 2.2. The Ida Tech fuel processor efficiencies using a variety of hydrocarbons.	29
Table 2.3. Experimental gas composition compared with equilibrium compositions.....	44
Table 3.1. Variables studied in the autothermal reforming process with methanol	62
Table 3.2. Variables studied in the autothermal reforming process with isooctane	62
Table 4.1. Different levels of O ₂ /fuel and H ₂ O/C ratios studied with methanol as a fuel.	63
Table 4.2. Replicate at a O ₂ /fuel=0.46; H ₂ O/C=0.76 at 900°F.....	66
Table 4.3. H ₂ /(CO+CO ₂) ratios at different levels and temperatures	78
Table 4.4. Isooctane exit gas product composition at different levels (dry basis).....	87
Table 4.5. Isooctane exit gas product composition, experimental and at equilibrium.....	89
Table 4.6. Replicate at a O ₂ /fuel=0.46; H ₂ O/C=0.76 at 900°F after coke formation.	90
Table 4.7. Methanol exit gas production at level 11 and 900°F without catalyst.....	92
Table 4.8. Isooctane production at level O/C=1; H ₂ O/C=1 and 900°F without catalyst...	93
Table B.1. Standard pure gases and their average retention times	112
Table C.1. Methanol product concentrations at different O ₂ /fuel and H ₂ O/C ratios... .	125

List of Figures

Figure 3.1. ANL Pt-based catalyst.....	53
Figure 3.2. The Bench Stirred Tank Reactor (BSTR) system.	55
Figure 3.3. BSTR without the insulator.....	55
Figure 3.4. Catalyst Basket.....	54
Figure 3.5. The BSTR system.....	56
Figure 3.6. Gas Chromatograph-TCD with the Integrator.....	57
Figure 3.7. Methanol and Isooctane Overall Autothermal Reforming Reaction.....	60
Figure 4.1. Reactor exit gas composition at $O_2/fuel = 0.27$; $H_2O/C = 0.46$	72
Figure 4.2. Reactor exit gas composition at $O_2/fuel = 0.27$; $H_2O/C = 0.76$	72
Figure 4.3. Reactor exit gas composition at $O_2/fuel = 0.27$; $H_2O/C = 1.12$	73
Figure 4.4. Reactor exit gas composition at $O_2/fuel = 0.39$; $H_2O/C = 0.46$	73
Figure 4.5. Reactor exit gas composition at $O_2/fuel = 0.39$; $H_2O/C = 0.76$	74
Figure 4.6. Reactor exit gas composition at $O_2/fuel = 0.39$; $H_2O/C = 1.12$	74
Figure 4.7. Reactor exit gas composition at $O_2/fuel = 0.5$; $H_2O/C = 0.46$	75
Figure 4.8. Reactor exit gas composition at $O_2/fuel = 0.5$; $H_2O/C = 0.76$	75
Figure 4.9. Reactor exit gas composition at $O_2/fuel = 0.5$; $H_2O/C = 1.12$	76
Figure 4.10. Hydrogen Selectivity ($O_2/fuel=0.27$) at different H_2O/C	80
Figure 4.11. Hydrogen Selectivity ($O_2/fuel=0.39$) at different H_2O/C ratios.	82
Figure 4.12. Hydrogen Selectivity ($O_2/fuel=0.5$) at different H_2O/C ratios.	83
Figure 4.13. Yield as a function of GHSV for ATR of methanol (800°F).	85
Figure 4.14. Catalyst before (yellow) and after coke formation (black).	91
Figure 4.15. Exit liquid mixture of reformed isooctane.....	91

Figure A.1. Control Temperature Profile of Reforming Reactor at 300°F.....	108
Figure A.2. Control Temperature Profile of Reforming Reactor at 350°F.....	109
Figure A.3. Control Temperature Profile of Reforming Reactor at 400°F.....	109
Figure A.4. Control Temperature Profile of Reforming Reactor at 450°F.....	110
Figure A.5. Control Temperature Profile of Reforming Reactor at 500°F.....	110
Figure A.6. Oxygen to methanol effect in the BSTR temperature.	111
Figure B.1. Hydrogen Calibration Curve-Low Concentrations.....	113
Figure B.2. Hydrogen Calibration Curve-High Concentrations	113
Figure B.3. Oxygen Calibration Curve	114
Figure B.4. Methane Calibration Curve.....	114
Figure B.5. Carbon Monoxide Calibration Curve	115
Figure B.6. Carbon Dioxide Calibration Curve.....	115
Figure C.1. Diagram of the system studied for the autothermal reforming of methanol.	116
Figure C.2. GC-TCD chromatograph of the product gas composition of methanol.....	118
Figure C.3. GC-TCD chromatograph of the product gas composition of methanol.....	119
Figure C.4. GC-TCD chromatograph of the product gas composition of isooctane	119
Figure C.5. Exit Hydrogen Concentration ($O_2/fuel = 0.27$; $H_2O/C = 0.46$)	120
Figure C.6. Exit Hydrogen Concentration ($O_2/fuel = 0.39$; $H_2O/C = 0.46$)	121
Figure C.7. Exit Hydrogen Concentration ($O_2/fuel = 0.50$; $H_2O/C = 0.46$)	121
Figure C.8. Exit Hydrogen Concentration ($O_2/fuel = 0.27$; $H_2O/C = 0.76$)	122
Figure C.9. Exit Hydrogen Concentration ($O_2/fuel = 0.27$; $H_2O/C = 1.12$)	122
Figure C.10. Exit Hydrogen Concentration ($O_2/fuel = 0.39$; $H_2O/C = 0.76$)	123
Figure C.11. Exit Hydrogen Concentration ($O_2/fuel = 0.50$; $H_2O/C = 0.76$)	123
Figure C.12. Exit Hydrogen Concentration ($O_2/fuel = 0.50$; $H_2O/C = 1.12$)	124

Figure C.13. Exit Hydrogen Concentration ($O_2/fuel = 0.39$; $H_2O/C = 1.12$)	124
Figure C.14. Oxygen, carbon monoxide and carbon dioxide chromatograph.....	125
Figure C.15. Hydrogen chromatograph ($O_2/fuel=0.27$; $H_2O/C=0.46$; $900^\circ F$).....	125
Figure C.16. Oxygen, carbon monoxide and carbon dioxide chromatograph.	126
Figure C.17. Hydrogen chromatograph ($O_2/fuel=0.5$; $H_2O/C=1.12$; $900^\circ F$).....	126
Figure C.18. Exit gas concentration with isooctane as a fuel at $600^\circ F$	131
Figure C.19. Exit gas concentration with isooctane as a fuel at $700^\circ F$	132
Figure C.20. Exit gas concentration with isooctane as a fuel at $800^\circ F$	132
Figure C.21. Exit gas concentration with isooctane as a fuel at $900^\circ F$	133
Figure D.1. Yield as a function of GHSV for methanol at $300^\circ F$	134
Figure D.2. Yield as a function of GHSV for methanol at $400^\circ F$	135
Figure D.3. Yield as a function of GHSV for methanol at $500^\circ F$	135
Figure D.4. Yield as a function of GHSV for methanol at $600^\circ F$	136
Figure D.5. Yield as a function of GHSV for methanol at $700^\circ F$	136
Figure D.6. Yield as a function of GHSV for methanol at $900^\circ F$	137
Figure E.1. Methanol exit product gas at equilibrium ($O_2/fuel=0.27$ and $H_2O/C=0.46$)	138
Figure E.2. Methanol exit product gas at equilibrium ($O_2/fuel=0.27$ and $H_2O/C=0.76$)	139
Figure E.3. Methanol exit product gas at equilibrium ($O_2/fuel=0.27$ and $H_2O/C=1.12$)	139
Figure E.4. Methanol exit product gas at equilibrium ($O_2/fuel=0.39$ and $H_2O/C=0.46$)	140
Figure E.5. Methanol exit product gas at equilibrium ($O_2/fuel=0.39$ and $H_2O/C=0.76$)	140
Figure E.6. Methanol exit product gas at equilibrium ($O_2/fuel=0.39$ and $H_2O/C=1.12$)	141
Figure E.7. Methanol exit product gas at equilibrium ($O_2/fuel=0.5$ and $H_2O/C=0.46$).	141
Figure E.8. Methanol exit product gas at equilibrium ($O_2/fuel=0.5$ and $H_2O/C=0.76$).	142
Figure E.9. Methanol exit product gas at equilibrium ($O_2/fuel=0.5$ and $H_2O/C=1.12$).	142

Figure E.10. Isooctane exit product gas at equilibrium (O/C=1 and H ₂ O/C=1).....	143
Figure E.11. Isooctane exit product gas at equilibrium (O/C=1 and H ₂ O/C=1.2).....	143
Figure E.12. Isooctane exit product gas at equilibrium (O/C=1 and H ₂ O/C=3)es.	144

List of Appendixes

APPENDIX A: CONTROL TEMPERATURE PROFILE.....	108
APPENDIX B: CALIBRATION PLOTS.....	112
B.1 Calibration plots for GC-TCD analysis.....	112
APPENDIX C: EXAMPLE RESULTS.....	116
C.1. Mass Balance for Methanol.....	116
C.2. GC-TCD chromatograms for the reformat analysis	118
C.3. Hydrogen in reformat at different O ₂ /fuel and H ₂ O/C ratios with methanol	120
C.4. Chromatograms	125
C.5. Product gas composition of methanol	127
C.6. Exit gas composition in the reformat (O/C=1 and H ₂ O/C=1) with isooctane...	131
APPENDIX D: YIELD AS A FUNCTION OF GHSV	134
APPENDIX E: REFORMING PRODUCTS PERCENTS AT EQUILIBRIUM.....	138
E.1. Methanol.....	138
E.2. Isooctane.....	143

1. INTRODUCTION

One of the major problems for fuel cells applications in automobiles is the delivery of hydrogen. Is it feasible to have a tank of hydrogen in a car? Is it feasible to have hydrogen stations? Obviously, this is a major problem to be solved. Thus, processes for reforming hydrocarbons and alcohols, into hydrogen, carbon monoxide and carbon dioxide are required. This process that involves liquid fuels and oxygen as feeds have been demonstrated to be feasible for use in fuel cell vehicles and stationary power applications. Reformers offer alternatives for delivery of hydrogen to fuel cells. For this reason, during the last decades, several investigators have been dedicated to the design and optimization of reformers and to the search of possible catalysts capable of being selective to hydrogen production. Since 1980 (41), Argonne National Laboratory (ANL) has been paying attention to these fuel processors as key players on the future development, so they focus on the development of reformer catalysts in addition to the enhancement of the reformer performance.

The Department of Chemical Engineering of the University of Puerto Rico in collaboration with Argonne National Laboratory (ANL) in Chicago, IL is developing and implementing a Reforming Catalyst Characterization Program. The specific objectives of this study are to: 1) convert various hydrocarbons, including methanol and isooctane to a hydrogen-rich product gas; 2) identify coke formation during autothermal reforming and 3) study the effects of oxygen, hydrocarbon and water flow rates, and reactor temperature

that maximize the selectivity to hydrogen and inhibit lateral reactions leading to methane formation and coke deposition.

1.1 Justification

Recently, President Bush emphasized “hydrogen fuel cells represent one of the most encouraging, innovative technologies of our era...let us promote hydrogen fuel cells as a way to advance into the 21st century” (43). The “hydrogen economy” will help to reduce our dependence on imported oil and will help the environment by reducing pollution from fossil fuels and by reducing the greenhouse gases emissions. If this idea is fully developed, the demand for oil will be reduced significantly by the year 2040.

Fuel cells are increasingly considered for widespread distributed generation and other stationary power applications. A fuel cell produces electricity from an electrochemical reaction of hydrogen and oxygen that can be obtained from air or in its pure form. Hydrogen is the most abundant element of the earth but before it can be fed to the fuel cell, it has to be derived from water or hydrocarbons such as gasoline, diesel, propane, methanol, ethanol, natural gas and renewable fuels (i.e. biodiesel).

Direct hydrogen fuel cell is the best choice because it does not produce dangerous emissions to the environment, its higher efficiency and a simple fuel system design. However, it has significant storage problems. This makes unrealistic in some aspect an automobile powered by fuel cell carrying a hydrogen tank. Also, an infrastructure for producing, storing and delivering hydrogen does not exist yet. The storage of hydrogen or production from other fuels on-board the vehicle is a fundamental problem in the fuel cell technology. Refueling stations will require sophisticated leak detection devices for

security reasons because hydrogen is colorless and odorless. Its low ignition temperature and wide flammability range are characteristics that make this gas a unique fire hazard. Obviously, this is dangerous and unrealistic at this time and another way of supplying or producing hydrogen must be developed.

Since an infrastructure is already in place for gasoline, natural gas, and diesel and exist in an easy, efficient storage of these compounds as liquids; hydrogen can be extracted from these existing sources using a device known as a reformer (located on the vehicle), eliminating the infrastructure problem. Three methods of reforming exist: steam reforming, partial oxidation and autothermal reforming in where the hydrocarbons react with a mixture of oxygen and steam in a reactor with a catalyst.

In this investigation, the reforming method of interest is to study the autothermal reforming which combines the endothermic steam reforming (fuel reacts with water) with the partial oxidation reaction (part of the fuel reacts with oxygen), balancing heat flow in and out of the reactor. The name “autothermal” refers to the heat exchange between the endothermic steam reforming process and the exothermic partial oxidation. These types of reformers systems are very productive, fast starting and compact making both the size and weight of a fuel processor important design considerations for automobiles deployment. But the principal advantage of autothermal reforming over other reforming systems is that does not require specialized materials reactors that resist high temperatures. This fact makes its manufacturability a lower cost option compared to the other steam reforming methods. Endothermic heat required by reforming reaction is

provided by the combustion of a portion of the fuel with controlled quantities of oxygen. Thus, lower reactor temperatures are required to reform the fuel.

These reformers are non-expensive and easy to manufacture and the process is similar to the automotive catalytic converters. Hydrogen-rich gas is produced at hundred degrees lower temperatures with greater product selectivity than the other reforming processes. All these characteristics make the autothermal reforming more feasible for automobile fuel cell applications.

ANL research involves the creation of a new catalyst that could be effective for all hydrocarbon types, selective to hydrogen and carbon dioxide, and inhibit methane and coke formation in the catalyst surface. They had tested these catalysts in a reactor that is capable of reforming many conventional fuels into a hydrogen-rich gas for feeding fuel cells using the autothermal reforming process. Using autothermal reforming could lead to side reactions due to the oxygen to fuel feed ratios and water to carbon feed ratios. Therefore, it will be important to study at what determined ratios, higher hydrogen production is obtained without the presence of side reactions such as methane, and coke formation.

The key objectives of this research is to study how this catalyst can convert methanol and isooctane to a hydrogen-rich product gas; study the effects of O_2 , hydrocarbon and H_2O flow rates; and study the reactor temperature that maximize the selectivity to H_2 and CO_2 and minimize side reactions.

1.2 Objectives

The ultimate objectives of this study were to establish the feasibility of using a new catalyst to:

- Obtain fundamental understanding in autothermal reforming process technologies utilizing a new Pt-based catalyst developed by ANL.
- Study experimental variables in order to obtain the highest hydrogen-rich gas production and selectivity for methanol and isooctane.
- Study combination of experimental variables where side reactions can be formed during autothermal reaction such as methane and carbon formation.

The specific objectives of this research were:

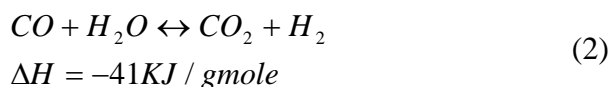
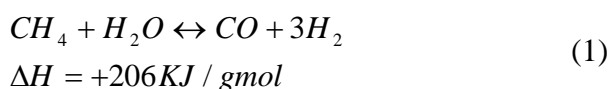
- To convert methanol and isooctane to a hydrogen-rich product gas.
- To study the effects of oxygen to fuel ratio, water to carbon ratio, and reactor temperature that maximize the selectivity to H₂ and decrease the production of CO and CO₂.
- To compare experimental gas product concentrations with thermodynamic simulation equilibrium results.

1.3 Theory

1.3.1. Reforming Technology

Hydrocarbon fuels (C_nH_m) can be reformed by partial oxidation (POX), steam reforming (SR), or autothermal reforming (ATR). *Steam reforming* combines fuel with water to produce hydrogen and carbon monoxide. The first steam reforming units to convert hydrocarbons into hydrogen rich gas were built by Standard Oil in 1930 (14). This technology is being used now worldwide to produce most of the hydrogen used for ammonia/methanol synthesis and refinery operations.

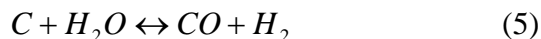
This reaction is highly endothermic and is conducted in large scale manufacturing processes in tube-fired furnaces at 800°C and pressures up to 30atm. Equations 1 and 2 represent steam reforming reactions for methane:



This process can be done catalytic or non-catalytic form. The non-catalytic way requires very high temperatures which are disadvantageous in fuel cell applications. If the steam to carbon ratio (ψ) used is too low, it leads to coke formation by thermal cracking (eq. 3) or by the Boudouard (eq. 4) reaction that results in catalyst deactivation.



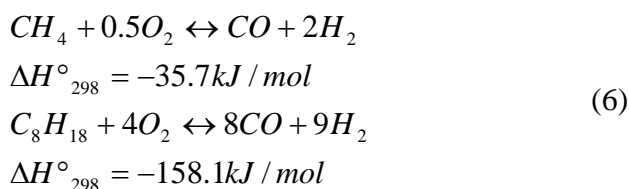
To reduce the coke formation is recommended to use an excess of steam in order to gasify all the carbon formed during the reaction (eq. 5).



Using methane as the hydrocarbon to reform, a steam to carbon ratio of 2.5 is enough to avoid coke formation. When using higher hydrocarbons, a ψ ratio of 6-10 is common.

The catalysts used in the catalytic steam reforming are commercial ones that consist of nickel supported in alumina, magnesia or calcium aluminate. The rhodium based catalysts have demonstrated to be more active and less susceptible to coking than the nickel catalysts, but they are more expensive (33).

Partial oxidation combines fuel and oxygen to produce hydrogen and carbon monoxide when the oxygen to fuel (x) ratio is less than the one required for complete combustion (CO_2 and H_2O) (eq. 6).

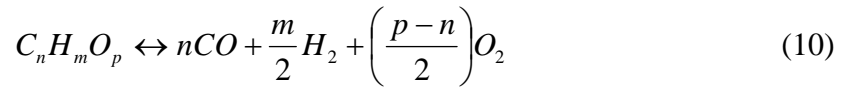
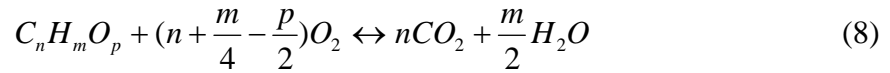
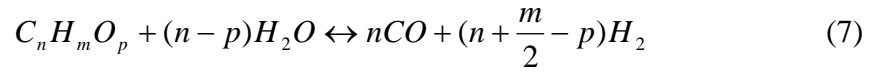


This reaction can be performed with or without a catalyst. The hydrogen production is less than that for steam reforming although the reaction rates are much higher for POX. Reaction temperatures above 1000°C are necessary to achieve rapid reaction rates for non-catalytic POX. Because the heat generated is not enough to preheat the feed to achieve optimal rates, some of the fuel must be combusted first, even though this reaction is exothermic. Catalytic POX operates at lower temperatures than the non-catalytic route providing better control over the reaction and less coke formation. These

characteristics have developed a big interest in this type of reforming since it allows for a wider choice of materials of construction for the reactor. The catalysts used are commonly from the VII Group metals such as rhodium, platinum, palladium, cobalt, etc., either supported on oxide substrates or used unsupported (33).

Autothermal reforming (ATR) is a combination of steam reforming and partial oxidation. This reaction involves steam, oxygen, and fuel to produce H_2 and CO_2 . The exothermic oxidation reaction provides the necessary heat for the endothermic steam reforming reaction. This characteristic allows a more rapid response to changing power demands and faster startup in transportation applications. There are three main advantages that low operating temperature catalytic ATR has over the high temperature operating POX and SR: (1) less complicated reactor design and lower reactor weight (heat exchange between the reactants and hot product) is required; (2) wider choice of construction materials; (3) lower fuel consumption during startup, because the energy required to heat the reactor to its operating temperature is proportional to its operating temperature (33). These characteristics make the autothermal reformer simpler and more compact than steam reformers, and it is likely that autothermal reformer will have lower capital costs. In an autothermal reformer, all the heat generated by the POX reaction is fully utilized to drive the steam reforming reaction. Therefore, autothermal reformers offer higher efficiency than POX systems where the heat that is in excess is not easily recovered. Water gas shift reactors (see eq. 2) are also needed in these three reforming ways to increase the hydrogen production and decrease the carbon monoxide content (44).

For hydrocarbons, the mechanism that involves autothermal reforming can be described by the following principal equations (51)



Thus, the overall reaction for ATR (including alcohols) is



As mentioned before, x is the oxygen to fuel ratio. This ratio and the steam to carbon ratio can be chosen independently, but it is important to add enough H₂O to convert all the CO to CO₂ by the water gas shift reaction (eq. 9). Also, undesired side reactions can occur, in where contaminant gases are produced and hydrogen production decreased. For example, carbon monoxide reacts according to reaction 12 with hydrogen to produce methane.



This side reaction is exothermic and is frequently observed at low reactor temperatures. Similar to other reforming systems, ATR has been studied with and without catalysts. The catalysts used are the same that are used in SR and POX, including platinum/palladium monolithic catalyst (14). Hydrocarbons to be reformed can contain

some contaminants, such as sulfur, that could poison the catalyst. The deactivation of the catalyst by poisoning or by coke formation has been always of great issue. But the catalyst is important because it permits a lower temperature operation with improved hydrogen selectivity.

Steam reforming, of the three reforming pathways, yields the highest hydrogen concentration in the product. Though, for practical and transportation applications, partial oxidation and autothermal reforming processes are more attractive because they are more energy-efficient and their hardware can be smaller and lighter (3).

1.3.2. Fuel Choices

Hydrogen is the most favored choice for all operations because of its higher efficiency and zero emissions. However, it has significant storage problems limiting its transportation applications. The principal fuels that investigators are considering as possible reformer fuels are: hydrogen, methanol, ethanol, biodiesel and gasoline. Methanol, gasoline and ethanol are more advantageous, but they should require on-board reformers to produce hydrogen (12).

In the following paragraphs it will be mentioned some of the characteristics of these fuels which offer some advantages and disadvantages to the fuel cells in automotive applications.

1. *Direct Hydrogen*

On-board hydrogen storages tend to be large and heavy due to its low energy density and boiling point. There are three types of hydrogen storages under development:

- *Compressed hydrogen* – offers the least expensive method. The real problem is the size. Automobiles have small platforms to accommodate multiple pressure vessels that compressed hydrogen requires.
- *Liquefied Hydrogen* – does not have the high storage size of compressed hydrogen but it is still bigger than gasoline storage systems. It has to be maintained at -253°C and its low boiling point requires excellent insulation of storage containers. Twenty-five percent (25%) of liquid hydrogen can be boiled off during refueling and 1% is lost per day in on-board storage.
- *Hydrides* – materials that absorb hydrogen into their crystal structure (metal hydrides). Hydrogen bonds to more than 80 metallic compounds forming weak attraction that stores hydrogen until heated. Hydride systems avoid safety concerns since heat is required to release the hydrogen. Though, these hydrides are very heavy resulting in storage of only 1.0 to 1.5% hydrogen by weight.
- *Other storage options* –the use of carbon nanotubes (microscopic carbon tubes synthesized in the laboratory) to absorb the hydrogen. Actually, it is not clear that this could offer significant advantages. Also, glass microspheres are considered. These are hollow glass spheres of 0.03-0.05mm in diameter that allow hydrogen to enter when heated to 200-400°C. Hydrogen becomes trapped once the temperature cools, and it is

released again when heated. This technology is in development yet and its performance implications are not clear.

Some agencies utilize on-site electrolysis (breaking water into hydrogen and oxygen) to supply hydrogen to their fuel cell vehicles as an alternative to manage H₂ storage problems.

2. *Methanol*

Other alternative to overcome hydrogen delivery problems is to use direct methanol powered fuel cells. United States produces about 2.6 million gallons of methanol per year and the major current market in automotive fuel applications is its use as a feedstock for the gasoline additive methyl butyl ether (MTBE). Since MTBE is being eliminated after 2002 due to environmental concerns, methanol quantities could be available for automobiles. One of the disadvantages that methanol have is its toxicity, which can result in blindness or death if ingested. It could also enter the body through the skin.

There are not very much refueling stations, among these there are M85 (85% methanol and 15% gasoline). The cost of converting a gasoline station to M100 is estimated at approximately \$60,000 (52). Methanol fuel cells could be considered as a transient solution, while a hydrogen distribution infrastructure is being built over the next decade or two. Methanol can also be used as fuel to be reformed for fuel cell applications in automobiles.

3. *Ethanol*

Over 1.4 billion of gallons of ethanol were produced in 1998 and it is expected that 2.7 billion gallons will be consumed (17). Recently, this renewable alcohol is being considered as a source of hydrogen for fuel cell. Ethanol is less toxic than methanol or gasoline and offers higher efficiency and lower technical risk. It can be used as E100, E95, or E85. Actually, there are approximately 76 E85 (85% ethanol and 15% gasoline) fueling stations in the United States.

4. *Gasoline*

Since gasoline infrastructure is already in place, using on-board reformers for the extraction of hydrogen from gasoline is one approach to commercialization of fuel cell vehicles (12). The most important issue is that producing hydrogen from gasoline is more difficult than methanol. The production can be achieved at 850-1000°C, making the system slow to start. Also, there is a concern about the sulfur and carbon monoxide levels that can poison the fuel cell membrane catalyst.

In general, methanol and gasoline are the most common fuels that are being considered for hydrogen fuel cells sources in automotive applications. They both have advantages and disadvantages as sources of hydrogen, and should continue to be developed before a commercialization choice is made. True “well-to-wheel” analysis will determine which is the best overall choice. It is important not only to consider the fuel processor technology, but safety and health considerations, overall infrastructure costs, and acceptance by the public of new technologies are important aspects in the development of this technology (9).

1.3.3. Reformer Systems

A significant issue for automotive applications, less for stationary power sources, is whether to carry out the reforming process before the fuel reaches the fuel cell system. External reforming could be carried out at a refinery or chemical plants delivered by pipeline to filling stations, or further downstream at the station itself for transporting or piping to the end user. As mentioned before, this option would allow to for a less complex system than the internal option, but it needs the introduction of on-board hydrogen facilities, which is highly expensive. Another alternative is the Direct Methanol Fuel Cell (DMFC) that runs on methanol without reforming. This technology is not yet fully functional and is also unlikely to be used for all applications (8).

On-board reforming systems experience packaging issues, extra weight, complicated controls and high cost. It is necessary to couple the systems together to carefully optimize the heat and energy economics, and turn the fuel-reforming technology into a compact, lightweight, efficient, and a low cost system. A good fuel processor offers the following advantages: (1) very-high purity product hydrogen, (2) high energy efficiency, (3) a compact device, and (4) a potential for low cost of manufacture (18). The following are existing reformer systems under development (44).

1. ***Sorbent Enhanced Reforming*** – An adsorbent, such as calcium oxide, is mixed with the reforming catalyst, eliminating the carbon monoxide and the carbon dioxide. The hydrogen production is higher than that produced in a catalytic steam-reforming reaction. Thus, it reduces the need of processing and purification of the syngas, which can be expensive in a small-scale steam

reformer. Furthermore, as CO₂ is adsorbed, the reaction will take place at a lower temperature (400-500°C) and pressure. This significantly reduces heat losses and material costs. Sorbent Enhanced reformers are in a demonstration stage and issues include catalyst, sorbent lifetime and system design (37, 50, 24, 27).

2. ***Ion Transport Membrane (ITM) Reforming*** – Some agencies and universities are developing ceramic membrane technology for generation of hydrogen and syngas. The non-porous membranes are composed by multicomponent metallic oxides that operate at high temperatures (>700°C). They have high oxygen flux and selectivity. Oxygen can be separated from air and is fed to one side of the membrane at ambient pressure or moderate pressure (1-5psig). Then it is reacted on the other surface with methane and steam at higher pressure (100-500psig) to form H₂ and CO. Initial estimates show a potential reduction of 27% in the cost of high pressure H₂ produced via this route. The development of this membrane is ongoing at Praxair with the Oxygen Transport Membrane Syngas Alliance (44).
3. ***Microchannel Reformers*** – The aim of using microchannel reactors is to reduce the automotive reformers size (56). This compact hardware is roughly an order of magnitude smaller than conventional technology and minimizes heat and mass transfer resistance. Their micron-scale dimensions permit the utilization of highly active catalysts, which take advantage of rapid surface reaction kinetics. These systems can be designed without large pressure drops

that are associated with small or complex flow structures. It is projected that a complete system volume of less than 8L could be used to produce a sufficient rate of hydrogen production and quality to produce 50kW_e for a PEM fuel cell (54).

1.3.4. Reformer efficiency

The thermal efficiency for a reformer reactor describes the relation of the lower heating values of the hydrogen produced to the lower heating value of the fuel processed.

The maximum theoretical efficiency can be defined as (3)

$$\eta_{eff,theo} = \frac{\text{lower heating value of H}_2 * \text{moles of H}_2 \text{ in the stoichiometric reaction}}{\text{lower heating value of the fuel fed} * \text{moles of fuel fed}} \quad (13)$$

To calculate the experimental efficiency, the numerator is replaced by the LHV multiplied by the moles of hydrogen obtained at the exit gas of the reactor. The denominator remains the same.

The temperature of the reactor feed influences the fuel processor efficiency. The higher the temperature of the reactor feed, the higher the reactor efficiency. As the feed temperature increases, less fuel has to be burnt to heat the feed to the necessary reactor temperature and more fuel can be steam-reformed. The vaporization of the fuel contributes to a higher efficiency because the heat of vaporization would be compensated by the combustion of a fraction of the fuel. However, vaporization of the fuel with a “downstream” heating source, leads to a slower load and might be difficult since it can result in fuel decomposition and soot formation. If it is desired to preheat air and water, it has to be around 200 and 400°C or vice versa. Higher temperatures will require more

heat exchangers that will increase weight and volume to the reformer. Pre-heating air and steam mixture around 300°C allows reformer efficiencies around 80% (16). The reformer efficiency is directly proportional to the hydrogen and carbon monoxide produced or generated. Besides of the objective of a high reforming efficiency, it is also important to obtain a higher concentration of H₂ than CO because the volume and weight of the shift reactors HTS and LTS are directly proportional to the CO concentration in the reformed gas (16, 28).

1.3.5. Reforming Catalysts

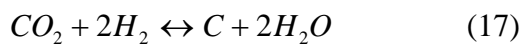
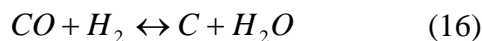
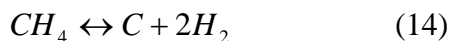
Fuel processors catalysts for automotive applications must have higher activity and better thermal and mechanical stability than the catalysts used in the production of H₂ for large-scale manufacturing processes. Reforming catalysts usually consist of a substrate and a promoter, where the substrate participates in the oxidation of the carbon and the promoter dehydrogenates the hydrocarbon or alcohol (4). Also, they should be able have to process feed at a GHSV of 200,000 h⁻¹ with a fuel conversion higher than 90% and a hydrogen production close to the equilibrium value. They are designed to resist deactivation with a lifetime of 5000h preferably (55). Catalysts used by various investigators for reforming fuels are Cu/ZnO/Al₂O₃; those consisting of nickel oxide (NiO), silica (SiO₂) and magnesium aluminate (MgAl₂O₃) (30); commercial naphtha reforming catalyst (NRC) (32.); rhodium-based supported on Al₂O₃ which may contain small amounts of Pt supported on metallic monoliths (51); Ni/(Fe,Co)/MgO/Al₂O₃) (31); ceria oxide impregnated with Pt (46); ruthenium/alumina and rhodium/alumina (45);

CuO-CeO₂ mixed oxide catalysts (45); and bimetallic PtSn catalysts (45); and Pt/ γ -Al₂O₃ and Au/ α -Fe₂O₃ (49).

Many research groups are developing these catalysts such as Engelhard Corporation, Johnson-Matthey and Argonne National Laboratory (ANL). ANL, one of the leading laboratories, is developing a transition metal catalyst supported on an oxide ion conducting substrate (ceria, zirconia or lanthanum gallate) for reforming systems. They have obtained excellent reforming activity between 500 and 800°C with high fuel conversion and selectivity using isooctane as a fuel and these catalysts (33). No-sulfur tolerant catalysts have been developed yet, requiring incorporating a large unit for removing the sulfur from the fuel to the fuel reformer systems (30).

1.3.6. Coke Formation

In steam reforming, hydrocarbons decompose at reforming temperatures in the absence of sufficient steam to form carbon and hydrogen. This is a highly undesirable product because it can deactivate the catalyst and can foul and shut down the reactors (2). The coke formation reactions reported in different systems are:



Coking can be avoided by operating at high temperatures and at high oxygen to fuel ratios. It is desirable that the oxygen feed be in the form of water, so the coke is reduced at high O/C and H/C ratios. In partial oxidation reforming the coke that can be formed is less, followed by autothermal reforming and steam reforming. The composition of the coke is related to its solubility. At a temperature lower than 550K, soluble coke predominates. When the temperature is increased, the soluble coke is transformed in insoluble coke (14).

1.3.7. Effect of Steam to Carbon Ratio(ψ) and Oxygen to Fuel Ratio(x)

As mentioned above, reformers are typically operated at high steam-to-carbon ratio in order to suppress coke formation. This effect in the fuel processor efficiency has been studied intensely. These studies consisted in varying ψ , keeping all the other input parameters and assumptions constant. As this ratio increased, the oxygen-to-fuel ratio (x) is adjusted too in order to maintain the thermoneutrality of the reaction. The thermoneutral value of x yields the maximum efficiency of the fuel processor, but sometimes, the reforming reaction is performed in a manner that will be slightly exothermic to compensate the heat loss from the fuel processor to the environment, and to maintain the exit reformat temperature higher than the reactant inlet temperature (2).

In order to vaporize the increasing amount of water in the feed, it was necessary to increase the amount of oxygen fed to the fuel processor. Though, increasing x led to lower hydrogen concentration and higher water contents in the product gas from the reformat fed to the fuel cell stack. These low hydrogen concentrations resulted in lower heating values of the reformer gas and lower fuel processor efficiencies. In addition,

keeping a constant exhaust gas temperature, the water vapor concentration will remain constant. Therefore, with increasing values of ψ or x , increasing amounts of water can be recovered at the condenser (38).

1.3.8. Carbon Monoxide and Sulfur Removal

The Polymer Electrolyte Fuel Cell (PEMFC) can be easily poisoned by residual concentrations of carbon monoxide (10ppm) remaining after the water gas shift reaction (14). It is preferentially adsorbed by Pt-catalyst, consequently blocking the access of hydrogen to these catalytic sites and significantly lowering the PEMFC efficiency. After the reforming process, it is necessary to have an additional process in order to reduce the CO concentration and to maintain an acceptable level of performance of the fuel cell. However, the Solid Oxide Fuel Cell (SOFC) oxidizes electrochemically CO to CO₂ to generate electric power without decreasing significantly its performance. The primary option to reduce CO concentration is the water gas shift reaction (eq. 2). The lower the reactor temperature, lower concentrations of CO can be achieved, based in thermodynamic equilibrium. There are several available commercial catalysts that are being used in this process such as iron-chrome oxide and copper-zinc oxide catalyst which operate at 300-450°C and 160-270°C, respectively. Water gas shift reactors are composed of two or more reaction stages and operate adiabatically based in the operating temperature of the catalyst used (33).

Other technologies that are being studied for reducing CO concentrations are (26, 8):

1. Membrane Separation - Palladium alloy membranes can remove the CO, but they require large differences in pressure and temperatures that reduce the efficiency of the system.
2. Methanation – CO is reacted with H₂ to produce methane and water, but the hydrogen required is three times the amount of CO removed.
3. Preferential CO oxidation (PrOX) - a small quantity of air is supplied to the fuel gas and CO is oxidized in CO₂ over the H₂ using Rh or Ru as catalysts supported on alumina.

For automotive or on-board applications PrOX is preferred over the methanation and the membrane separation because the lower energy requirement.

Other concerns under study are the poisoning of the PEMFC and SOFC by sulfur. Sulfur, in the form of H₂S will be present in the fuel gases in gasoline and diesel fuel and can reduce the catalyst activity significantly. Also, it decreases irreversibly the performance of the PEMFC with a concentration of 200 ppb. At low concentrations of 1ppm no degradation in SOFC performance has been observed. The gasoline fuel may contain as high as 3-8ppm of equivalent H₂S and it is necessary to remove all the sulfur that can damage the fuel cell. There are two different possibilities:

1. Desulfurization prior to reforming – The sulfur is removed from the fuel gas before it is reformed. International Fuel Cells has developed a Ni-based adsorbent in order to reduce the sulfur from the fuel (10, 34).
2. Desulfurization after reforming – The sulfur-content fuel is first reformed and then desulfurized using ZnO, an oxide adsorbent (13).

2. LITERATURE REVIEW

2.1 Fuel Cells Systems

Fuel cells are electrochemical devices that are being developed for transportation and for stationary and portable power generation. They have the potential to develop high efficiency and lower emissions (32). To succeed, fuel cell developers have to compete with the conventional power-generation technologies such as internal combustion engines, microturbines, or batteries. These systems need to be efficient and inexpensive. Higher energy efficiency will lead in a reduction in carbon dioxide emissions (contributes to the global warming), and eliminate the carbon monoxide, nitrogen oxides (NO_x), and sulfur oxides (SO_x) that are being considered as atmospheric pollutants (3, 42).

Fuel cells provide increased efficiency and energy density compared to the internal combustion of the engines and second batteries. By producing electricity from the reaction of hydrogen and oxygen, less thermal waste is created than in a heat engine. Fuel-cell technology has the potential to improve both the efficiency and the environmental impact of automobile travel because it can achieve much higher overall system efficiency (45%) than an internal combustion (IC) engine (20%). The fuel consumption of automobiles per mile traveled will decrease significantly, since the improvement in efficiency on that order slows the drain on our fuel resources. An advantage of the fuel cell is that its output is more environmentally friendly than the IC engine. The waste stream from the fuel cell is a mixture of water and air, compared to the high temperature combustion products such as NO_x, SO_x and particulates that exit with the effluent from an IC engine. Several types of fuel cells are being studied with special interests, such as Molten Carbonate Fuel Cell (MCFC), Solid Oxide Fuel Cell (SOFC), Phosphoric Acid Fuel Cell (PAFC), Direct Methanol Fuel Cells (DMFC) and Proton Exchange Membrane Fuel Cells (PEMFC) (20).

Molten Carbonate Fuel Cells (MCFC) and Solid Oxide Fuel Cells (SOFC) are considered as higher temperature fuel cells and have potential for central power plants, while the Polymer Electrolyte Membrane Fuel Cells (PEFC or PEMFC) predominate among smaller power generators. These generators are developed for residential units and for propulsion power in automobiles. The PEFC has the best potential to replace the IC engine since it can be easily fit under the hood (size and weight), it has the ability to startup quickly, the ability to meet the dynamic response typical in a driving cycle, and

cost. However, PEFC contains platinum as the electrocatalyst and it is poisoned at low temperatures (80°C) by carbon monoxide and sulfur, as well as ammonia. Since the CO fraction has to be less than 20ppmv to ensure a good behavior of the cell, an effective purification system has to be added before entering the membrane (2).

Hydrogen is the best fuel to feed the PEMFC. But, the lack of a hydrogen refueling infrastructure, and storage capacity combined with a shorter driving range (because of its low energy density) results in a “hydrogen-fueled vehicle” less attractive to the consumer. It is more viable to carry liquid fuels (hydrocarbons or alcohols) with high energy densities and convert them to a hydrogen rich gas. This process is accomplished by reforming units in vehicles. The consumer will not sacrifice the performance of the vehicles, such as the ability to “start-and-drive” capability or rapid acceleration. Consequently, the fuel processor or reformer, which will going to be part of the fuel cell engine, must also meet the requirements of size, weight, be able to start up very quickly and be dynamically responsive to power demands (3, 46, 9). Thus, one of the key areas in the development of fuel cell technology that had been studied is the ability to obtain the reactant gases (i.e. H₂ and O₂). Oxygen can be obtained from the air. However, achievement to obtain pure hydrogen from fuel sources without contaminant gases that do not affect the fuel cell performance is the principal issue of interest.

At the beginning of this technology, the primary fuel candidate for stationary fuel cells considered was natural gas, which is used in those cells that has an internal natural gas reformer. In case of no access to natural gas, propane, methanol and other alcohols, diesel and synthetic fuels (i.e. dimethyl ether) could be used. The development of fuel

flexible fuel cells systems could enable their application initially to the available fuel infrastructure. SOFC and MOFC can oxidize carbon and hydrogen in the anode compartment and could eventually support the use of coal, biomass, petroleum distillates, methanol, ethanol or other hydrocarbons as primary fuels. As solutions to the hydrogen sources, ANL and other research groups proposed to produce hydrogen for feeding the cells using a process called electrolysis where the water is broken in the hydrogen and oxygen elements in a non-polluting process. As long-term solutions, when all the hydrogen infrastructure and storage problems have been eliminated, it can be produced from water at large plants using more efficient chemical processes and heat or power from nuclear power plants. The hydrogen would be sent for large fuel cell systems to produce electricity or it can be stored for later use (7).

In the next section, reformers units to obtain the hydrogen to be fed to the fuel cell and the differentials between reformer systems that are being studied will be discussed.

2.2 Reformer Systems

In the fuel delivery process, it is possible to carry out the reforming step at several stages which can be divided into external and internal reforming. This is a significant issue for automotive fuel cell applications. External reforming is carried out before the fuel reaches the fuel cell system and internal reforming refers to the process occurring inside the fuel cell stack. External reforming could be done in a chemical plant or refinery and deliver the hydrogen through pipelines to filling stations. For automotive applications, on-board reformers may be used so that the vehicles can use liquid fuels that are going to be converted to a hydrogen-rich gas in a processor attached to the fuel cell

system. This option will increase the cost and the complexity of the vehicle's power system. Using external reformers will eliminate this problem, but the need of an introduction of hydrogen storage facilities is still an engineering challenge (8).

In 1990, the DOE began a program to develop technologies of fuel processing than could fit under the hood of a car, respond to power demands and can utilize a variety of candidate fuels. Nuvera Fuel Cells (before Arthur D. Little) began its work on a fuel-flexible reformer concept that could contain a partial oxidation reactor, a catalytic reforming section, a shift reactor to convert CO to CO₂ and, if necessary, a sulfur removal bed. In October 1997, Nuvera Fuel Cells produced electricity using gasoline as a fuel for the reformer and a PEMFC. On January 9, 2002, the Secretary of DOE, Spencer Abraham, announced the FreedomCAR, an initiative that focus on technologies for hydrogen production that could make fuel cell vehicles affordable and to develop an infrastructure of a hydrogen supply to support them. The announcement of the FreedomCAR is evidence that this commitment is getting to the highest level of the federal government. This commitment has to be backed up by a national program that can create sufficient funding to the test and demonstrations of hydrogen fueling and hydrogen vehicles on a large scale (41).

In the next section, different types of reforming that are available nowadays will be discussed.

2.2.1 Steam Reforming

Freiburg ISE (22) advises that at the moment of designing a reformer processing unit it is necessary to know that a hydrogen generator which supplies a fuel cell for an

electric motor must react immediately to the rapid load fluctuations that occur during driving. They had studied the reforming process for vehicle applications. In their processing unit, a reactor gives a hydrogen-rich gas product by reacting natural gas with steam at temperatures between 700 and 900°C. This mixture contains high levels of carbon monoxide and then it is processed in shift reactors (two subsequent catalytic converters) to give carbon dioxide gas and additional hydrogen gas. A gas purification step, which is the final one, removes the CO from about 0.5% volume to a low residue of 10ppmv. This low value guarantees the efficiency of the PEFC membrane fuel cell.

In the steam reformer, the endothermic reaction and the combustion reaction used to maintain it are in separated zones and the housing wall transfers much of the required heat from the combustion zone to the reforming zone. A low emission burner heats the metallic honeycomb catalyst. The reactor efficiency (the ratio of the lower heating value of the hydrogen produced to that of the fuel used) value was 0.65 to 0.68.

Edlund (18) studied the technology of producing hydrogen based on steam reforming at Ida Tech, Oregon, USA. This company scaled down the process and coupled it directly to a multi-stage hydrogen purifier, resulting in very high purity hydrogen, good enough for use in fuel cells.

Table 2.1. Comparison of the Ida Tech Fuel Processor with major reformer technologies.

Type	Process	Typical Hydrogen Purity
Ida Tech Fuel Processor	Steam Reforming	99.95%; <1ppm CO and <5ppm CO ₂
Autothermal Reforming	Partial Oxidation Coupled with Steam Reforming	50-60%; 10-100ppm CO and 20-30% CO ₂

Partial Oxidation Reactors	Partial Oxidation	40-50%; 10-100ppm CO and 20-30% CO ₂
----------------------------	-------------------	--

The hydrogen purifier unit consist of two stages: the first one consist of hydrogen selective membrane and provides a separation of hydrogen from the crude reformat gas mixture; and the second polishing catalytic stage removes trace levels of CO and CO₂. The membrane consists of a palladium alloy and exhibits a high selectivity (600-1000) for hydrogen over other gases. The catalyst used is a methanation bed and these two stages are integrated with the steam reformer region of the fuel processor. Impurities that poison the fuel cell anode catalyst such as amines and organic nitrogen compounds are almost totally removed from the first stage of the hydrogen purifier. Table 2.1 compares the hydrogen purity obtained from their system from the principle types of commercial reformers and fuel processors. Steam reforming uses hot steam as the oxidant rather than using air as a source of oxygen as in the case of partial oxidation (POX) and autothermal reforming (ATR). About of 30% of the hydrogen is derived from steam. This characteristic increases fuel economy and make this a benefit of using steam reforming. They used catalysts supported-nickel formulations that are usually used for steam reforming of hydrogen feedstocks. These catalysts are very sensitive and poisoned easily with sulfur compounds and it will be necessary to desulfurize the feedstock prior or post reforming. If some type of catalyst tolerant to sulfur would be available, the need of desulfurizing the hydrocarbon won't exist because the hydrogen purification system rejects all impurities and the palladium alloy membrane used is not poisoned by sulfur content.

Ida Tech also measured and compared energy efficiencies for the fuel processor using several different feedstocks. Any loss of heat from the fuel processor, decreases the energy efficiency but here the waste gases from the steam reforming process serve as fuel to heat the fuel processor giving an overall efficiency very close to the theoretical limit. Table 2.2 shows the measurements of the experimental and theoretical efficiencies for different types of hydrocarbons. The theoretical efficiency was calculated assuming that the steam to carbon ratio remains constant at 1:1 for methanol and 3:1 for the other feedstocks. Obviously, this is a source of discrepancy between the experimental and theoretical efficiencies because this ratio will vary during experimental measurements. Also, the system is assumed to be ideal reaction stoichiometric to calculate the theoretical values, giving rise to another source of discrepancy between theoretical and experimental efficiency values.

Table 2.2. The Ida Tech fuel processor efficiencies using a variety of hydrocarbons.

Feedstock	Experimental Efficiency (%)	Theoretical Efficiency (%)
Methanol	86-90	87
Methane	67	66
Biodiesel	55	61
Diesel	70	66

G.A. Whyatt and et al. (57), agree with Ida Tech in the advantages of steam reforming over POX and ATR. The hydrogen content in the product stream will be higher because it is not diluted with nitrogen; high pressures to the reformat could be applied by pumping liquid fuel and water without needing to compress air to the reaction

pressure; and it can use the waste fuel cell anode gas as a fuel to combust and provide the necessary heat input, being more efficient. They emphasize that ATR and POX cannot use the waste fuel cell anode gas for being thermally neutral and exothermic, respectively.

2.2.1.1 Microchannel Reactors

Sean P. Fitzgerald et. al. (20), evaluated steam reforming in microchannel reactors, as a method to generate a hydrogen-rich gas product needed for automotive PEMFC applications. They performed tests with a gasoline analogue, isooctane, in a compact microchannel reactor using a catalyst that enable a residence time of 2.3 milliseconds of the reactants. The use of a catalyst synthesized by themselves lead to a high conversion of isooctane and high selectivity to hydrogen. With an experimental steam to carbon ratio of 6:1 and residence times of 7.4 ms, they found that at 650°C, the isooctane reached almost 100% and the selectivity to hydrogen was almost 92%. The selectivity of CO₂ was 65%, more favored than CO and hydrocarbons with selectivities of 27% and 8%, respectively. Their catalyst was studied during 90 hours without noticeable deactivation. They used microchannels reactors to add heat efficiently to the strongly endothermic reaction, and the heat exchange fluid used to heat the reactor zone was combustion gas. It was built by them with a total of 30cm³, large enough to produce 1.0kWe power in a PEM fuel cell. This reactor achieved 90% conversion of isooctane and 90% selectivity to hydrogen at a residence time of 2.3ms, three orders of magnitude faster than conventional technology. Based in these results, it is believed that a 50kWe

gasoline-based steam reforming system will have a volume less than 4 liters and a volume smaller than 8 liters for a complete 50kWe fuel processor.

Tonkovich et al. (54) developed and demonstrated that the fuel vaporizer is a one-step of the multi-component fuel processor, at both bench and fuel scale for automotive applications at 50kW size. They emphasized that the microchannel reactor-based fuel processors are small, efficient, modular, lightweight and inexpensive. These reactors can reduce the size of conventional chemical without lowering the throughput. Other systems, such as steam reforming, partial oxidation reforming and autothermal reforming exist to produce synthesis gas (H_2+CO) and are based in a fixed-bed reactor technology. These systems do not scale linearly with throughput because of the inefficient heat transfer. The heat and mass transport limitations are minimized in the microchannel reactors while in conventional reactors the observed reaction rates are slower. The process efficiency is increased by fast heat and mass transfer which permits process miniaturization without lowering the productivity. The technology used in their investigation was based upon combusting the waste hydrogen from the cell anode to provide the latent heat of vaporization of the fuel. The anode effluent stream is comprised of nitrogen, carbon dioxide, water and hydrogen (6-8% volume). Catalytic combustion of the diluted hydrogen was performed using palladium catalyst supported on porous ceramic foam, metal monolith, or silica powders.

Tonkovich et. al. (53), with other group of investigators also developed, a compact microchannel gasoline vaporizer in a full scale using commercial-grade gasoline. This vaporizer utilizes integrated catalytic combustion of a simulated PEMFC

anode effluent to supply heat to evaporate liquid gasoline. This compact unit vaporizes gasoline at nearly 300mL/min and its weight is only 1.8kg and displaces about 0.3L. The results indicate that this component is more than an order of magnitude smaller than a conventional fuel vaporizer and a complete system volume of less than 8L produce hydrogen at a sufficient rate and quality to produce 50kWe from a PEM fuel cell.

G.A. Whyatt et.al. (57), also demonstrated a high energy-efficient microchannel steam reforming system. They also agree with Fitzgerald in the fact that using this reactor produces rapid heat and mass transport, which enables fast kinetics for the highly endothermic reaction. The microchannels architecture also ensures the construction of very compact and highly effective heat exchangers. The overall volume of the reactor was 4.9 liters and that of the supporting heat exchangers was 1.7 liters. To provide heat to the reaction, the reactor contains alternating reaction and combustion gas channels, arranged in crossflow. A network of microchannel heat exchangers permit to recover the heat in the product of the reformat and combustion exhaust streams for use in vaporizing the fuel and water, preheating the combustion air and preheating the reactants to reactor temperature. The combustion gas had a temperature of almost 50°C and 130°C for the reformat product and the reactor operated at 750°C. Reforming isooctane at a rate sufficient to supply a 13.7kWe fuel cell, the system achieved 98.6% conversion with an estimated overall efficiency (electrical output/LHV fuel) of 44% after integration of a water gas shift reactor (WGS) and PEMFC.

2.2.1.2 Plasma Reactors

Cormier et. al. (15), studied another type of steam reformer reactor, known as plasma device. Plasma is a mixture of electrons, highly excited atoms and molecules, photons, ions, etc. The chemistry is very complex and the understanding is very limited. To predict theoretically the final products and their concentration is difficult. They made a comparative analysis between the autothermal reformers, including their improved variants, and the plasma reactors. The study was based in the advantages and disadvantages coming from methane conversion, selectivity, energy efficiency, and investment cost. Plasma reactors used for chemical applications are acceptable due to its high operating power with a selective energy input while maintaining a non-equilibrium condition. Depending of their energy, temperature and ionic density, plasmas are classified as thermal or non-thermal (non-equilibrium) plasmas. Thermal plasma reactors, or plasmatrons, comprise two water cooled metallic tubular electrodes. The electrodes are made of copper or of some improved alloys, such as beryllium bronze and tungsten-copper-nickel.

Bromberg et. al. (11) demonstrated that the autothermal reformer reaction without a catalyst in a plasmatron resulted in a hydrogen yield of 40% for an input power of 3.5kW. The plasma process resulted in a low methane conversion of 40% at low values of input power. The productivity was about $4000\text{m}^3/\text{h}$ H_2 per cubic meter of reactor. Without heat recovery, the minimum power consumption was 100MJ/kg H_2 . In order to decrease this specific power consumption a catalyst nickel-based supported on alumina was used. The hydrogen yield increased to 80%, for an input power of 2.7kW and a

methane conversion of almost 70%. The reformat had a composition of 35% H₂, 5%CH₄, 3.7%CO, 15%CO₂, 41%N₂ and traces of C₂ hydrocarbons. The productivity increased to 10,000m³/h H₂ per cubic meter of reactor and the required specific energy was reduced to less than 17MJ/kg H₂.

Cornier emphasizes that plasma reactors represent an innovative alternative due to their simplicity, compactness and low price. For small scale units to produce hydrogen in automobile applications, the choice of technology may be dictated by parameters like simplicity and quick response. Although the autothermal reformers seem to be the most efficient chemical reactors, the use of plasma reactors may soon become the preferred choice.

2.2.2 Autothermal Reforming

One of the most attractive technologies is steam reforming with oxygen (SRO), also known as autothermal reforming because it has the lower energy requirements. It provides high space velocity, a lower process temperature than partial oxidation (POX) and the H₂/CO ratio is easily regulated by the inlet gas ratio. The shortcomings of the SRO reformers concern size, large investments, and extreme operating conditions that limit the lifetime of the reactor, safety, operability and limitations on rapid response.

In the autothermal reactor, it is only needed one reaction zone and both processes occur together. The combustion runs in parallel and provides the heat for the reforming reaction, giving optimal heat transfer. Freiburg, ISE (22) were interested in autothermal reforming and constructed a test reactor with a thermal hydrogen generation power of 20kW. A mixture of fuel, air and water flows through a metal active honeycomb catalyst,

leading this direct thermal coupling of the combustion and reforming reactions to keep the operating temperature as low as 800°C. Since the reactor has an integrated heat exchanger, efficiency values exceed 70%.

Researchers of General Electric Company (35), has developed a hydrogen generating system for vehicle refueling. This system is named the Autothermal Cyclic Reforming (ACR) process which is a technology that can be applied for the production of hydrogen or syngas from many fuels, including natural gas, coal, diesel fuel, and renewable feed-stocks, such as biomass. The ACR process operates in a three-step cycle. The first step involves steam reforming of the fuel in a catalyst of Ni which is the reforming step. The second step is air regeneration where the reactor is heated by oxidizing the Ni catalyst. The final step (fuel reduction step) consists in reducing the catalyst to its original state. During the exothermic oxidation of Ni to NiO, the system is giving the heat required for the endothermic reforming reaction. The overall objective of the General Electric Company project is to design, fabricate and install a reliable and safe H₂ refueling system, based on its patented ACR process. The system includes a Pressure Swing Adsorption (PSA) unit to purify the hydrogen produced, a hydrogen compressor, a high-pressure storage tanks and a dispensing unit to deliver the H₂ from the storage tanks to the vehicle in a safely way. The company Praxair developed the PSA unit, the hydrogen storage tanks and the hydrogen compressor. Hydrogen Components Inc. (HCI) will be responsible of developing the H₂ dispenser and BP will analyze the refueling logistics and safety. The system will produce sufficient refueling for 1 bus or 8 cars daily (40kg/day) with an efficiency of 80% (based on the high heating value (HHV) of pure H₂

produced to the HHV of fuel consumed ratio). The cost will be less than \$2.50/kg based on a natural gas price of \$4.00/MMBtu.

Hagh (23) developed a methodology for optimization of an autothermal reactor with respect to a various system parameters. He performed a theoretical interpretation of reforming reactions using atomic balance in order to determine the reforming reaction space and maximum monolith temperature for a methane reformer. The hydrogen yield was determined based on energy and material balance coupled with chemical equilibrium requirements. The assumptions taken were: (1) complete consumption of oxygen without formation of carbon soot, (2) steam reforming and water gas shift reaction to be at equilibrium at ATR outlet temperature, and (3) adiabatic reaction or a known heat loss. Hagh found that the $\text{CO}/\text{CO}_2 = 0$ and $\text{CO}/\text{CO}_2 = \infty$ were the possible boundaries of the ATR reaction space in the full range of combustion to steam methane reforming. He stated that the reaction space is independent of conversion, steam to carbon ratio, pressure, temperature, heat loss and assumption of equilibrium. Heat loss and higher pressure have inhibitory effect on the hydrogen-to-methane feed, shifting to a maximum hydrogen production with higher O_2/CH_4 feed. Hydrogen production increased with decreasing levels of oxygen in the reactor with pressure giving an inhibitory effect. Also, Hagh demonstrated that the rate of change of maximum hydrogen yield with respect to inlet feed temperature was dependent on S/C. He suggested that in cases where the ATR feed is pre-heated, inlet temperature and S/C may not be truly independent parameters and a higher inlet temperature may require lower S/C.

Ersoz et al. (19) was interested to maximize the hydrogen content while decreasing the carbon monoxide and methane formation. Their study presented the performance of the ATR of two different average molecular weight hydrocarbon fuel mixtures, one lower molecular weight hydrocarbon (LHCM) and one higher molecular weight hydrocarbon (HHCM), with no sulphurous compounds under several operation conditions. LHCM was composed of 33.6% of hexane (C_6H_6), 28% hexene (C_6H_{12}) and 38.4% xylol, similar to gasoline and with a average molecular weight of 95 kg/kmol. The HHCM chosen was $C_{12}H_{26}$ with a molecular weight around 200kg/kmol. Also, they calculated the efficiency of the fuel processor defined as the ratio of the lower heating value (LHV) of the total hydrogen produced to the LHV of the hydrocarbon fuel fed into the reformer. A simulation software named HYSYS was utilized for simulations and calculations of the fuel processing reactions. Ersoz agrees with Hagh that the thermodynamic equilibrium in a reforming reaction depends on several parameters such as: (1) chemical composition of the fuel, (2) preheat temperatures of the reactor feed air, steam, and fuel, (3) relation of S/C and O/C ratios, (4) heat loss/gain of the reactor, and (5) pressure inside of the reactor. The primary operating variables selected were fuel composition, temperature of the preheated air-steam-fuel mixture, S/C and O/C ratios and reforming temperature. The pressure was constant at 3 bar. Although a catalytic reaction was not analyzed, a wide ratio of S/C was selected (2.0-3.5) to see the effect on H_2 yield, because lower S/C ratios favor soot and coke formation, which is not desired in catalytic operations. The results of these investigators showed very similar behavior for the LHCM and HHCM fuels. They concluded that the major operational parameters that

affected the reformat gas composition were O/C and S/C ratios, and the process temperature. They found that increasing O/C ratios decrease hydrogen and carbon monoxide formation. Hydrogen production was almost diminished above a certain O/C ratio. This effect was observed at lower O/C ratios for LHCM. The effect of S/C on hydrogen was more pronounced at lower O/C values. An increase in S/C ratio favored hydrogen formation and CO formation was depressed especially at higher operation temperatures. The results indicated that there should be an optimum temperature and S/C and O/C ratios for a given fuel. The selection of the right operation parameters was very important in terms of the efficiency of the reactor. They concluded that the difference observed for both fuels were due to their different molecular structures.

2.3 Argonne National Laboratory (ANL) (41)

In the late of 1980's, the U.S. Department of Energy (DOE) had a program to build a fuel cell bus. ANL was working in the catalytic conversion of gasoline to hydrogen inside a solid oxide fuel cell and General Motors Company (GM) realized that developing a fuel cell system was going to be very expensive and considered the partnership with the government. In spring 1999, four ANL researchers (S. Ahmed, R. Kumar, M. Krumpelt and R. Sutton) received the Partnership for a New Generation of Vehicles (PNGV) Medal for their work for trying to make fuel cell vehicles a reality.

Kumar and Ahmed recommended catalytic partial oxidation reforming for a faster, lighter and smaller processor compared to that used for conventional steam reforming. DOE began to contract with this industry to create and develop fuel processors for methanol, ethanol and gasoline. Finding the right catalyst to promote the

hydrogen conversion at significant lower temperatures was an enormous challenge to them and, eventually, they discovered a catalytic material that was successful in the hydrogen production of gasoline. In 1996, ANL showed a catalytic methanol processor that generated 5kW of electricity. By 1997, they developed a bench-scale reformer to produce hydrogen from commercial gasoline and natural gas. Switching to a new catalyst made a big difference, the processor could be very compact and the automobiles could have rapid startups. For example, a steam reformer designed by GM to produce 30kW is about 80-100L, however, ANL developed a device of 20L to generate 25kW using their own catalyst.

Many investigators have developed fuel cell systems using hydrogen for powering homes and vehicles, but this gas is not yet convenient to use as a fuel. ANL developed a reactor that can be used as a “transition technology” until H₂ is readily available. This reactor can reform many hydrocarbon fuels, making it a “fuel flexible device”. That means that fuels such as gasoline, methanol, and natural gas can be reformed to a hydrogen-rich gas for use in fuel cells. The fuel processor is inexpensive, easy to manufacture and uses a process similar to that used in the catalytic converter in the automobiles. The process consisted of a first stage of mixing the vaporized fuel with air and sent to a partial oxidation catalyst packed cylinder. Hydrogen is released to feed the fuel cell at temperatures that are hundred degrees lower than in conventional processes. The catalyst used is one created by ANL based in a combination of selected metals and an oxygen conducting ceramic material. The carbon monoxide produced by this reforming process is converted to carbon dioxide and more hydrogen when passes

through the second stage catalyst (in a water-gas-shift reactor). Finally, a cartridge absorbs sulfur (another component that can damage the performance of the fuel cell) if it is present in the hydrocarbon fuel. This step ensures the reliable, long-term fuel cell operation.

Autothermal reforming is commonly carried at temperatures higher than 1,000°C in industrial process (40) and the necessity of having a catalyst that can fulfill the requirements of accomplish the size, weight and cost for automotive applications is very difficult. Also, the reactions that involve hydrocarbons with larger chains need large amounts of steam to keep the catalyst cleaned and avoid coke fouling. For a practical automobile processes, it is necessary to reduce this amount of water on board. An important challenge is to find alternative materials for fuel reforming catalysts (5). Then, their effort has been focused in synthesizing new catalysts with the purpose to convert fuels, including gasoline, to a hydrogen-rich product at lower temperatures (enables the use of inexpensive materials) and lower steam requirements. Their new catalysts contain either noble metals or non-noble transition metals bonded to an oxide ion conductor substrate, such as ceria, zirconia and lanthanum gallate. Catalysts known as “noble metals” such as platinum and rhodium are preferred due to their ability to resist oxidation. However, these metals are very expensive and identifying more affordable options could make the ATR option to be more commercially viable. Non-noble metals (nickel, copper, cobalt and iron) when bonded to a substrate are more active than expensive noble-ones at temperatures lower than 700°C. The hydrogen production has shown to be of high quality with these non-noble catalysts. But, the platinum containing

catalysts are very resistant to sulfur, a contaminant that is present in the fossil fuels. The first and second row transition elements in combination with each other are very effective in the autothermal reforming of methane or isooctane.

2.3.1 Polymer Electrolyte Membrane (PEM) Fuel Cells

The **Polymer Electrolyte Membrane (PEM) Fuel Cell** is the most promising in transportation applications of the “green” fuel cell technologies for the investigators in Argonne (39). A PEMFC is attached to a fuel processor which converts a hydrocarbon fuel from an onboard fuel tank. This processor produces hydrogen-rich gas required to operate a PEM fuel cell properly. In 2001, ANL developed and patented a catalyst for the process that involves gasoline as a fuel for PEMFC processors (40). This catalyst was capable to convert a mixture of gasoline, air and water into a hydrogen rich gas product and convert it at 700°C. The product stream also has some byproducts of carbon monoxide and carbon dioxide and traces of sulfur. The carbon monoxide is converted to more carbon dioxide and to additional hydrogen, while the sulfur goes to a replaceable cartridge where it is removed. The hydrogen is sent to the PEM fuel cell to make electricity for the electric motor that “drives the wheels”. The Argonne’s major objective with the processor is to reduce vehicle to near-zero emissions for a better environment and to reduce the United States of America dependence on imported oil.

ANL (1) also has developed a catalytic reactor that can be used in powered fuel cells light-duty vehicles based on partial oxidation reforming or autothermal reforming. This ANL reformer uses a catalyst in their processes because it helps to give a lower temperature operation with a greater selectivity. The reactor built by these researchers is

a bench-scale autothermal reformer and is tested with methanol fuel at various fuels, water and oxygen (as air) feed rates. Methanol was chosen due to its advantages as a fuel such as being liquid, easy to reformate, low boiling point, water soluble, etc. They used gasoline too as a fuel because of its existing infrastructure. Since this fuel is a blend of different hydrocarbons it is more difficult to convert to hydrogen and carbon dioxide. Thus, it is necessary to build a catalyst capable of reforming all different type of hydrocarbons is obvious. The catalyst has to be selective to hydrogen and carbon dioxide and inhibit coke and methane formation due to side reactions.

In addition, ANL had been used a micro-reactor apparatus where the desired temperature was attained placing a tube furnace inside it, and 2g of catalyst that consisted of a substrate (participates in the oxidation of the carbon) and a promoter (participates in the dehydrogenation of the hydrocarbon). They demonstrated that a 1.8L reactor can generate hydrogen with a LHV of 12.6kW when the fuel used was methanol (higher values were obtained after converting CO to CO₂ and additional hydrogen in a water gas shift reactor). The product gas composition from this process typically contains over 50% hydrogen and less than 1% carbon monoxide. These results were obtained with a methanol rate of 56mL/min and an oxygen to methanol ratio of 0.27.

ANL also compared their catalyst to commercial catalysts for isooctane reforming. Using a feed of water and a feed of oxygen to octane ratio (x) equal to 4, their catalyst produced over 50% of hydrogen at 600°C while the other catalyst produced only 30%. The ANL catalyst tested other hydrocarbons such as toluene, pentene, cyclohexane

and ethanol showing to be active above 500°C. The hydrogen selectivity, defined as the theoretically percent available hydrogen at the value of x given, was always over 80%.

They had synthesized a similar catalyst to reform gasoline which was obtained from a local gas station. The product gas analyzed contained 60% hydrogen, 19% carbon dioxide, 18% carbon monoxide and 3% methane at 760°C. When air is used as a source of oxygen, lower values will be obtained because of the dilution effect of nitrogen as an inert. In the short term tests, the gasoline components had completely converted to hydrogen rich gas at 800°C and a gas hourly space velocity of 15,000/h. Conversions were over 95% under these conditions. Aromatic compounds (trimethylbenzene and toluene) require higher temperatures than olefins (1-octene). Olefins require higher temperatures than naphthenes (methylcyclopentane and methyl-cyclohexane) which require higher temperatures than straight chain and branched paraffins (n-octane and isooctane). The hydrogen production for trimethylbenzene decreased dramatically from 0.8L/mL of fuel + water to 0.15L/mL of fuel + water, when the reactor temperature decreased from 800°C to 600°C. This gasoline compound showed sensitive changes to space velocities because the hydrogen yield dropped when the space velocity was increased from 15,000/h to 75,000/h.

Gasoline blends containing 20% aromatics were reformed for more than 1,000 hours (long-term experiments) with start-up and shut down cycles and there was not any evidence of coke formation. The hydrogen production was about 35% and decreased about 5% after 1,000 hours of operation. The percentages of CO and CO₂ were 15% and 10%, respectively. To test their catalyst from sulfur content in some hydrocarbons, they

used reforming fuels with benzothiophene to obtain sulfur levels of 50, 300 and 1,000ppm by weight. The hydrogen production was higher than the fuel sulfur-free ones (39% to 34%) at short and long terms. When a commercial nickel catalyst was used for autothermal reforming process, hydrogen production decreased in comparison with ANL catalyst that did not show this behavior and demonstrated to be resistant to sulfur and coke formation.

ANL had performed several studies in micro-reactors (4) using different types of fuels such as isooctane, toluene, 2-pentene, ethanol and methanol. In these experiments, the oxygen feed rate was adjusted so that the oxygen to carbon ratio was 1. The water rate was maintained to provide a water to carbon ratio greater than 1. The next table (2.3) shows the fuels studied, the maximum conversion temperature and the hydrogen, CO and CO₂ percentages obtained for each one of the fuels. The last three columns of the gases represent the percentages that would exist at equilibrium at these temperatures. It can be seen that the experimental values for H₂ and CO are higher than the values that can be obtained at equilibrium. Using their catalyst, conversions at less than 700°C were achieved. The same hydrogen production results obtained for gasoline (60% at 760°C) was again obtained.

Table 2.3. Experimental product gas composition compared with equilibrium compositions at ANL feed mixture.

Fuel	Temperature (°C)	Experimental (%, dry, N ₂ -free)			Equilibrium (%, dry, N ₂ -free)		
		H ₂	CO	CO ₂	H ₂	CO	CO ₂
Isooctane	630	60	16	20	57	20	19
Toluene	655	50	8	42	49	23	26
2-Pentene	670	60	18	22	56	21	21

Ethanol	580	62	15	18	62	18	16
Methanol	450	60	18	20	60	19	17

Based on the composition of the gasoline and the oxygen to fuel ratio was estimated that the maximum achievable hydrogen percentage is 67%. The catalyst was tested once more; no deactivation occurred after 40 hours and demonstrated to be sulfur tolerant. Experiments with natural gas and diesel were performed and both fuels had been tested to be reformed at 800°C.

Also, Argonne has designed a scale bench-reactor to study their catalysts under more realistic operating conditions reforming isooctane fuel. This reactor consists of a cylindrical tube filled with 1.7L of the ANL catalyst pellets. An electrically heated coil gives immediate ignition and the gases flow down the catalyst bed and exit at the bottom. These gases are analyzed using an on-line gas chromatograph. At the beginning of the experiments, the hydrogen production was over 45% due to the low fuel flow rate of 16mL/min. Carbon monoxide and carbon dioxide were at 16% and 6%, respectively. As the processing rate and the air to fuel ratio were increasing, the production of hydrogen and carbon dioxide decreased and the CO levels increased. This behavior could be attributed to the possibility of the combination of the very high feed rates and, consequently, the reduced residence time in the catalyst. The methane level was almost constant at 0.6% and the CO₂/CO dropped from 3 at the start to 2 near the end of the experiment.

Gasoline and natural gas were used as fuels in this reactor. The gasoline, water and air feed rates were 22mL/min, 24mL/min, and 45mL/min, respectively. The product

gas contained 38% H₂, 12% CO₂ and 10% CO. The gas is sent to a water-gas-shift reactor (WGS) and the hydrogen percentage could increase to 43%. With isooctane, gas compositions of hydrogen and CO₂/CO higher than gasoline were obtained because of its lower H/C ratio in gasoline. The autothermal reformer produced from gasoline 40mL/min of hydrogen, sufficient to operate a 3kW fuel cell stack.

The natural gas experiments were performed with feed rates of 6L/min of fuel, the water feed rate was 8mL/min and air was maintained at 14-17mL/min. There was a hydrogen production of 45%, 6%CO, 14%CO₂, and nearly 5% of unreacted methane when a low oxygen to fuel ratio was operated. As this ratio was increased, the temperature also increased, improving the methane conversion. Hydrogen and CO₂ decreased and CO increased. Like gasoline, these results are partly due to the lower residence time resulting from the increased air feed rate; and the presence of nitrogen resulted in a greater dilution of the product gases.

Other Argonne's combustible of interest for the PEM Fuel Cell is diesel. Reforming diesel fuel could bring several problems related to degradation of catalysts over time because the nature of the fuel (47). Diesel typically has a higher fraction of sulfur than other fuels and many of the causes of degradation include poisoning of catalysts by sulfur. Startup and shutdown thermal cycling leads to thermal shock, and an extensive coke formation that could deactivate the catalyst because of the low hydrogen to carbon ratio and high molecular weight of diesel. High temperatures improve conversion (better system efficiency), but reduce material stability. Three-diesel type fuels were tested with an Argonne's catalyst in a 0.41cm ID tubular reactor within a tube

furnace: hexadecane, certified low-sulfur grade 1 diesel, and a standard grade 2 diesel. The autothermal catalyst was prepared at ANL in a monolithic form and was placed in a tubular reactor within tube furnace. At the top of the reactor, the fuel and water were fed, vaporized and mixed with the incoming oxygen and nitrogen (used as an internal standard). The reactant stream was passed over the catalyst, and the hydrogen-rich gas products were analyzed with a gas chromatograph (GC). Also, an infrared detector was used to continuously measure the carbon monoxide concentration in the product exit from the water-gas shift beds. In addition, water-gas shift catalysts (see section 2.3.3) were fabricated as extrudates, and commercial zinc oxide and iron-chromium oxide catalysts were obtained from United Catalysts, Inc., for sulfur removal and high temperature shift, respectively.

Since the diesel fuel is of a complex nature (several hundred separate components have been identified), a complete chemical breakdown of the fuel was not feasible. After some analyses, they showed that grade 1 diesel was significantly richer in alkanes than the grade 2 diesel. Grade 2 is significantly richer in aromatic compounds, particularly naphthalenes and naphthene benzenes. Because of these differences in composition, the hydrogen yields obtained with the reforming catalyst were different too. Grade 2 diesel yielded a greater fraction of hydrogen in the product, although it has lower hydrogen to carbon ratio (hydrogen poor). They concluded that maybe aromatics are easier to reform than cyclic aliphatics.

With a water to carbon ratio of 1.25 and an oxygen to carbon ratio of 1 used to perform the experiments, they found that at thermodynamic equilibrium, the formation of

hydrogen was maximized close to 700°C. These results are comparable to those obtained for hexadecane, where the hydrogen fraction in the product at this temperature was 57% on a dry, nitrogen-free basis. The methane formation increased and the hydrogen yield decreased when the temperature was reduced. Reforming a certified low-sulfur diesel fuel at a water:fuel ratio of 20 and oxygen:fuel ratio of 8, showed an hydrogen production to be at its maximum value at 875°C. ANL stressed that this temperature was higher than that obtained with hexadecane because using a similar O:C and water-to-fuel ratios, hydrogen production was maximized at 800°C with a product hydrogen (on a dry, nitrogen-free basis) of 60%. For the certified fuel, the average hydrogen fraction in the product at 840°C was 46%, while at 880°C it was 50%. These values are higher than Pereira's data of the same fuel (47), but are lower than the ANL results obtained for grade 2 diesel where there was 52% hydrogen product at 850°C.

The composition of the product effluent from diesel reforming was also examined as a function of GHSV, oxygen:fuel ratio and water:fuel ratio. Reducing the oxygen feed rate from 8 to 6 O₂ per mole of fuel, with a water:fuel ratio of 20, resulted in a much greater variety and larger fraction of hydrocarbons in the product stream such as aromatics. A greater fraction of the hydrocarbons was not cracked or oxidized effectively with less oxygen in the feed. Increase in coke formation was observed with an increase in pressure drop. Methane was the most hydrocarbon present at 840°C with a oxygen:fuel ratio of 8 and a water:fuel ratio of 20 and no increase in pressure drop was observed. The GHSV was varied from 2,000 to 10,000/h at 840°C and from 2,000 to 4000/h at 880°C. There was not significant changes in the product distribution over the

range of space velocities tested; therefore, the reformer hydrogen yield in the product gas should be reasonably consistent over this range of diesel fuel. When the water:carbon ratio was increased from 1 to 2, at a constant oxygen:fuel ratio of 8, the hydrogen yield increased. With lower water:fuel ratios, as observed with oxygen, the coke or soot formation increased due to the increase in pressure drop across the reactor. The catalyst did not show evidence of coke formation, although soot deposits were observed in the reactor above the catalyst bed. Analysis with gas chromatography, demonstrated that a greater fraction and mixture of hydrocarbon products were observed at lower temperatures, as observed too for low oxygen:fuel ratios.

The researchers of ANL had developed a monolithic catalyst of a composition like the extruded form, but with a microchannel form. When the temperature was increased from 850°C to 900°C at 10,000/h in the reactor packed with this catalyst, the hydrogen yield increased from 50 to 55%. This microchannel monolith can reduce the size of the diesel reformer, maintaining or improving the hydrogen yield over a packed bed system. Since microreactor tests are much more rapid and permit to determine better the operating conditions for a large-scale unit, they are studying an entire diesel fuel process by connecting the reformer microreactor with a series of sulfur and carbon monoxide scrubbers that consist of a sulfur removal bed, high temperature shift (HTS) and low temperature shift (LTS) beds and a preferential oxidizer. This process is similar to the 5 kW(e) unit, but it is much more flexible (reactor configuration and feeds can be made quickly). They sent a portion of the hydrogen-rich gas product from the reformer microreactor through a sulfur scrubber and the HTS and LTS beds. The carbon

monoxide content was reduced of the reformat from 20% to less than 2% on a dry basis with the two water-gas shift reactors and sulfur, as H₂S could not be measured with on-line instruments.

2.3.2 Water-Gas Shift (WGS) Catalysis (6)

Argonne National Laboratory has worked with the reduction of CO in the reformat product. Depending on the fuel and the reforming process used, the CO content could be up to 16% by volume. If the product contains at least 100 ppm of CO, the performance of the PEM fuel cell is severely degraded and is necessary to reduce its concentration to lower traces. Current fuel processors have two-step catalytic process where CO is reduced to 1% using WGS reaction ($\text{CO} + \text{water} = \text{CO}_2 + \text{H}_2$) and then reduced to less than 100 ppm using preferential oxidation (PrOx) of CO. The industrial chemical processes currently use iron-chrome oxide and copper-zinc catalysts. The first one operates at temperatures of 300°C to 450°C and it is referred to as the high-temperature shift catalyst (HTS); copper-zinc catalysts operate at temperatures of 160-250°C and are known as the low-temperature shift (LTS) catalyst. These catalysts have several disadvantages, and one of them, is that they have to be reduced in H₂ prior to the exposure to the fuel gas and cannot be exposed to air in the reduced state. Transportation systems have highly intermittent duty cycle and size/weight constraints, so a good catalyst must be capable of eliminate the need to activate it “in situ”; eliminate the need to sequester it during system shutdown; increase tolerance to temperature excursions; and reduce the size and weight of the shift reactors.

ANL has investigated bifunctional catalysts for WGS reactions where one component of them could adsorb or oxidize CO and the other component dissociates water. They believe that metal support combinations could promote this mechanism. Platinum, rhodium, palladium, PtRu, PtCu, Co, Ag, Fe, Cu and Mo are examples of the metallic components chosen to adsorb CO at intermediate adsorption strengths. A mixed-valence oxide with redox properties or oxygen vacancies under the highly reducing conditions of the fuel gas was chosen to adsorb and dissociate water. The researchers at this laboratory developed a copper/oxide catalyst with the same activity as the commercial copper-zinc oxide catalyst. The ANL catalyst can operate above 250°C without deactivation and retains its activity after exposure to air at 230°C, making it feasible to be used in both LHT and HTS stages. This catalyst demonstrated to reduce dramatically the size and weight of the HTS stage since it has higher water-gas shift activity than the iron-chrome catalyst. The LTS stage could run at a higher temperature inlet (300°C rather than 200°C with copper/zinc oxide) because of the copper/oxide catalyst temperature stability. The size and weight of this stage could be reduced too, due to its improved kinetics afforded by a higher operating temperature.

For the near to mid terms the ANL team is continuing to work on reforming gasoline, diesel and other types of hydrocarbons. Robert Sutton, a member of ANL, believes that the automakers will initially favor methanol in this country: “In the years after 2010, the focus may shift to a fuel processor based on an infrastructure that is readily available here...some type of distillate or gasoline-based fuel. Both DaimlerChrysler and GM have run methanol-fueled cars and demonstrated them at auto

shows. I think the goals that the automobile companies have set for a pre-production prototype by 2004 are reasonable” (41). Fuel cell processors for fuel cell systems that are based in autothermal reforming have many advantages over steam reformers by not requiring any indirect (through a wall) heat transfer. These processors are compact and lightweight as well as suitable for power systems that require quick-starting and load-following capabilities (4). These facts make ANL to continue in its research for the next five years to find materials and processes that will make the reformer even smaller, lighter and faster.

3. EXPERIMENTAL METHODS AND APPARATUS

The main objective of this study was to establish the feasibility of using a new platinum based catalyst provided by Argonne National Laboratory to convert methanol and isooctane, to a hydrogen-rich product gas to be fed to fuel cells in automobile applications. In this chapter, the materials, equipment, and methods that were used to accomplish the objectives will be discussed. The first section describes the materials and equipment used; the second section mentions the analytical method used for the determination of coke and hydrogen composition in the product gas; the third section describes the procedure; and in the last section the statistical experimental design used will be presented.

3.1 Materials and equipment

3.1.1 Materials and reagents

Anhydrous methanol and isooctane (HPLC grade) were purchased from Fisher Scientific (Cayey, Puerto Rico). Oxygen ultra high purity (99.99%), hydrogen ultrahigh purity (99.99%) and nitrogen high purity gases were supplied by Linde (Hormigueros, Puerto Rico).

The catalyst used in this investigation was supplied by Argonne National Laboratory. It is a Pt-based catalyst, but its physical and chemical characteristics are confidential nature. It consists of a substrate which participates in the oxidation of the carbon, and a promoter which dehydrogenates the hydrocarbon fuel. Figure 3.1 shows a picture of this catalyst.



Figure 3.1. ANL Pt-based catalyst

3.1.2 Equipment

A stainless steel bench-scale basket stirred tank reactor (BSTR) Model 4575 with a total capacity of 500mL and a temperature range up to 500°C was operated at

atmospheric pressure and used to perform the reforming experiments (see Figure 3.3). Figure 3.2 shows the jacket around the reactor that minimizes heat losses during reaction. Also, it shows part of the system, including gases flow meters (rotameters), thermo-par selector, rheostats, coil heating tapes, condenser, and a flash drum. Figure 3.5 shows the whole system with pump drives and temperature controller. Two Masterflex L/S peristaltic pumps #7524-50 were used to feed the reactants (fuel and water) to the reactor at a desired volumetric flux. Master Flex tube #96410-16 and a Master Flex tube #6412-14 were used for the water and the fuel to the reactor, respectively. The oxygen and nitrogen volumetric flux were controlled by rotameters with a flowrange from 0 to 1,709 ccm supplied by Cole Palmer. A temperature measurement board (TMB), also supplied by Cole Palmer, was used to measure the temperature of each stream. Two voltage controllers, with a maximum load capacity of 115V, were used to control electric power to the coil heaters (heating tapes) to heat the oxygen and nitrogen streams. These heating tapes are covered with Zetrix insulator and have a maximum temperature exposure of 900°F.

The reagents stream gases entered the BSTR, which contained 2g of the catalyst inside a basket (Figure 3.4), through 1/16-inch stainless steel tubes. The products were cooled using a condenser equipped with a serpentine, which permitted the re-circulation of water from a constant bath temperature at 11°C. After the products were cooled at 11°C, they entered to a flash drum where both liquid (bottom exit) and gaseous samples (top exit) were separated and analyzed. The gas product was sampled with a 1 mL gas-tight chromatography syringe (Microliter Gas-tight Syringe #1001 1mL). The liquid

product was analyzed by density for methanol concentration using picnometers of 10mL (Fisher Scientific, Cayey, PR).



Figure 3.2. The Bench Stirred Tank Reactor (BSTR) system.



Figure 3.3. BSTR without the insulator



Figure 3.4. Catalyst Basket



Figure 3.5. The BSTR system including the peristaltic pumps and the temperature controller.

3.2 Analytical analysis

3.2.1 Gas chromatography analysis

Gas chromatography was used to evaluate the composition in the product gases obtained from the autothermal reforming reaction. Specifically, hydrogen, oxygen, carbon monoxide, methane and carbon dioxide were analyzed. Analyses were performed using a Hewlett Packard 5890, Series II Gas Chromatograph coupled with a Thermal Conductivity Detector (see Figure 3.6). The capillary column used was a ViCi GC

Valcobond with a solid phase of Molecular Sieve 5A, a length of 30m, a film thickness of 15 μ m, an upper temperature limit of 350°C, and an internal diameter (ID) of 0.53mm.

For the reactor exit gas composition analyses, the GC-TCD injector temperature was set to 155°C and the detector temperature was 200°C. The oven temperature was held at 100°C for the first 5 minutes during the run of every analysis. After that, the oven temperature was programmed to increase from 100 to 200°C at 20°C/min, and then was held at 200°C for 12.0 min. The total analysis time was 22.0 min. Helium was used as the carrier gas because of its high difference in thermal conductivity with the gases under analysis. A flow rate of 30.0mL/min and a backpressure of 500 kPa (72psi) of carrier gas were used. One milliliter samples were injected manually with a syringe (Microliter Gas-tight Syringe #1001 1mL; Hamilton Co., Nevada). The injector septa (Alligent long life 11mm) used was changed at the beginning of each experiment. After the end of the day, the oven temperature was raised to 300°C for 15 minutes to eliminate impurities and humidity that could interfere in the future chromatograms results.



Figure 3.6. Gas Chromatograph-TCD with the Integrator

3.3 Procedure

The autothermal reforming process was studied with two types of fuels at atmospheric pressure. In addition, seven different temperatures and three water to carbon and oxygen to fuel ratios were chosen. In section 3.4, a detailed description of the experimental design is given.

The procedure consisted in turning on the reactor temperature controller and giving it the desired temperature set point. The oxygen rheostat, used to heat the reagent streams, is turned on to allow the heating tape to achieve a coil temperature of approximately 300°C. The nitrogen rheostat and flowmeter are turned on to purge the system with a volumetric flow rate of 387 cm³/min. during 15 minutes. After this time, the nitrogen rotameter and its heating tape were turned off. The oxygen rotameter and the water and fuel pumps were turned on simultaneously at the respective desired flows (see section 3.4).

Once the reactants were fed, the reactor temperature was maintained at the setpoint with a temperature variation range between -10°F to +10°F. In previous experiments, it was demonstrated that the controller could be successfully “controlled” within this temperature range by turning on and off the heater (see Appendix A). The exit gas products from the BSTR were passed through a condenser connected to a temperature bath, which recirculated cooling water at a constant temperature of 11°C. At the top exit of the flash drum, the gases that were previously condensed separated in liquid and gas phases. The liquid product at the bottom exit was collected in a flask and a density analysis was performed to determine its composition.

Before the gas sample was analyzed, the bottom valve of the flash drum was closed and the top valve was opened. The gas sample was permitted to flow by approximately one minute to ensure a purging of the sample point. Then, 1mL gas samples were taken with a 1mL gas chromatography syringe and injected to the GC-TCD. The samples were taken and injected every half hour to let the chromatogram run and stabilize itself before another injection.

The duration of each experiment was approximately 4.5 hours at a constant temperature with a variation range between -10°C to $+10^{\circ}\text{C}$. This time is acceptable because preliminary experiments showed that the hydrogen production stabilized quickly and it allowed taking at least five (5) injection samples (see Appendix C.3). With the HP Integrator, it was possible to determine the desired gas concentrations such as hydrogen, oxygen, methane, carbon monoxide, and carbon dioxide. The integration area could be easily converted in volume percentages using the calibration curves (see Appendix B). The calibration curves were done injecting several amounts (0.10, 0.20, 0.30, 0.40, 0.50, 0.60, 0.70, 0.80, 0.90 and 1.0 mL) of each of the gases mentioned above. Each gas had a purity of almost 99.999%. The value of the integration value was plotted vs. its volume percent (i.e., $(0.10\text{mL}/1.0\text{mL}) * 100$).

3.4 Experimental Design

The objective of this experimental design was to investigate the effects of the reaction temperature, fuel type, water to carbon ratio, and oxygen to fuel ratio. A quantitative analysis was used to determine, in the range studied, the better conditions where methanol achieved the maximum hydrogen production and minimum side

reactions (carbon and methane formation) were not observed. In addition, a brief study of isooctane was made to see if there was some hydrogen production at the conditions studied.

Seven different temperatures were selected: 300, 400, 500, 600, 700, 800 and 900°F. These temperatures were chosen because in previous experiments done by ANL, hydrogen production reached its maximum achievable concentration in equilibrium (60%) near 900°F. Also, the effect of temperature on hydrogen production was studied. Experiments over 900°F were not considered due to the equipment limitations. Methanol and isooctane were the fuels studied. For methanol and each reaction temperature, a 3² design experiment with one replicate was considered. For isooctane, a few experiments with set water-to-carbon and oxygen-to-fuel ratios and temperatures were performed.

The H₂O/carbon ratio and the O₂/fuel ratio were evaluated at three levels each one for methanol and reaction temperature. The levels of the oxygen to fuel ratio (x) considered were 0.27, 0.39 and 0.50 for methanol. The partial oxidation autothermal reaction is thermally neutral at $x = 0.23$ at 25°C (see figure 3.7); over this value will be exothermic. The value of x should not be higher than 0.5, since no water will be reacting and the autothermal reaction will not occur. The O₂/methanol ratio of 0.27 corresponds to the ratio studied by ANL investigators, where maximum hydrogen production was observed (near the thermoneutral level at 25°C) (1). A ratio in the exothermic range of 0.39 and the exothermic ratio of 0.5 were chosen as the other levels. The levels of water to carbon ratio were 0.46, 0.76 and 1.12. The level of H₂O/C ratio of 0.46 was the stoichiometric ratio corresponding to an O₂/fuel ratio of 0.27. ANL previous studies with

methanol emphasize that the used H₂O/C ratios were always greater than one (to suppress coke formation) feeding the fuel two times the volumetric flow of water. The fixed flow chosen for methanol was 3mL/min, thus, the water volumetric flow should be 1.5mL/min. This volumetric flow corresponds to the H₂O/C=1.12 ratio. The H₂O/C=0.76 is the middle value between 0.46 and 1.12 (see table 3.1).

The levels of the oxygen to fuel ratio (x) and water to carbon (ψ) ratio for isooctane considered at each one of the seven temperatures were 3.5 and 1.0, respectively. This reaction is thermally neutral at x = 2.94 at 25°C (see figure 3.7); over this value will be exothermic. Ahmed et al. used values of x between 0 and 4 (1). The 3.5 ratio was used due to the rotameter capacity. Other oxygen-to-fuel and water-to-carbon ratios were chosen randomly at 900°F to look if there was any hydrogen production (see table 3.2). After running these experiments with isooctane the same catalyst was used to perform at least one methanol replicate. This was done in order to know if the catalyst was deactivated because the production of hydrogen using isooctane as a fuel, in the range studied, was never observed or detected.

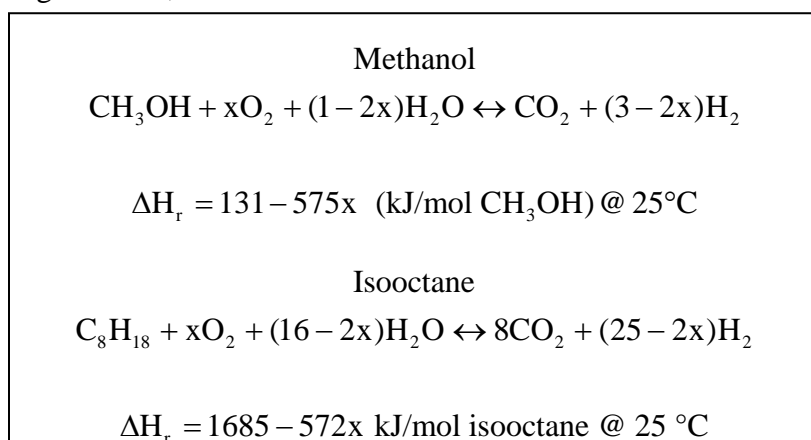


Figure 3.7. Methanol and Isooctane Overall Autothermal Reforming Reaction

Table 3.1. Variables studied in the autothermal reforming process at each temperature with methanol (300, 400, 500, 600, 700, 800 and 900°F).

Fuel	O ₂ /fuel	H ₂ O/C	Fuel Flow (mL/min)	Water Flow (mL/min)	Oxygen Flow (mL/min)
Methanol	0.27	0.46	3.0	0.61	489.07
	0.39	0.76	3.0	1.0	707.65
	0.50	1.12	3.0	1.5	907.24

Table 3.2. Variables studied in the autothermal reforming process with isooctane as a fuel

Fuel	Temperature (°F)	O ₂ /fuel	H ₂ O/C	Fuel Flow (mL/min)	Water Flow (mL/min)	Oxygen Flow (mL/min)
Isooctane	600	3.5	1.0	3.0	2.6	1,780.2
	700	3.5	1.0	3.0	2.6	1,780.2
	800	3.5	1.0	3.0	2.6	1,780.2
	900	3.5	1.0	3.0	2.6	1,780.2
	900	3.3	1.2	3.0	3.1	1,466.27
	900	3.5	3.0	3.0	7.9	1,780.2

4. RESULTS AND DISCUSSION

4.1. Experimental Design

The exit gas compositions of the reformat were analyzed based on the areas given by the Gas Chromatograph. Using the areas of each peak and the calibration curves it was obtained the volume percent (dry basis) of hydrogen, oxygen, carbon monoxide, methane and carbon dioxide at every level studied (see table 4.1). The levels of the oxygen-to-fuel and water-to-carbon ratios used for both methanol and isooctane are given below.

Table 4.1. Different levels of O₂/fuel and H₂O/C ratios studied with methanol as a fuel.

Level	O ₂ /fuel	H ₂ O/C	Fuel Flow (mL/min)	Water Flow (mL/min)	Oxygen Flow (mL/min)
00	0.27	0.46	3.0	0.6	489.07
11	0.39	0.76	3.0	1.0	707.65
22	0.50	1.12	3.0	1.5	907.24
01	0.27	0.76	3.0	1.0	489.07
02	0.27	1.12	3.0	1.5	489.07
10	0.39	0.46	3.0	0.6	707.65
12	0.39	1.12	3.0	1.5	707.65
20	0.50	0.46	3.0	0.6	907.24
21	0.50	0.76	3.0	1.0	907.24

It was necessary to calculate which volumetric flow rates were going to be used from each of the levels chosen. The densities (ρ) of the fuels and water were taken from Perry and Chilton (48). Example of the calculations for water and oxygen flows made for both fuels (methanol and isooctane) are as follows:

A. Methanol - it was fixed to 3mL/min:

$$MeOH \text{ volumetric flow} * MeOH \text{ density} * \frac{1}{MW_{MeOH}} = \frac{\text{moles}}{\text{min}} MeOH \text{ (fixed)} \quad (19)$$

$$3 \frac{mL}{\text{min}} * (0.791 \frac{g}{cm^3}) * \frac{1 \text{ mol}}{32 g} = 0.0742 \frac{\text{moles}}{\text{min}} MeOH$$

B. Water

For the overall autothermal reforming equation (0.46 H₂O/C ratio):



$$\frac{\text{water}}{\text{C}} \text{ratio} * \frac{1 \text{ mol C}}{1 \text{ mol fuel}} * \left(\frac{\text{moles fuel}}{\text{min}} \right) \text{MW}_{\text{water}} * \frac{1}{\rho \text{ of water}} \quad (21)$$

= volumetric flow of water

$$0.46 \frac{\text{moles water}}{\text{mol C}} * \left(\frac{1 \text{ mol C}}{1 \text{ mol CH}_3\text{OH}} \right) * \left(\frac{0.0742 \text{ moles CH}_3\text{OH}}{\text{min}} \right) * \left(\frac{18 \text{g water}}{1 \text{ mol}} \right) * \left(\frac{\text{cm}^3}{1 \text{g}} \right)$$

$$= 0.6 \frac{\text{cm}^3}{\text{min}}$$

C. Oxygen (For x = 0.27 O₂/fuel)

$$\frac{\text{moles Oxygen}}{\text{mol fuel}} \text{ratio} * \left(\frac{\text{moles fuel}}{\text{min}} \right) = \frac{\text{moles Oxygen}}{\text{min}} \quad (22)$$

$$V = \frac{nRT}{P} \quad (23)$$

$$0.27 \frac{\text{moles Oxygen}}{\text{mol MeOH}} \text{ratio} * \left(\frac{0.0742 \text{ moles MeOH}}{\text{min}} \right) = 0.02 \frac{\text{moles Oxygen}}{\text{min}}$$

$$V = 0.02 \frac{\text{moles Oxygen}}{\text{min}} * 82.06 \frac{\text{cm}^3 \cdot \text{atm}}{\text{mol} \cdot \text{K}} * \frac{298 \text{K}}{1 \text{atm}} = 489.07 \frac{\text{cm}^3}{\text{min}}$$

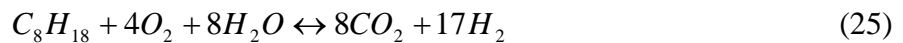
For isooctane, the same calculations for the O/C and H₂O/C ratios studied were performed (see Table 3.2):

A. Isooctane – it was fixed to 3mL/min.

$$\text{isooctane volumetric flow} * \text{isooctane density} * \frac{1}{\text{MW}_{\text{Isooc}}} = \frac{\text{moles}}{\text{min}} \text{isooctane (fixed)} \quad (24)$$

$$3 \frac{\text{mL}}{\text{min}} * \left(\frac{691.87 \text{kg}}{\text{m}^3} \right) * \left(\frac{1 \times 10^{-6} \text{m}^3}{\text{mL}} \right) * \frac{\text{mol C}_8\text{H}_{18}}{0.114 \text{kg}} = 0.0182 \frac{\text{moles}}{\text{min}} \text{C}_8\text{H}_{18} \text{ (fixed)}$$

For the overall autothermal reforming equation:



B. Water

Following equation 21:

$$\begin{aligned} & \frac{1 \text{ mol H}_2\text{O}}{1 \text{ mol C}} * \left(\frac{8 \text{ moles C}}{1 \text{ mol C}_8\text{H}_{18}} \right) * \left(\frac{0.0182 \text{ moles C}_8\text{H}_{18}}{\text{min}} \right) * \left(\frac{18 \text{ g H}_2\text{O}}{\text{mol H}_2\text{O}} \right) * \left(\frac{\text{cm}^3}{1 \text{ g}} \right) \\ & = 3.1 \frac{\text{cm}^3}{\text{min}} \end{aligned} \quad (26)$$

C. Oxygen

To verify the moles of oxygen required to have an O/C =1:

$$\left(\frac{1 \text{ mol O}}{1 \text{ mol C}} \right) * \left(\frac{1 \text{ mol O}_2}{2 \text{ mol O}} \right) * \left(\frac{8 \text{ moles C}}{1 \text{ mol C}_8\text{H}_{18}} \right) = 4 \frac{\text{moles O}_2}{\text{mol C}_8\text{H}_{18}} \quad (27)$$

Following equations 22 and 23:

$$\begin{aligned} & 4 \frac{\text{moles O}_2}{\text{moles C}_8\text{H}_{18}} * \left(\frac{0.0182 \text{ moles C}_8\text{H}_{18}}{\text{min}} \right) = 0.0728 \frac{\text{moles O}_2}{\text{min}} \\ & V = 0.0728 \frac{\text{moles Oxygen}}{\text{min}} * 82.06 \frac{\text{cm}^3 \cdot \text{atm}}{\text{mol} \cdot \text{K}} * \frac{298\text{K}}{1 \text{ atm}} = 1,780.2 \frac{\text{cm}^3}{\text{min}} \end{aligned}$$

After the experiments were performed as described in section 3.3, the exit gas composition from the flash drum was analyzed in order to determine the best variables combination. The compounds concentrations were calculated as described in section 3.2.1. Hydrogen production was reproducible at each temperature and was constant throughout the 4.5 hours of operating conditions studied, indicating that the catalyst was not deactivating during a run and the reactor was operating at steady-state conditions (see Appendix C.3). The desired gas exit concentration is when the hydrogen composition is close to the theoretical equilibrium value (~60%) and the minimal CO and CO₂ concentration are obtained (4.). Carbon monoxide composition is a known poison for

PEM fuel cell. For the variable range studied, the best combination was observed at level 11.

Appendix C.3 illustrates that at this condition ($O_2/\text{fuel} = 0.39$ and $H_2O/C = 0.76$) and 900°F can give a reaction product concentrations (dry basis) of 59.8% H_2 , 14.6% CO , and 12.6% CO_2 (see Appendix C.4 for chromatograms). In section 4.2 the effect of the different level combinations to the exit flash drum gas composition will be discussed.

In order to verify the reproducibility of the experiments, a replicate at level 01 at 900°F ($O_2/\text{fuel} = 0.46$; $H_2O/C = 0.76$) was performed after the first replicate was finished. Table 4.2 shows the results obtained from each one of the trials done. From this table, it can be observed that the experiments were reproducible, obtaining similar gas concentration with difference percents as low as 0.57%.

Table 4.2. Replicate at a $O_2/\text{fuel} = 0.46$; $H_2O/C = 0.76$ at 900°F .

Gas	Concentration (% , dry basis)		Difference (%)
	Trial 1	Trial 2	
H₂	52.6	52.9	0.57
O₂	16.0	16.1	0.62
CO	18.6	18.4	1.08
CO₂	12.1	12.5	3.25

Also, it is important to mention that at condition of $O_2/\text{fuel} = 0.5$ and $H_2O/C = 1.12$ (level 22) at 900°F , the reaction product concentrations (dry basis) were 58.5% H_2 , 20.4% CO , and 18.7% CO_2 (see Appendix C.4 for chromatograms). These concentrations

were very close to those obtained at equilibrium (60% H_2 , 19% CO , and 17% CO_2) by Ahmed et al. at the same temperature and feed conditions (4).

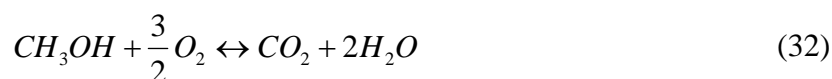
4.2. Reactor Exit Gas Composition, Methanol

In this section, a comparison will be given between the production of the reaction products of methanol reforming that would exist at equilibrium and the ones obtained experimentally at each one of the conditions studied. The equilibrium results were performed using a thermodynamic simulation program, and were provided by Dr. Theodore Krause, ANL (see Appendix E.1). The concentration of the products, H₂, CH₄, CO, and CO₂, includes the molar percent of water present at the reactor exit (before reaching the condenser). Also, it includes the moles of O₂ and methanol that did not react. For a more detailed explanation of the mass balance done for the system, see Appendix C.1.

Figures (4.1 to 4.9) show that the experimental and equilibrium curves have the same behavior for the product gases. The most notable difference is the absence of methane formation in the experimental results. Also, differences between experimental quantity produced and equilibrium compositions were observed. First, the water production observed experimentally was less than that at equilibrium, due to that the equilibrium calculations assumed the formation of methane. Methane is formed by the reaction of 1 mole of CO and 3 moles of hydrogen to produce 1 mole of methane and 1 mole of water (eq. 28). Thus, the formation of methane besides increasing the water composition at the exit reactor gas also decreases hydrogen and carbon monoxide compositions.



At low temperatures, the methane formation is favored increasing the water composition at temperatures less than 200°C. For example, at level 00 (Figure 4.1), at 300°F water concentration at equilibrium is 55%, while the experimental value was just 23%. The water curves, both at equilibrium and experimentally, coincide in the fact that the exit gas concentration decreases as the temperature increases. Figure 4.1 shows the water decreased at equilibrium from 55% to 37.3%, and an experimental decrease from 23% to 18.3%. Methane formation is not favored at temperatures higher than 300°C (572°F), causing a decrease in the equilibrium methane composition. In addition, at higher temperatures, water could be more consumed in the steam reforming reaction (endothermic, eq. 29) and was not anymore favored in the combustion reaction (exothermic, eq. 32).



Carbon dioxide is produced by the WGSR (eq. 31), by the combustion reaction (eq. 32), and by the steam reforming reaction (eq. 29). At lower temperatures, the CO₂ existence is attributed to WGSR and to the combustion reaction. After that, when the temperature rises, more carbon dioxide will be produced due to the steam reforming reaction. The CO₂ found experimentally was lower than that at equilibrium because the steam reforming reaction may not be occurring at the same level as expected by the equilibrium calculations. Figure 4.2 (level 01) demonstrates that at equilibrium and

900°F, the carbon dioxide concentration is 17.9% while the experimental concentration was 6.8%. At level 02 and 900°F (figure 4.3), CO concentration at equilibrium is 1.6% and experimentally was 8.5%. This means that most of the methanol was cracked (eq. 30) instead of reformed (eq. 29). That is why the experimental production of CO is higher than the equilibrium value. Another reason for the increase in the carbon monoxide composition is that CO is expected to react with hydrogen to produce methane and, as said before, methane was not seen experimentally. The exothermic reaction (eq. 32) is favored at low temperatures. The CO at equilibrium is not seen at low temperatures (before 370°C) because, besides for being consumed to produce methane, it is also consumed by the WGSR. At higher temperatures, it is produced by the cracking reaction mentioned before. Also, this explains why in the experimental results the CO concentrations were higher at low temperatures compared to those at equilibrium.

The experimental hydrogen composition found was greater than the one that would exist at equilibrium for all the experiments. Figure 4.4 (level 10) at 900°F shows that hydrogen concentration at equilibrium is 22.9% and experimentally was 32.8%. According to equation 28 is necessary to consume 3 moles of hydrogen in order to produce 1 mole of methane. These moles were not consumed and are reflected in its greater concentration in the exit gas than at equilibrium. Furthermore, since the steam reforming reaction is not occurring properly, most of the hydrogen production can be accredited to the cracking reaction as well. When a precious-metal based catalyst is used, these tend to promote decomposition rather than reforming, especially between 200-500°C (392-932°F) (unpublished data).

When the O_2 /fuel ratios were increased (leaving the H_2O/C constant), at low temperatures, hydrogen production rose considerably. Increasing the oxygen flowrate at the entrance of the reactor gave additional heat to the steam reforming and cracking reactions. Therefore, these reactions were more favored at lower reactor temperatures than if they were occurring without additional oxygen flowrate. Figure 4.1 shows that at an O_2 /fuel ratio of 0.27, the hydrogen product concentration at $204.4^\circ C$ ($400^\circ F$) was (wet basis) 2.3% H_2 . With an $x = 0.39$ (figure 4.4), the product concentration at $204.4^\circ C$ ($400^\circ F$), was 9.73%. The increase of carbon dioxide at low reactor temperatures, when more oxygen was added to the reforming systems, is attributed to the combustion reaction because it is favored to produce more CO_2 . As mentioned above, when x increases, more heat is added to the cracking reaction which produces CO . At an O_2 /fuel ratio of 0.27, and $900^\circ F$ the CO and CO_2 were 10.4% and 5.57%, respectively. When x was increased to 0.39 (figure 4.4), the product concentrations at $900^\circ F$ of CO and CO_2 were (wet basis) 13.0% and 8.5%, respectively.

If x remained constant and increased the water-to-carbon ratio, a slightly decrease in carbon monoxide at high temperatures was observed. With more water present in the reactor, the CO reaction to carbon dioxide is favored (WGSR). Figure 4.1, with a H_2O/C ratio of 0.76 and at $900^\circ F$, the concentration of CO found was 9.96%. At a H_2O/C ratio of 1.12 and at $900^\circ F$ (see figure 4.3), the concentration of CO found was 8.47%.

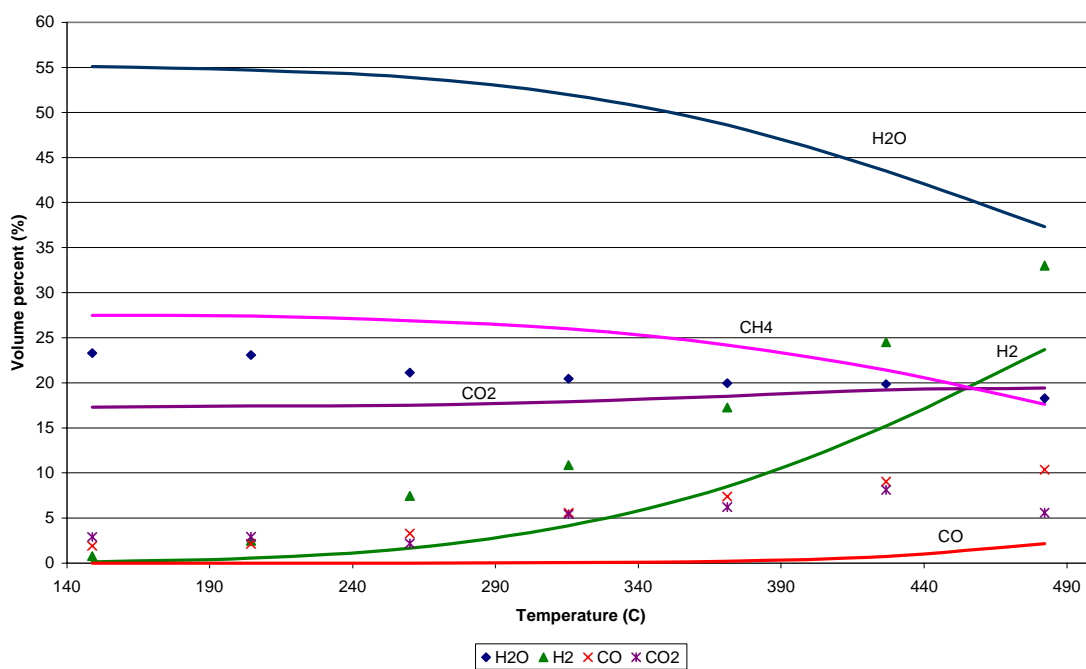


Figure 4.1. Reactor exit gas composition at $O_2/\text{fuel} = 0.27$; $H_2O/C = 0.46$ and different temperatures.

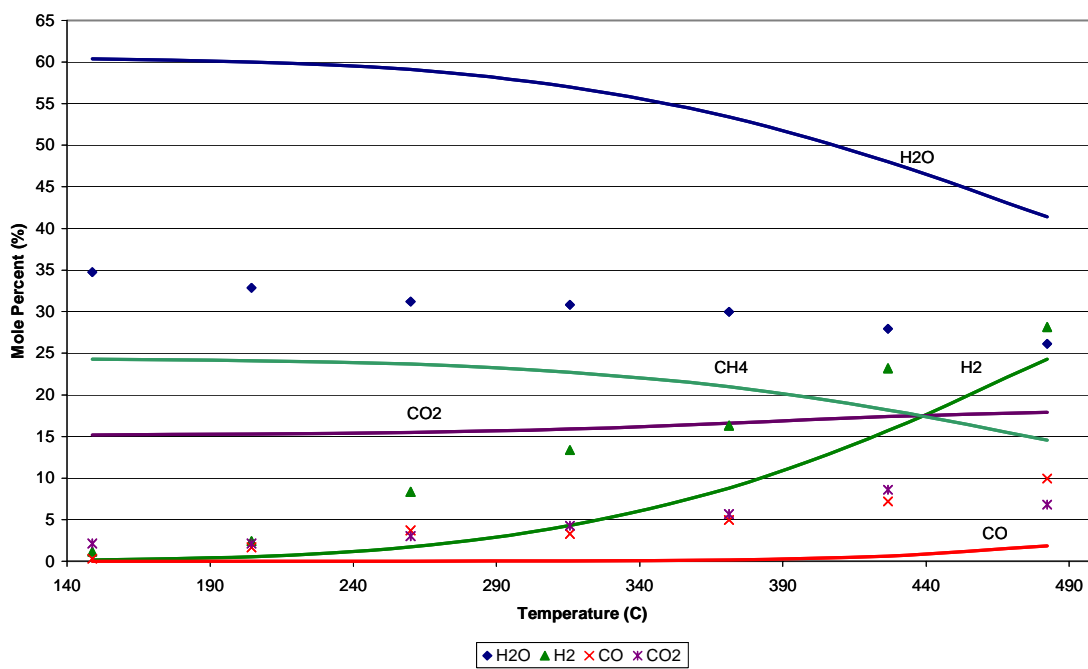


Figure 4.2. Reactor exit gas composition at $O_2/\text{fuel} = 0.27$; $H_2O/C = 0.76$ and different temperatures.

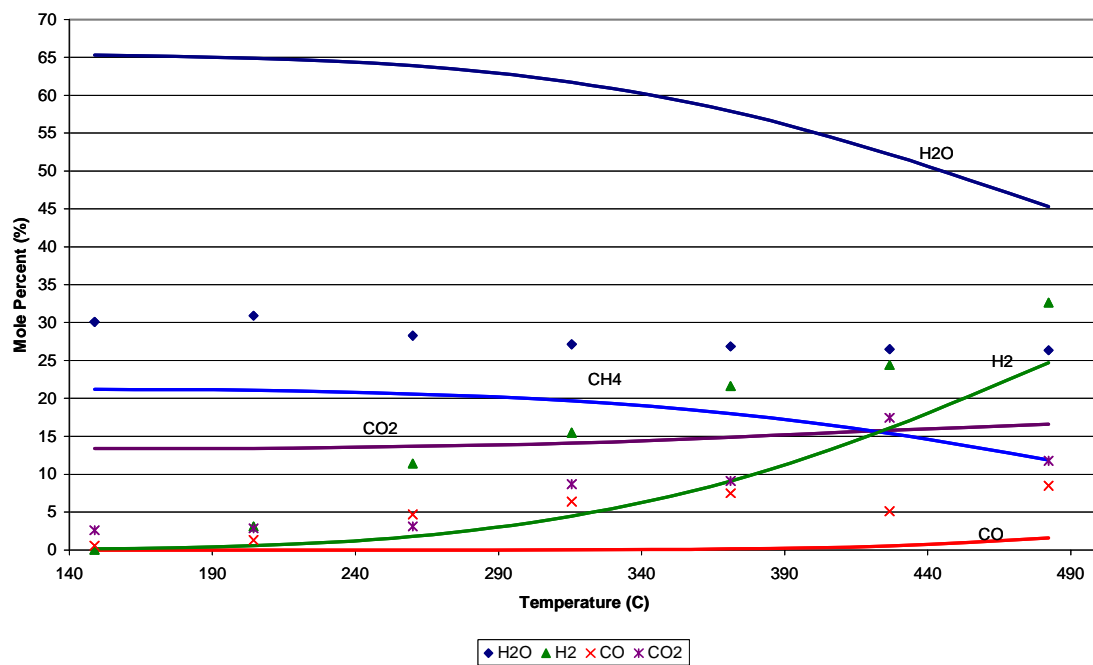


Figure 4.3. Reactor exit gas composition at $O_2/\text{fuel} = 0.27$; $H_2O/C = 1.12$ and different temperatures

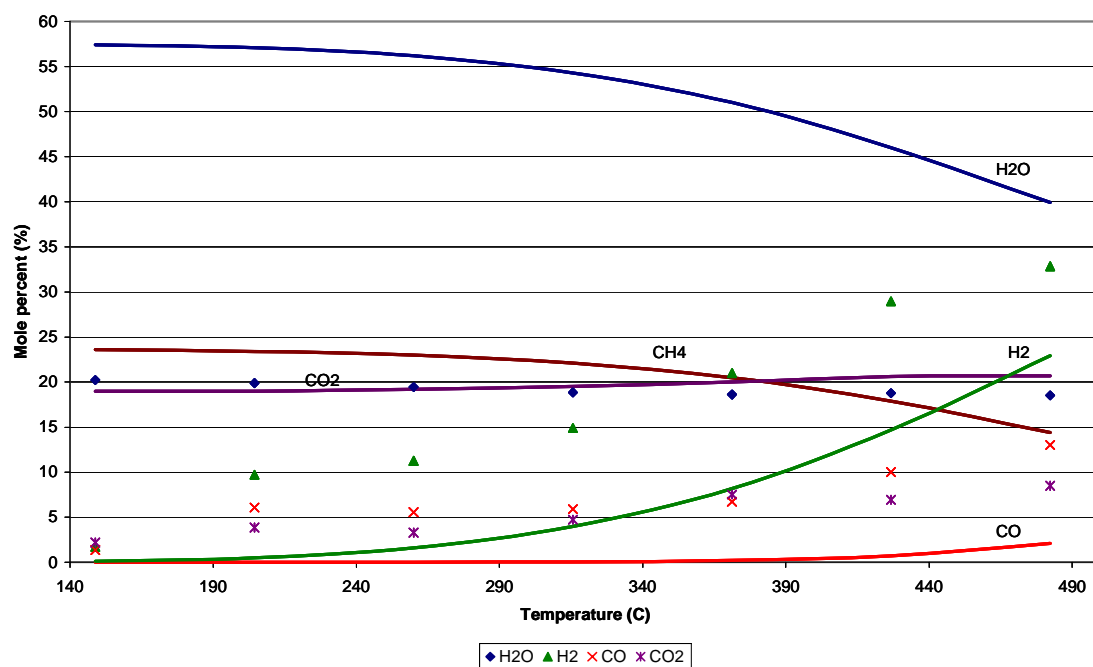


Figure 4.4. Reactor exit gas composition at $O_2/\text{fuel} = 0.39$; $H_2O/C = 0.46$ and different temperatures.

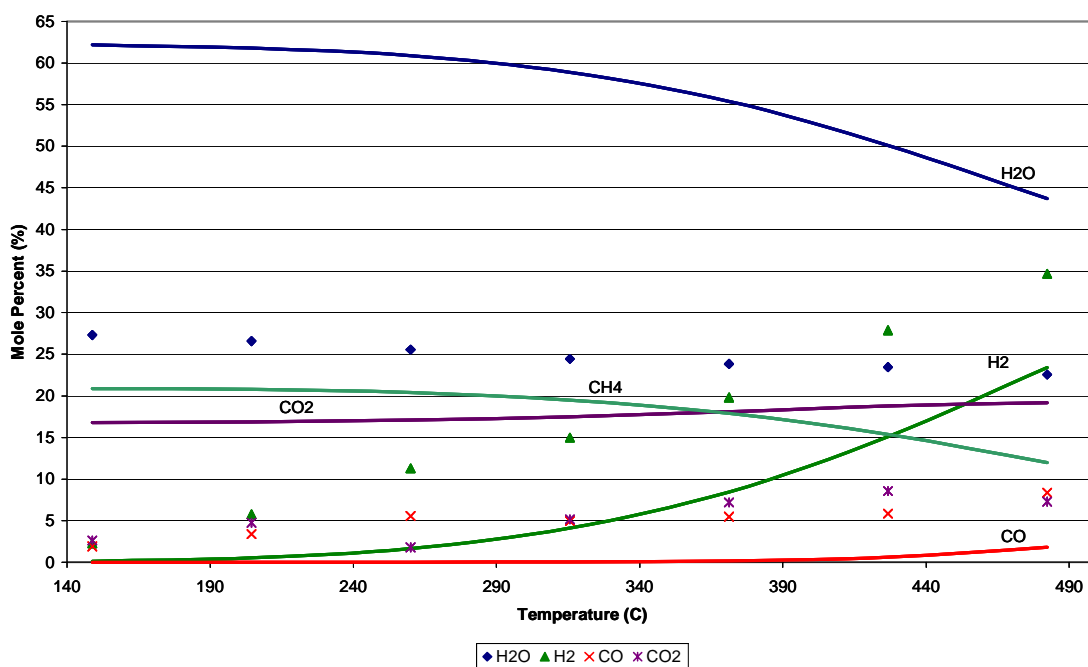


Figure 4.5. Reactor exit gas composition at $O_2/\text{fuel} = 0.39$; $H_2O/C = 0.76$ and different temperatures

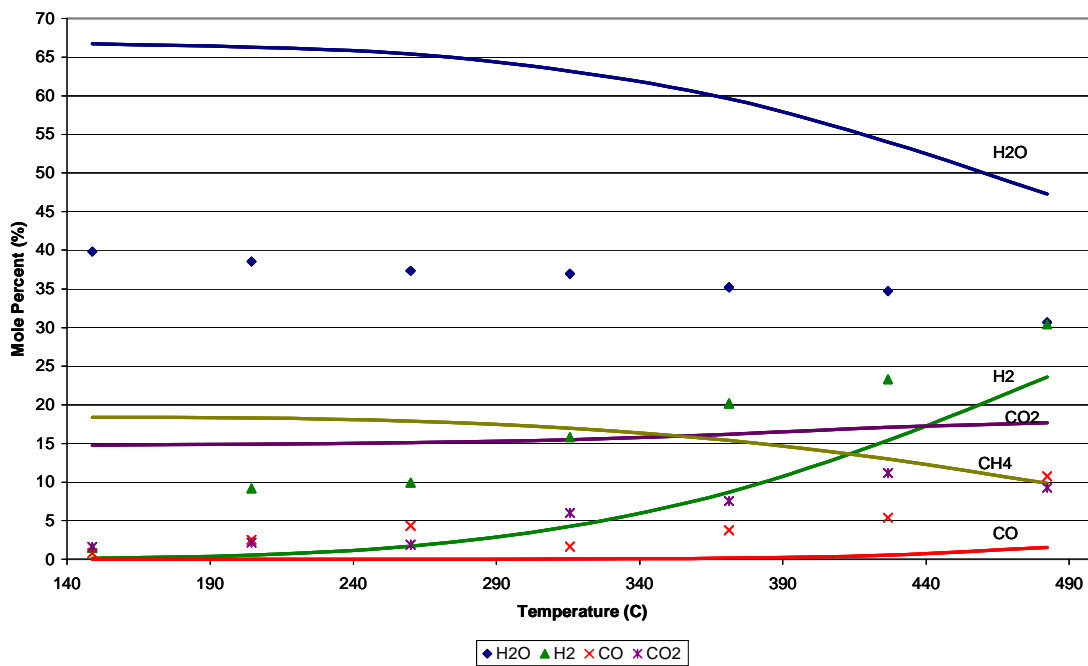


Figure 4.6. Reactor exit gas composition at $O_2/\text{fuel} = 0.39$; $H_2O/C = 1.12$ and different temperatures.

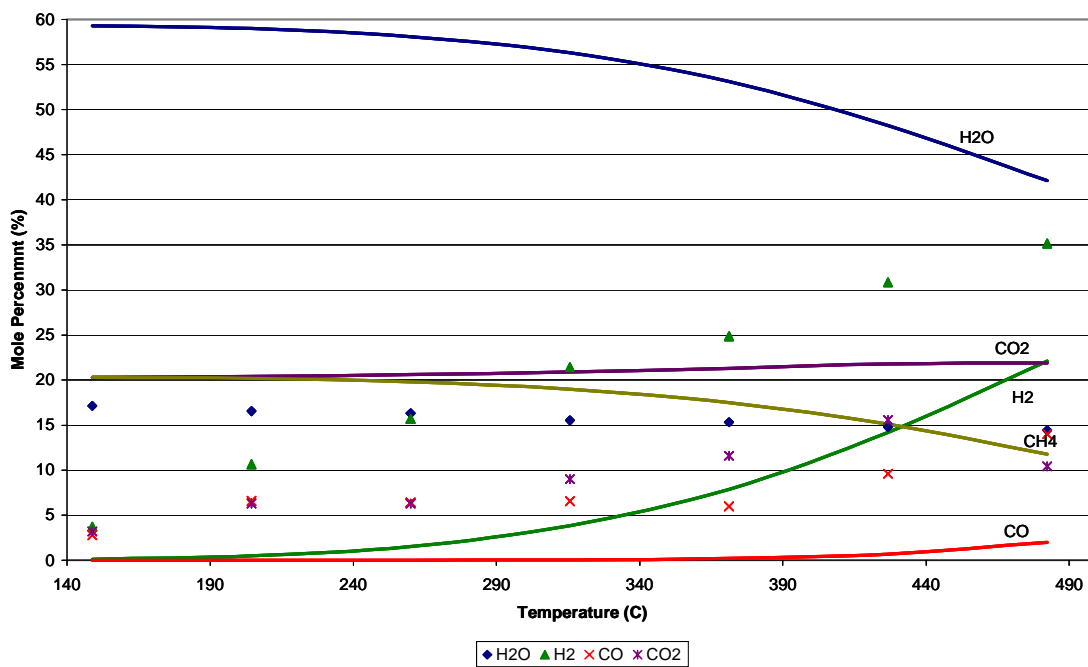


Figure 4.7. Reactor exit gas composition at $O_2/\text{fuel} = 0.5$; $H_2O/C = 0.46$ and different temperatures.

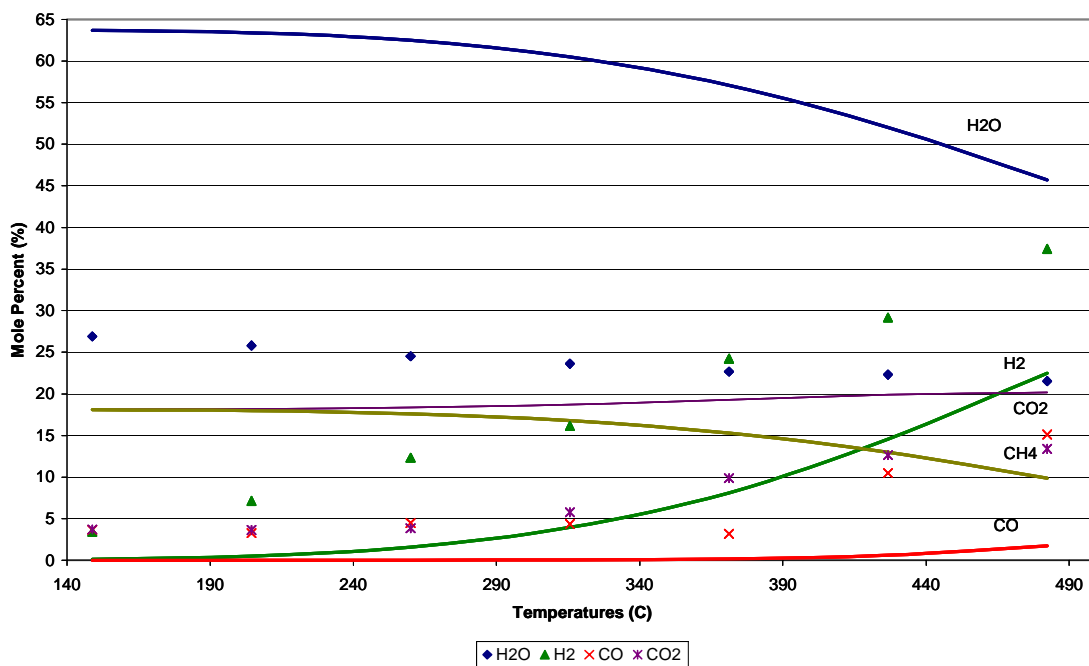


Figure 4.8. Reactor exit gas composition at $O_2/\text{fuel} = 0.5$; $H_2O/C = 0.76$ and different temperatures.

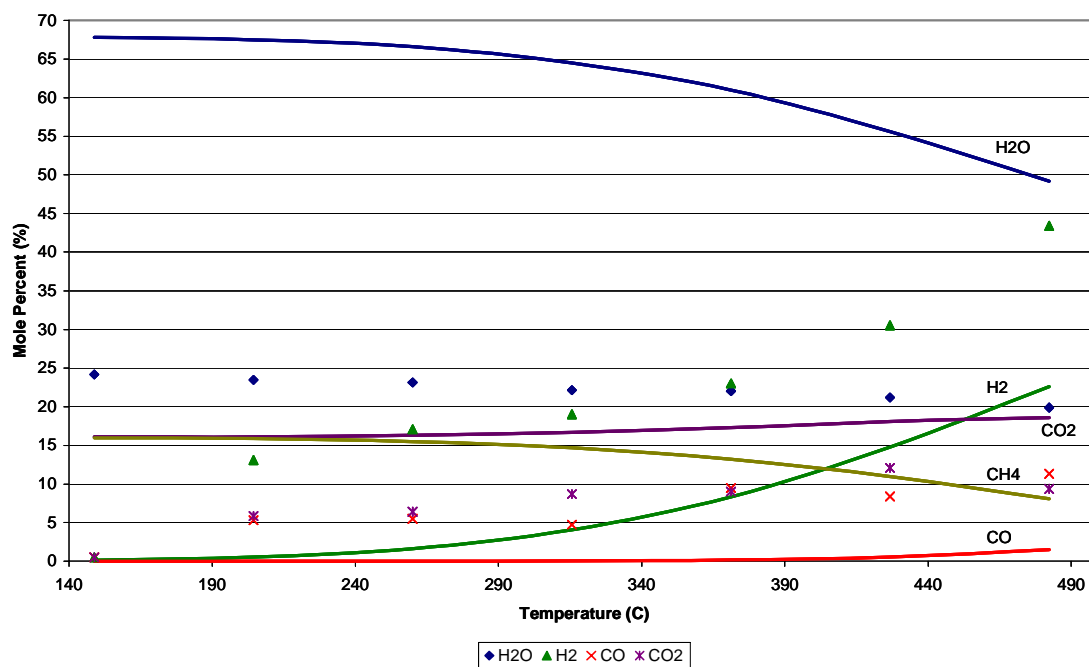


Figure 4.9. Reactor exit gas composition at $O_2/\text{fuel} = 0.5$; $H_2O/C = 1.12$ and different temperatures.

4.3. Hydrogen to (CO + CO₂) ratio

$H_2/(CO+CO_2)$ ratio can be used as a factor to describe the behavior of each one of the reactions that take part in the overall autothermal reforming reaction inside the reforming system. For reforming, this value is 3, and for cracking is 1 or 2 (unpublished data). The ratios calculated for each level and temperatures were frequently around 1 and 2 (see table 4.3). Then, it can be concluded that at the experimental conditions studied, the reaction favored for the reactor and catalyst used, was mostly the one of cracking or decomposition of methanol rather than reforming. Moreover, this assumption was verified with the analysis of the exit reactor gas composition done in last section. At temperatures between 300 and 400°F, $H_2/(CO+CO_2)$ ratio was smaller than 1, because neither the reaction of cracking nor reforming were favored at low temperatures for being endothermic. It was favored the partial oxidation reaction. As is expected, for level 11 ($O_2/fuel=0.39$ and $H_2O/C=0.76$) and 900°F, the $H_2/(CO+CO_2)$ ratio of 2.21 was greater than the other ones. A combination of steam reforming and cracking reactions was occurring, since $H_2/(CO+CO_2)$ of both reactions together, is equal to 2.5. As discussed in section 4.1, at this level was observed the maximum production of hydrogen with the minimal composition of CO and CO₂.

In general, it can be seen from table 4.3, that at higher reactor temperature the $H_2/(CO+CO_2)$ ratio increases. The reactor temperature provides more heat to the endothermic steam reforming reaction (eq. 29). If $O_2/fuel$ ratio increases (constant H_2O/C ratios) the partial oxidation equation (eq. 32) will be displaced to the products liberating more heat that could be used by the endothermic steam reforming reaction.

This effect is observed better at low temperatures and low H₂O/C ratios. For example, at level 00 (O₂/fuel=0.27 and H₂O/C=0.46) at 300°F, the H₂/(CO+CO₂) ratio was 0.16, and at level 10 (O₂/fuel=0.39 and H₂O/C=0.46) at 300°F, the H₂/(CO+CO₂) ratio increased to 0.480. When the H₂O/C is greater than 0.46 (second level number of 1 or 2) is observed that the H₂/(CO+CO₂) ratio slightly increased with an increase in O₂/fuel ratio. The addition of water can affect the partial oxidation reaction equilibrium by displacing it to the reactants. But when more oxygen is added at the same time, the effect of increasing H₂O/C and O₂/fuel ratios is canceled in the of case the partial oxidation reaction.

At higher temperatures (>500°F), the most observed value was around 1.5. Equations 30, 31, and 32 give together an H₂/(CO+CO₂) ratio of this value. Probably, these equations were happening simultaneously without the steam reforming reaction which leads to an increase in this ratio.

Table 4.3. H₂/(CO+CO₂) ratios at different levels and temperatures

Level	Temperature (°F)						
	300	400	500	600	700	800	900
00	0.16	0.50	0.99	1.3	1.4	1.4	2.1
10	0.48	0.83	1.2	1.4	1.5	1.7	1.5
20	0.82	1.0	1.5	1.4	1.4	1.2	1.4
01	0.47	0.64	1.2	1.6	1.5	1.5	1.7
11	0.50	0.71	1.3	1.8	1.9	1.9	2.2
21	0.51	0.73	1.3	1.5	1.6	1.3	1.3
02	0.47	0.75	1.5	1.0	1.3	1.1	1.6
12	0.51	0.80	1.6	2.1	1.8	1.4	1.6
22	0.53	0.82	1.7	1.4	1.2	1.5	2.1

4.4. Hydrogen Selectivity

In this section, the results obtained for hydrogen selectivity will be discussed. It was calculated at each different water and oxygen levels and temperatures. Only hydrogen selectivity was calculated for methanol since hydrogen was not observed in the range studied for isooctane.

The hydrogen selectivity at the same conditions was calculated as (33)

$$\text{H}_2 \text{ selectivity} = \frac{\text{moles of H}_2 \text{ produced}}{\text{moles of methanol reacted}} \quad (33)$$

The denominator is obtained from the mass balance for methanol in the whole system.

For level 00 ($\text{O}_2/\text{fuel}=0.27$ and $\text{H}_2\text{O}/\text{C}=0.46$) and at 900°F :

$$\begin{aligned} \text{moles of methanol reacted} &= \text{moles fed to the reactor} - \text{moles in the reactor exit gas} \\ &= 0.074156 - 0.06804 = 0.006116 \text{ moles of methanol reacted} \end{aligned}$$

$$\text{H}_2 \text{ selectivity} = \frac{0.01508 \text{ moles of H}_2 \text{ produced}}{0.006116 \text{ moles of methanol reacted}} = 2.47 \frac{\text{moles H}_2 \text{ produced}}{\text{moles methanol reacted}}$$

The next figures show (4.10-4.12) the behavior of H_2 selectivity at the different feed ratios and temperatures studied. At an $\text{O}_2/\text{fuel}=0.27$ ratio and temperatures lower than 500°F , the hydrogen selectivity was approximately the same for all the $\text{H}_2\text{O}/\text{C}$ ratios (see figure 4.10). The steam reforming reaction (eq. 29) is highly endothermic and is generally conducted at reactor temperatures above 800°C (14). In order to make this reaction to occur at lower reactor temperatures, it is needed to supply additional heat with the exothermic partial oxidation reaction (eq. 32). If more water is added, equation 32 will not be favored to the products side and it will not give sufficient heat to the steam reforming reaction which is endothermic. A combination of the reactor temperature with

the heat supplied by equation 32, will favor the steam reforming equation. Thus, at these conditions, a less concentration of water feed will allow a displacement of the partial oxidation equation to the products and will supply heat to the steam reforming equation. This effect can be seen at high temperatures where hydrogen selectivity increased as the H_2O/C ratio decreased. The maximum hydrogen moles that can be produced for each mole of methanol reacted, according to the overall autothermal reaction (eq. 11), are 2.46 moles. Figure 4.10 shows that only the level with less water feed concentration, at temperatures higher than $600^\circ F$, reached the maximum hydrogen moles that can be produced.

Figure 4.11 shows the hydrogen selectivity for an $O_2/fuel=0.39$ and different H_2O/C ratios and temperatures. There could be an interaction between both $O_2/fuel$ and H_2O/C ratios at temperatures higher than $500^\circ F$. The reaction of steam reforming was favored maybe because the negative effect that could have the increase in water feed concentration mentioned before, could be compensated by the partial oxidation reaction when there was an increase in the oxygen feed. When there is more H_2O/C ratio, is observed higher hydrogen selectivity at lower temperatures ($<500^\circ F$). There is enough oxygen to react and to displace the partial oxidation reaction to the products and give heat. The water excess could be used as a driving force to the product displacement of the steam reforming reaction. The maximum hydrogen moles that can be produced for each mole of methanol reacted, according to the overall autothermal reaction (eq. 11), are 2.22 moles. Figure 4.11 shows that the three levels of H_2O/C ratios, at high temperatures, reached the maximum hydrogen moles that can be produced.

When O_2 /fuel ratio was increased to 0.50 (figure 4.12), the hydrogen selectivity was almost constant at all combination of levels studied. With an increase in water feed concentration, the partial oxidation equation is not favored at low temperatures. But with the addition of a sufficient oxygen feed, the equilibrium of this equation would not be affected. At lower temperatures and more water added, equation 32 (partial oxidation) will be displaced to the reactants and there will be less heat production. When too much water is added ($H_2O/C=1.12$), the partial oxidation equation is not going to be favored and would not give the necessary heat to the steam reforming reaction that occurs at higher temperatures. Maybe, at higher temperatures ($800^\circ F$) the controlling variable of the hydrogen selectivity is the reactor temperature. The maximum hydrogen moles that can be produced for each mole of methanol reacted, according to the overall autothermal reaction (eq. 11), are 2.0 moles. Figure 4.12 shows that the levels of H_2O/C ratios of 0.76 and 1.12, at high temperatures, reached the maximum hydrogen moles that can be produced.

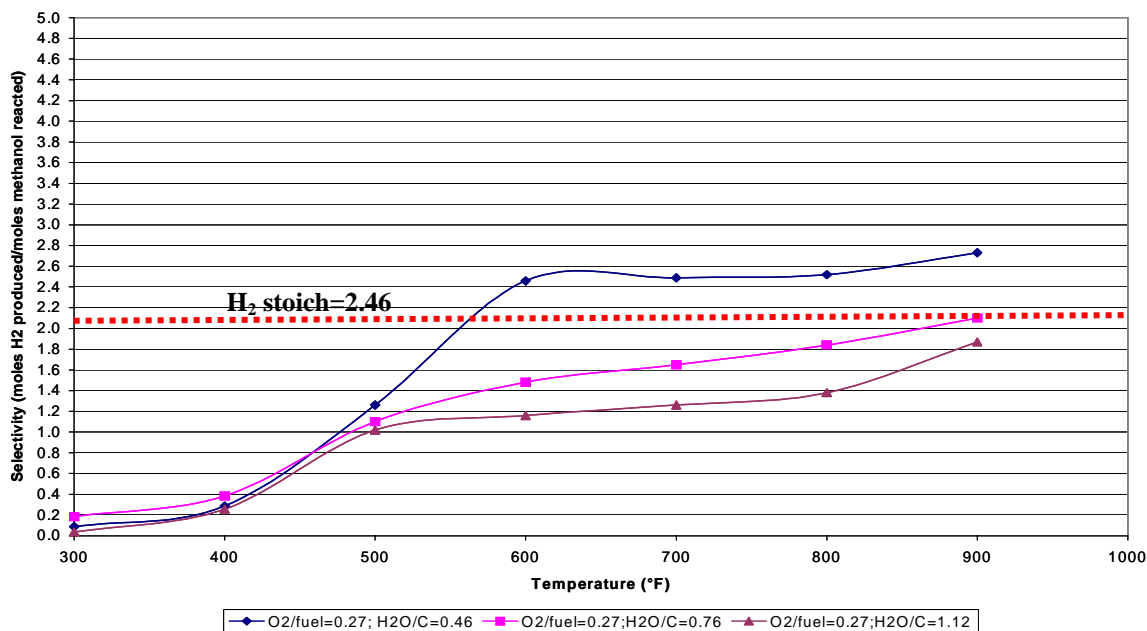


Figure 4.10. Hydrogen Selectivity ($O_2/\text{fuel}=0.27$) at different H_2O/C ratios and temperatures.

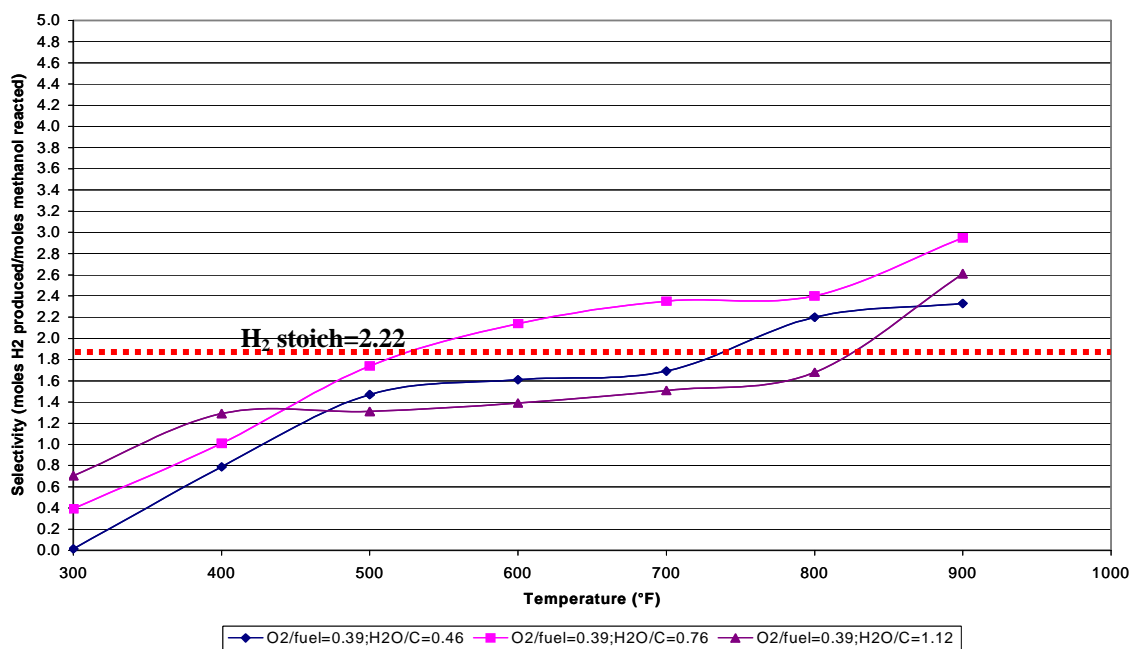


Figure 4.11. Hydrogen Selectivity ($O_2/\text{fuel}=0.39$) at different H_2O/C ratios and temperatures.

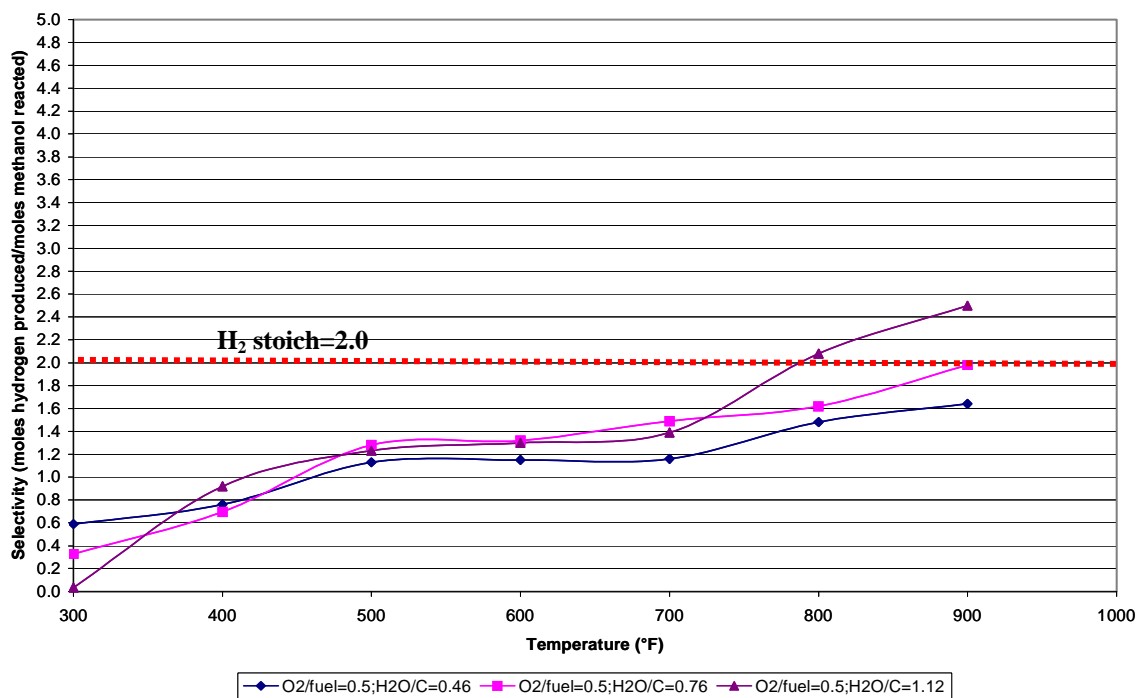


Figure 4.12. Hydrogen Selectivity (O_2 /fuel=0.5) at different H_2O/C ratios and temperatures.

4.5. Gas Hourly Space Velocity (GHSV)

The gas hourly space velocity in the catalyst reactor, based on the mass of the catalyst, gives a measure of the reactant throughput relative to the catalyst, and is defined as (28, 21):

$$\text{GHSV} = \frac{\text{mass flow rate of the exit gas of the reactor}}{\text{weight of the catalyst}} \quad (34)$$

The weight of the Pt-based catalyst used was ~2.0g.

At an $\text{O}_2/\text{fuel}=0.27$ and $\text{H}_2\text{O}/\text{C}=1.12$ (level 02):

$$\text{GHSV} = \frac{4.5094\text{g}}{2.0\text{ g} * \text{min}} * \left(\frac{60\text{ min}}{\text{hr}} \right) = 135.28\text{ hr}^{-1}$$

Figure 4.13 shows the yield for the reaction products (H_2 , CO , CO_2 and H_2O) produced from reforming methanol as a function of the GHSV at a temperature of 800°F . Every product gas decreased its yield with increasing the GHSV. Even at the highest GHSV, some H_2 (~0.9105 moles per mole of methanol observed) was present in the fuel gas. The hydrogen yield reached to ~1.25 moles per mole of methanol observed as the GHSV decreased.

The same behavior of the products yield of the methanol reforming reaction was observed at each temperature studied (see Appendix D). These results coincide with the results obtained by some investigators (33, 21, 29). Krumpelt et. al. (33), suggested that the initial yield of hydrogen that is observed at the highest GHSV investigated is produced by reactions of the fuel and O_2 . Partial oxidation, which produces CO and H_2 , is occurring together with the total oxidation reaction, which produces CO_2 and H_2O . Also, these reactions occur at a time scale that is less than the contact time corresponding

to highest GHSV. Thus, the steam and possibly CO₂ reforming are the predominant reactions for the production of hydrogen.

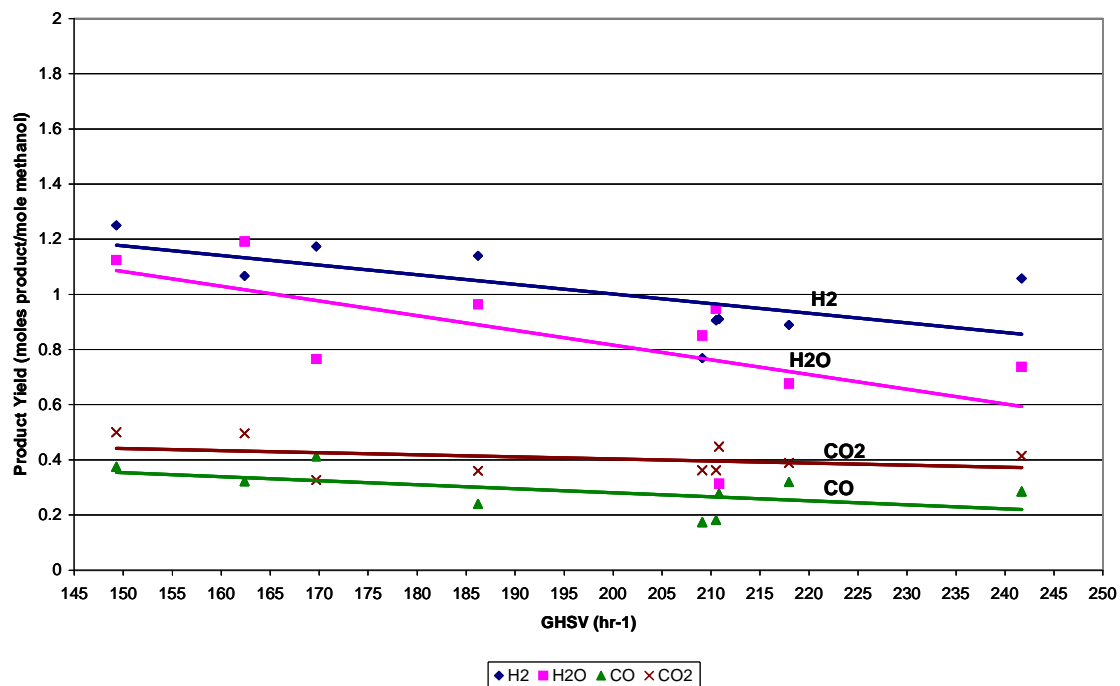


Figure 4.13. Yield of reaction products as a function of GHSV for ATR of methanol (800°F).

4.6. Reforming of isooctane (2,2,4-trimethylpentane)

The experiments done for reforming isooctane are summarized in table 4.4. No hydrogen was detected at all the conditions studied. The detection limit of the analytical equipment for hydrogen is near 6%. This means that the concentration of the hydrogen present at all conditions studied was below this detection limit (see Appendix B). Previous studies have demonstrated that hydrogen is produced during isooctane reforming at exit gas temperatures above 700°C (32, 3, 30). Methane and other hydrocarbons (C₁-C₆) were not seen in the isooctane chromatograms. The GC-TCD was very sensitive to methane and its detection limit was 2%. So, it can be deduced that this gas was not present in the exit reactor gas (see Appendix B). Higher hydrocarbons were not seen in the gas phase because they exist at very low concentrations and the detector was not able to detect them. Also, the compositions of C₁-C₆ hydrocarbons at equilibrium are in the order of 10⁻⁶ (unpublished data). As in methanol reforming experiments, the exit gas composition was reproducible at each temperature and was constant throughout the 4.5 hours of operating conditions studied, indicating that the catalyst was not deactivated and the reactor was operated at steady-state conditions (see Appendix C.6).

The influence of H₂O/C ratio on CO concentration was more evident since at 900°F, its value decreased from 22.1% at the ratio of 1.0 to nearly 5.21% at a molar ratio of 3. A high molar ratio of H₂O/C is preferred for generating the fuel gas mixture containing low concentration of CO. As the temperature increased from 300 to 900°F at a O/C=1 and H₂O/C=1 ratios, CO concentrations increased quickly from 0.62% to

22.1%. This concentration should increase more drastically above 700°F as in previous studies (32). At 900°F, carbon dioxide concentration decreased from 23.8% to 6.61% as more water was added. Raising the temperature at O/C=1 and H₂O/C=1 ratios, CO₂ remained almost constant at temperatures between 600°F and 800°F (~16%), and slightly increased to 23.8%.

Table 4.4. Isooctane exit gas product composition at different levels and temperatures (dry basis).

Ratio	Temp. (°F)	H ₂ (%)	O ₂ (%)	CO (%)	CO ₂ (%)	CH ₄ (%)	Total (%)
O/C=1; H ₂ O/C =1	600	<6	83.0	0.62	16.6	<2	100
	700	<6	83.8	1.33	15.5	<2	100
	800	<6	79.5	5.55	15.9	<2	100
	900	N.D.*	84.0	22.1	23.8	<2	100
O/C=1; H ₂ O/C =1.2	900	N.D.*	58.1	20.4	22.9	<2	100
O/C=1; H ₂ O/C =3	900	N.D.*	89.2	5.21	6.61	<2	100

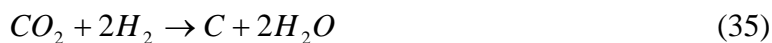
* Non-detected or integrated by the integrator.

4.6.1. Coke Formation

Generally, the reforming of hydrocarbons has the potential to form carbon or coke. This occurs when the reactor is not properly designed or operated and could avoid a satisfactory production of hydrogen. Coke may deactivate the catalyst by depositing on the active sites, responsible for dehydrogenation and oxidation, blocking the catalyst pores or causing the metal to separate from the support (36). Extreme care must be taken to prevent carbon formation. It is a function of fuel constituents, oxygen to fuel molar ratio, $H_2O/fuel$ molar ratio and reaction temperature. An O/C higher than 0.6 and H_2O/C between 1 and 2 is desirable for vehicle applications.

If the feed consists in a 1gmol of isooctane and air at O/C of 1, coke of more than 1.0×10^{-9} $\mu\text{mol/hr}$ will form at temperatures up to 950°C . If the feed consists of 1gmol of isooctane and water, the same quantity of coke will form up to 800°C . If water is maintained to be $H_2O/C=1$ and oxygen to be $O/C=1$, the temperature of the reactor can be lowered to 560°C before coke formation occurs (30).

At every experiments performed, coke formation was observed (see figures 4.14 and 4.15). This observation agrees with the previous studies mentioned before since the higher experimental operating temperature condition used was below 500°C . Figure 4.20 shows the catalyst before (yellow) and after coke formation (black). Figure 4.21 shows the exit liquid mixture of reformed isooctane where is clearly seen the immiscibility of isooctane, water and carbon from coking. Some of the side reactions that take place during isooctane reforming are the coking reaction (eq. 35) and the reaction given by equation 36 (30):



The coking reaction shows that coke formation comes from the reaction of 1 mol of carbon dioxide with 2 moles of hydrogen. Since carbon deposits were observed in the experimental conditions studied, it can be deduced that carbon dioxide and hydrogen concentrations at the reactor exit will be lower than those that would exist at equilibrium where no carbon is formed. Equation 36 shows that the carbon that is formed during the experiment can react with oxygen to produce carbon monoxide. That could be the reason of obtaining higher experimental concentrations of CO than if it would exist at equilibrium (see Appendix E.2 and table 4.5). When H₂O/C ratio increases, the hydrogen concentration at equilibrium will be higher and the CO and CO₂ concentrations at equilibrium will be lower.

Table 4.5. Isooctane exit gas product composition, experimental and at equilibrium, at different levels and temperatures (dry basis).

Ratio	Temp (°F)	H ₂ (%)		CO ₂ (%)		CO (%)	
		Eq.	Exp.	Eq.	Exp.	Eq.	Exp.
O/C=1; H ₂ O/C=1	600	0.32	<6	26.9	16.6	0.0046	0.62
	700	14.0	<6	40.8	15.5	0.4397	1.33
	800	23.2	<6	38.3	15.9	1.45	5.55
	900	34.0	<6	34.6	23.8	3.9	22.1
O/C=1; H ₂ O/C=1.2	900	36.5	<6	33.4	22.9	3.66	20.4
O/C=1; H ₂ O/C=3	900	52.0	<6	13.3	6.61	2.48	5.21

Apparently, the Pt-based catalyst used for these experiments, is not feasible for reforming isooctane as a fuel at low temperatures because it does not prevent large quantities of coke at temperatures below 500°C and, therefore, leads to a poor hydrogen production

(32). Docter and Lamm said that some catalysts might be able to enhance the other reactions and not to suppress the coke formation reaction (16).

After performing the isooctane experiments, a methanol reforming experiment with the black catalyst was done in order to verify if any deactivation was present. This replicate was done at 900°F, $O_2/\text{fuel}=0.46$ and $H_2O/C=0.76$. Table 4.6 shows the results obtained from each one of the trials done. The deactivation, based in a decrease of hydrogen concentration in the reactor exit gas, was not observed because the concentrations of hydrogen, oxygen, carbon monoxide, and carbon dioxide were the same. Hence, regardless of the deposition of carbon in the catalyst, it was not deactivated. Thus, it can be deduced that the catalyst used can resist the deactivation by coke accumulation, but it can not prevent coke formation for isooctane.

Table 4.6. Replicate at a $O_2/\text{fuel}=0.46$; $H_2O/C=0.76$ at 900°F after coke formation.

Gas	Concentration (% , dry basis)	
	Trial 1	Trial 2
H₂	52.6	53.1
O₂	16.0	15.8
CO	18.6	18.3
CO₂	12.1	12.3



Figure 4.14. Catalyst before (yellow) and after coke formation (black).



Figure 4.15. Exit liquid mixture of reformed isooctane
(isooctane + water + coke).

4.7. Methanol and isooctane reforming without catalyst

In order to compare the difference in product concentrations, a condition for both fuels was done again without the presence of a catalyst inside the reactor. For methanol, condition that was chosen was level 11 where the best results were obtained. Table 4.7 shows the difference between the concentrations of hydrogen, carbon dioxide, and carbon monoxide (dry basis) that were observed. At a $O_2/\text{fuel}=0.39$ and $H_2O/C=0.76$ ratios and 900°F , is seen that without the catalyst, H_2 concentration decreased by $\sim 10\%$. Carbon dioxide and carbon monoxide increased by approximately 25% and 4%, respectively. Although it was mentioned that the major reaction occurring at the conditions studied was cracking (see section 4.2), the presence of a Pt-based catalyst in some way also favors methanol reforming. It seems to improve the hydrogen production and reduce carbon monoxide and carbon dioxide concentrations, which are the requirements that should have an effective fuel processor in automotive applications (9, 36).

Table 4.7. Methanol exit gas production at level 11 and 900°F without catalyst (dry basis).

Ratio	Temp. ($^\circ\text{F}$)	H_2 (%)		CO_2 (%)		CO (%)	
		with	without	with	without	with	without
11 ($O_2/\text{fuel}=0.39$; $H_2O/C=0.76$)	900	59.79	49.33	12.57	37.35	14.46	18.20

The condition repeated without catalyst for isooctane was $O/C=1$ and $H_2O/C=1$ ratios and a temperature of 900°F . The hydrogen production was less than the detection limit of the gas chromatograph for both with and without catalyst. Contrary to the differences observed with methanol, the absence of the catalyst did not significantly

changed carbon dioxide and carbon monoxide concentrations (see table 4.8). Without the catalyst, CO₂ and CO increased only by ~2% and ~1%, respectively. This fact proves again that autothermal reforming of isooctane was not favored at the temperatures and conditions studied with a precious-metal catalyst used. In the range studied, the reactions that governed the system were the formations of coke and hydrocarbons between C₁-C₆ (see previous section).

Table 4.8. Isooctane exit gas production at level O/C=1; H₂O/C=1 and 900°F without catalyst (dry basis).

Ratio	Temp. (°F)	H ₂ (%)		CO ₂ (%)		CO (%)	
		With	Without	with	without	with	without
(O ₂ /C =1; H ₂ O/C=1)	900	<6	<6	22.09	23.76	21.35	22.29

5. CONCLUSIONS

As part of the development of a methanol and isooctane reforming systems for integration with the PEM fuel cell, the autothermal reforming reaction of methanol and isooctane over a Pt-based catalyst at different O_2/fuel and H_2O/C ratios and at different temperatures was investigated. The catalyst was provided by Argonne National Laboratory.

Based on the product gas composition of methanol reforming the following conclusions were drawn from the experimental results:

1. The best condition in the range studied that can obtain high hydrogen concentration and the minimal carbon dioxide and carbon monoxide concentrations was level 11 at 900°F. This level consists of an $O_2/\text{fuel}=0.39$ and $H_2O/C=0.76$ and the concentrations produced (dry basis) were 59.8% H_2 , 14.6% CO , and 12.6% CO_2 .
2. When an $O_2/\text{fuel}=0.5$ and $H_2O/C=1.12$ ratios at 900°F were used, the concentrations obtained were very close to that obtained at equilibrium by Ahmed et. al. (4) at the same temperature and feed conditions. The equilibrium concentrations are 60% H_2 , 19% CO , and 17% CO_2 , while the experimental concentrations obtained were 59% H_2 , 20% CO , and 18% CO_2 . The $H_2/(CO+CO_2)$ ratio was 2.21.
3. A thermodynamic simulation program was used to calculate the equilibrium concentrations at each one of the levels and temperatures studied. The data obtained in the equilibrium model (supplied by Dr. Krause, ANL) was compared

with the experimental data. The following conclusions were based in this comparison:

1. Different experimental gas compositions values in comparison with equilibrium values were observed, but with similar trends.
2. The experimental water production was less than that at equilibrium. According to the simulation, methane and water are produced from the reaction of hydrogen and carbon monoxide. Since no methane was formed, less water composition was obtained at the exit gas of the reactor.
4. The water curves, both at equilibrium and experimentally, coincide in the fact that the exit gas concentrations decreases as the temperature increases. Water was more consumed at high temperatures in the steam reforming reaction and was not favored anymore in the combustion reaction at higher temperatures.
5. The carbon dioxide existence at low temperatures is attributed to the water gas shift reaction (WGSR) and to the methanol combustion reaction. As the temperature increases, CO_2 will be produced from the steam reforming reaction. The CO_2 found experimentally was lower than that at equilibrium because maybe the reforming reaction was not occurring as expected. Thus, most of the methanol was cracked instead of reformed.
6. The CO production increased and the one obtained experimentally was higher than at equilibrium. Carbon monoxide could react with hydrogen to produce methane and water and no methane production was observed. At equilibrium and low temperatures, CO concentration is not observed because it is consumed to

produce methane and consumed in the WGSR. When the temperature rises, this gas will be produced by the cracking reaction of methanol.

7. The hydrogen concentrations found experimentally were greater than at equilibrium. The hydrogen moles necessary to produce methane were not consumed. Also, the steam reforming reaction was not as expected and the additional hydrogen produced can be attributed to the cracking reaction.
8. The effect of increasing O_2/fuel and leaving H_2O/C constant led to a hydrogen production increase at low temperatures. If more oxygen is fed to the reactor, additional heat is added to the reactions of steam reforming and cracking and will be more favored at lower temperatures. Cracking reaction produces CO, thus, its concentration increased too. Carbon dioxide increased at higher temperatures because when more oxygen is fed to the reactor, there is more possibility that the reaction could arrive to a complete combustion and produce more CO_2 .
9. The effect of increasing H_2O/C ratio leads to a slightly decrease in carbon monoxide at high temperatures. When more water was added to the fuel processor, more CO is converted to CO_2 due to the WGSR.
10. At the temperature range studied, the platinum catalyst did not permit methane production inside the reactor. Also, this catalyst promoted methanol decomposition rather than reforming because the $H_2/(CO+CO_2)$ ratios calculated at each level and temperature were frequently between 1 and 2 (decomposition ratio).

The hydrogen selectivity were also studied and analyzed for each level and temperature. The conclusions found were:

1. At an $O_2/\text{fuel}=0.27$ ratio and temperatures lower than 500°F , the hydrogen selectivity was approximately the same for all the H_2O/C ratios. At these conditions and high temperatures, a less water feed will favor the partial oxidation equation to the products and will supply enough heat to the steam reforming equation. Only the level with less water feed concentration, at temperatures higher than 600°F , reached the maximum H_2 moles that can be produced (2.46).
2. For an $O_2/\text{fuel}=0.39$ and different H_2O/C ratios and temperatures, it could be an interaction between both ratios at temperatures higher than 500°F . The negative effect that could have the increase in water feed concentration in the steam reforming reaction could be compensated by the partial oxidation reaction when there was an increase in the oxygen feed. The three levels of H_2O/C ratios, at high temperatures, reached the maximum H_2 moles that can be produced (2.22).
3. When O_2/fuel ratio was increased to 0.50, the hydrogen selectivity was almost constant at all combination of levels studied. But with the addition of a sufficient oxygen feed, the equilibrium of this equation would not be affected by an increase in water feed concentration. Levels of H_2O/C ratios of 0.76 and 1.12, at high temperatures, reached the maximum hydrogen moles that can be produced (2.0).

Differences between the concentrations of hydrogen, carbon dioxide, and carbon monoxide (dry basis) were observed when the reaction was performed with and without the catalyst. The Pt-based catalyst in some way also favors methanol reforming because it improves the hydrogen production and reduce carbon monoxide and carbon dioxide concentrations.

The methanol reforming exit gas production was plotted against the gas hourly space velocity (GHSV). Every product gas (H_2 , CO, CO_2 , and H_2O) decreased its yield with increasing the GHSV. This behavior was observed at each temperature studied and the results coincide with the ones obtained by some investigators (33).

The following conclusions were drawn from the experimental results of reforming isooctane:

3. No hydrogen was detected at all the conditions studied. The concentration of the hydrogen present at all conditions studied was below the gas chromatograph detection limit.
4. Coke formation is a function of fuel constituents, oxygen to fuel molar ratio, H_2O/C molar ratio and reaction temperature. At every experiments performed, coke formation was observed. Previous studies demonstrate that at $H_2O/C=1$ and $O/C=1$ ratios, coke formation occurs at lower temperatures than $560^\circ C$ (30).
5. Carbon dioxide and hydrogen concentrations were lower than those at equilibrium (where no carbon was formed), since carbon deposits were observed in the experimental conditions studied.
6. Higher experimental concentrations than at equilibrium of CO were observed because the carbon formed during the experiment could react with oxygen to produce carbon monoxide.
7. The Pt-based catalyst used for these experiments, is not feasible for reforming isooctane at low temperatures because it does not prevent large quantities of coke at temperatures below $500^\circ C$ and, therefore, leads to a poor hydrogen production (30).

8. Regardless of the carbon deposition inside the reactor, deactivation of the catalyst was not observed because the concentrations of hydrogen, oxygen, carbon monoxide, and carbon dioxide were the same when a methanol replicate of one condition was done with the catalyst used with isooctane (black catalyst).
9. The absence of the catalyst did not significantly changed carbon dioxide and carbon monoxide concentrations when an isooctane replicate of one condition was performed. Autothermal reforming of isooctane was not favored at the temperatures and conditions studied with a precious-metal catalyst. The reactions that governed the system were the formations of coke and hydrocarbons between C_1 - C_6 which could not be detected with the analytical equipment used.

6. RECOMMENDATIONS FOR FUTURE WORK

After completing the scope of this work, some recommendations or suggestions can be made based in the results from this study. This section will provide some additional information that could help in a better development and analysis in autothermal reforming of methanol and isooctane.

1. A different fuel processor must be used in order to make it possible to study higher temperatures.
2. Since the catalyst studied promoted more decomposition rather than reforming of the fuels, it will be necessary to prove other catalysts (copper-based) to avoid the reaction of cracking.
3. Coke formation was observed in the reactor exit product of isooctane and not in the reactor exit product of methanol. Making an analysis of the catalyst surface used in the experiments should give a better explanation about why this fact was occurring.
4. More sensitive analytical detectors and measurement of condensables are recommended.
5. The residence time of the reactants inside the reformer is critical in the concentration of the exit product gases. Utilizing less feed flows and maintaining the same O_2/fuel (or O/C) and H_2O/C ratios will increase the residence time (lower GHSV) inside the reactor. The product gas concentration results can be compared to the ones obtained in this work. It is expected that higher residence times could benefit the reforming reaction.

6. As a future work, Biodiesel, another fuel source, will be reformed at $H_2O/C=2$, and $O_2/C= 0.4-0.6$ ratios with a Rhodium-based catalyst (ANL), in a plug flow reactor that can resist higher temperatures (up to $1100^\circ C$). The product gas will be injected in the GC-MS to analyze the hydrocarbons formed such as metha-, para-, ortho-xylene, ethane, propylene and isobutene. Also, the product gas will be injected in the GC-TCD to analyze hydrogen concentration.

7. BIBLIOGRAPHY

1. Ahmed, S., Doshi, R., Lee, S.H.D., Kumar, R., and Krumpelt, M., "Partial Oxidation Reformer Development for Fuel Cell Vehicles," ANL, IL.
2. Ahmed, S., Kopaz, J., Kumar, R., and Krumpelt, M., "Water Balance in a Polymer Electrolyte Fuel Cell System," *Journal of Power Sources*, 112: 519, 2002.
3. Ahmed, S., Krumpelt, M., "Hydrogen from Hydrocarbon Fuels for Fuel Cells", *International Journal of Hydrogen energy*, 26:291, 2001.
4. Ahmed, S., Krumpelt, M., Kumar, R., Lee, S.H., Carter, J.D., Wilkenhoener, R., and Marshall, C., "Catalytic Partial Oxidation Reforming of Hydrocarbon Fuels," *Transportation Technology R&D Center, Conference Paper, Fuel Cell Seminar*, 1998.
5. ANL, "Taking Catalytic Autothermal Reforming to the Next Stage with Commercially Viable Catalysts," <http://cartech.doe.gov/research/fuelcells>.
6. ANL, "Water Gas Shift Catalysts", <http://www.cmt.anl.gov>.
7. ANL, Fuel Processor Catalysts, <http://cmt.anl.gov/scence-technology/fuelcells>
8. Baird, S., Fuel Reforming, <http://myhome.naver.com>.
9. Berlowitz, P.J., and Darnell, C.D., "Fuel Choices for Fuel Cell Powered Vehicles," *SAE Technical Paper Series*, 2000.
10. Bonville, Z.J., DeGeorge, C.L., Foley, P.F., Garow, J., Lesieur, R.R., Preston, J.L., Szydowski, D.F., US Patent 6,159,256 (2000).
11. Bromberg, L., Cohn, D.R., Rrubinovich, A., and Alexeev, N., "Plasma Catalytic Reforming of Methane," *International Journal of Hydrogen Energy*, 24: 1131, 1999.
12. Browning, L., *Projected Automotive Fuel Cell use in California*, California Energy Commission, October, 2001.
13. Carter, J.D., Krause, T., Mawdsley, J., Kumar, R., Krumpelt, M., "Sulfur Removal Form Reformate," *Proceedings of the Argonne National Laboratory R&D Meting, DOE Fuel Cells for Transportation Program, Tennessee*, June 2001.

14. Colucci, J.A., and Cabrera, C.R., "Argonne Reformer Catalyst Characterization by X-Ray Photoelectron Spectroscopy," Research Pre-proposal to Argonne, 1999.
15. Cornier, J.M., and Rusu, I., "Syngas Production Via Methane Steam Reforming with Oxygen: Plasma Reactors versus Chemical Reactors," *Journal of Physics D: Applied Physics*, 34:2798, 2001.
16. Docter, A., and Lamm, A., "Gasoline Fuel Cell Systems," *Journal of Power Sources*, 84:194, 1999.
17. DOE Office of Transportation Technologies, *Future US Highway Energy Use: A Fifty Year Perspective*, 2001.
18. Edlund, D., *A Versatile, Low Cost, and Compact Fuel Processor for Low Temperature Fuel Cells*, Ida Tech, Oregon USA, 1999.
19. Ersoz, A., Olgun, A., Ozdogan, S., Gungor, C., Akgun, F., and Tiris, M., "Autothermal Reforming as a Hydrogen Fuel Processing Option for PEM Fuel Cell," *Journal of Power Sources*, 5244:1, 2003.
20. Fitzgerald, S.P., Wegeng, R.S., Tonkovich, A.Y., Wang, Y., Freeman, A.D., Marco, J.L., Roberts, G.L., and Vandewiel, D.P., "A compact Steam Reforming Reactor for Use in Automotive Fuel Processor," Pacific Northwest National Laboratory, Richland, WA, 1999.
21. Fogler, H.S., *Element of Chemical Reaction Engineering*, Third Edition, Prentice-Hall, Inc., New Jersey, 1999.
22. Freiburg, ISE, *Reforming Unit for Hydrogen from Fossil Energy Carriers*, <http://www.hydrogen.org>, 1997.
23. Hagh, B.F., "Optimization of Autothermal Reactor for Maximum Hydrogen Production," *International Journal of Hydrogen Energy*, 28(12): 1369, 2003.
24. Han, C., and Harrison, D., "Simultaneous Shift Reaction and Carbon Dioxide Separation for the Direct Production of Hydrogen," *Chemical Engineering Science*, 49(24B):5875, 1994.
25. Himmelblau, D.M., *Basic Principles of Chemical Engineering*, Sixth Edition, Prentice-Hall, Inc., New Jersey, 1996.
26. Hirschenhofer, J.H., Stauffer, D.B., Engleman, R.R., Klett, M.G., *Fuel Cell Handbook*, Fourth Edition, US Department of Energy, DOE/FETC-99/0176, 1999.

27. Hufton, J., Waldron, W., Weigel, S., Rao, W., Nataraj, S., and Sircar, S., "Sor bent Enhanced Reaction Process for the Production of Hydrogen," Proceedings of the 2000 Hydrogen Program Review, NREL/CP-570-28890, 2000.
28. Jamal, Y., Wagner, T., and Wyszynki, M.L., "Exhaust Gas Reforming of Gasoline at Moderate Temperatures," International Journal of Hydrogen Energy, 21(6):507, 1996.
29. Jones, M.R., "Feasibility Studies of the Exhaust Gas Reforming of Hydrocarbon and Alcohol Fuels", PhD Thesis, Automotive Engineering Center, School of Manufacturing and Mechanical Engineering, University of Birmingham, April 2002.
30. Ju D., Woo, J., Deuk, S., and Sung, B., "Partial Oxidation (POX) Reforming of Gasoline for Fuel-Cell Powered Vehicles Applications", Korean Journal of Chemical Engineering, 19(6):921, 2002.
31. Ju, D., and Woo, J., "Partial Oxidation Reforming Catalyst for Fuel Cell Powered Vehicles Applications," Catalysis Letters, 8:3, 2003.
32. Ju.D., Sreekumar, K., Deuk, S., Gwon, B., and Hoon, S., "Studies on Gasoline Fuel Processor System for Fuel Cell Powered Vehicle Applications," Applied Catalysis A: General, 215:1, 2001.
33. Krumpelt, M., Krause, T.R., Carterm J.D., Kopasz, J.P., and Ahmed, S., "Fuel Processing for Fuel Cell Systems in Transportation and Portable Power Applications," Catalysis Today, 77:3, 2002.
34. Kumar, R., Ahmed, S., Krumpelt, M., and Myles, K.M., "Improved Fuel Cell System for Transportation Applications," Patent No. 5,246,566 (1993).
35. Kumar, R.V., Kastanas, G.N., Barge, S., Zamansky, V., and Seeker, R., "Hydrogen Refueling System Based on Autothermal Cyclic Reforming", Proceeding of the 2002 US DOE Hydrogen Program Review, NREL/CP-610-32405, 2002.
36. Loffler, D.G., Taylor, D., and Mason, D., "A light hydrocarbon Fuel Processor Producing High-Purity Hydrogen", Journal of Power Sources 117(1-2): 84, 2003.
37. Lyon, R., Private Communications, Energy and Environmental Research Corp., 1996.
38. Middle East Petrotech, "Hydrogen Plants for the New Millennium," Conference and Exhibition, October 2001.

39. Miller, J., "New Argonne Technologies Help in the Transition to the Hydrogen Fueled Vehicles," Chemical Technology Division, ANL, 2001.
40. Milliken, J., Krumpelt, M., and Osborne, S., "New Partial Oxidation Catalysts for Liquid Fuel Reforming in Fuel Cell Systems," Transportation for the 21th Century, 2001.
41. News from Argonne's Transportation Technology R&D Center, Transforum, 2(1), Spring 1999.
42. Newson, E., and Truong, T.B., "Low-Temperature Catalytic Partial Oxidation of Hydrocarbons (C₁-C₁₀) for Hydrogen Production," International Journal of Hydrogen Energy, 28: 1379, 2003.
43. Office of the Press Secretary, "Hydrogen Fuel Initiative Can Make Fundamental Difference," <http://www.whitehouse.gov/news/release>, 2003.
44. Ogden, J.M., Review of Small Stationary Reformers for Hydrogen Production, Princeton University, New Jersey, 2002.
45. Oh, S.H., and Sinkevitch, R.M., "Carbon Monoxide Removal from Hydrogen Rich Fuel Cell Feedstream by Selective Catalytic Oxidation," Journal of Catalysis, 142 (1): 254, 1993.
46. Pacheco, M., Sira, J., and Kopaz, J., "Reaction Kinetics and Reactor Modeling for Fuel Processing of Liquid Hydrocarbons to produce Hydrogen: Isooctane Reforming," Applied Catalysis A: General, 250:161, 2003.
47. Pereira, C., Bae, J.M., Ahmed, S., Krumpelt, M., "Liquid Fuel Reformer Development: Autothermal Reforming of Diesel Fuel," Proceedings of the 2000 Hydrogen Program Review, NREL/CP-570-28890, 2000.
48. Perry, R.H., Green P.W., and Maloney J.O., Perry's Chemical Engineer's Handbook, Seventh edition, McGraw-Hill Professional, New York, 1997.
49. Schubert, M.M., Kahlich, M.J., Gasteiger, H.A., Behm, R.J., "Correlation between CO Surface Coverage and Selectivity/Kinetics for the Preferential CO oxidation over Pt/ γ -Al₂O₃: an in-situ-Drifts Study," Journal of Power Sources, 84: 175, 1999.
50. Sircar, S., Anand, M., Carville, B., Hufton, J., Mayorga, S., and Miller, B., "Sorption Enhanced Reaction Process (SERP) for Production of Hydrogen", Presented at the USDOE Hydrogen R&D Program Review Meeting, 1996.

51. Springman, S., Friedrich, G., Himmen, M., Sommer, M., and Eigenberger, G., "Isothermal Kinetic Measurements for Hydrogen Production for Hydrocarbon Fuels using a Novel Kinetic Reactor Concept," *Applied Catalysis A: General*, 235:101, 2002.
52. Thijsen, "Cost Analysis of Fuel Cell System for Transportation-Pathways to Low Cost", Presentation to DOE, 2001.
53. Tonkovich, A.L., Fitzgerald, S.P., Zilka, J.L., LaMont, M.J., Wang Y., Vander Wiel, D.P., and Wegeng, R.S., *Microchannel Chemical Reactors for Fuel Processing Applications, II, Compact Fuel Vaporization*, Pacific Northwest National Laboratory, Richland, WA, 1999.
54. Tonkovish, A.L., Jiménez, D.M., Zilka, J.L., LaMont, M., Wang, Y., and Wegeng, R.S., *Microchannel Chemical Reactors for Fuel Processing*, Pacific Northwest National Laboratory, Richland, WA, 1997.
55. US Department of Energy, Office of Transportation Technologies, Annual Progress Report, 2001.
56. Wegeng, R.S., "Reducing the Size of Automotive Fuel Reformers," presented at IQPC Fuel Cells Infrastructure Conference, Chicago, IL, 1999.
57. Whyatt GA, Tegrotenhuis W.E., Geeting J., Davis J.M., Wegeng R.S., and Pederson L.R., "Demonstration of Energy Efficient Steam Reforming in Microchannels for Automotive Fuel Processing", *Proceedings of the Fifth International Conference on Microreaction Technology*, Springer, Berlin, 2002.

APPENDIX

APPENDIX A: CONTROL TEMPERATURE PROFILE

The objective of these experiments was to improve the reactor temperature control by maintaining an interval between -10 to $+10^{\circ}\text{F}$. When the reactor reached the desired temperature, the switch of the controller was turned off. The temperature continued increasing several degrees and then began to decrease. Once the temperature was in the desired temperature range again, the switch was turned on. After the temperature decreased several degrees and began to increase by one or two degrees, the switch was turned off again. This procedure was repeated continuously until an appropriate temperature profile of $\pm 10^{\circ}\text{F}$ range was obtained. The temperatures chosen to do these experiments were 300°F , 350°F , 400°F , 450°F , and 500°F . Experiments with other temperatures were not performed since the reactor behavior, using the same technique, was always the same (see graphs below)

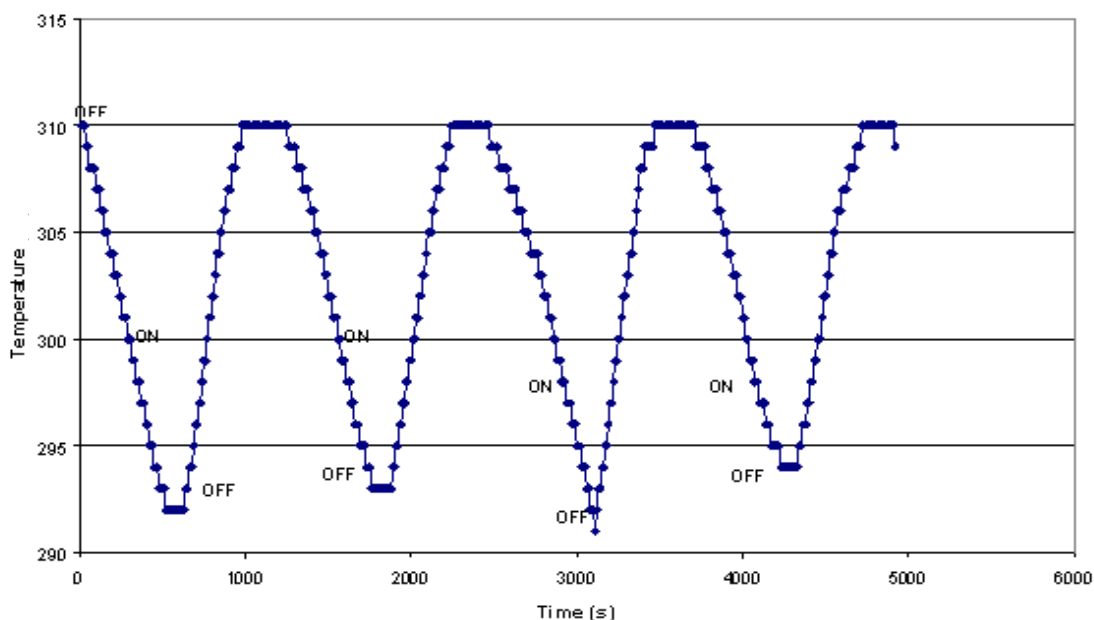


Figure A.1. Control Temperature Profile of Reforming Reactor at 300°F .

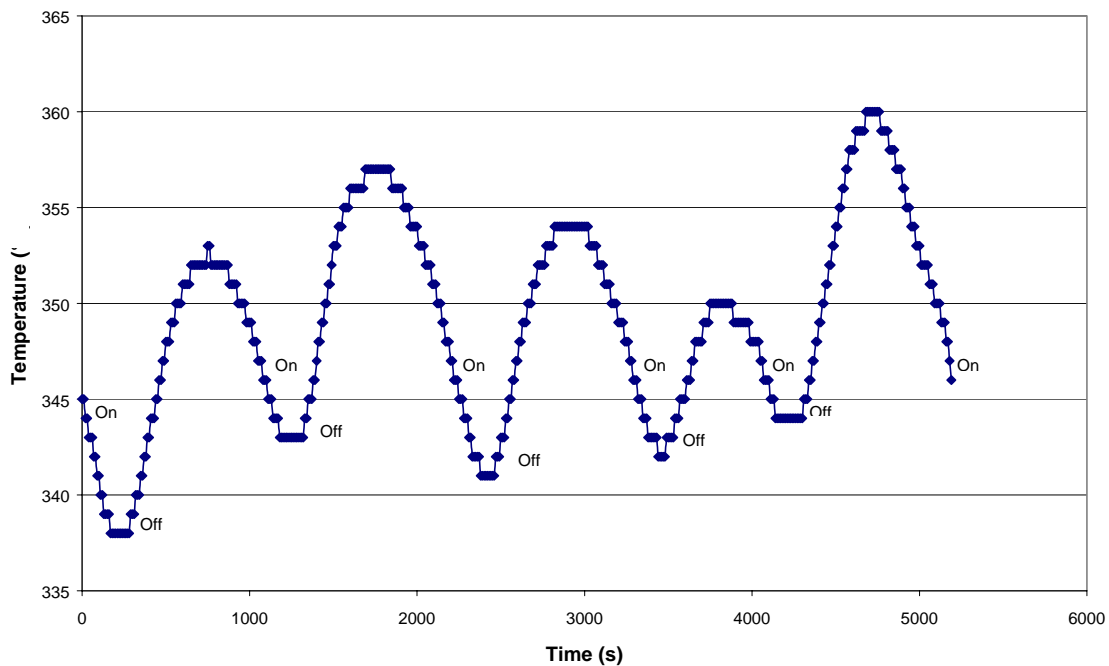


Figure A.2. Control Temperature Profile of Reforming Reactor at 350°F.

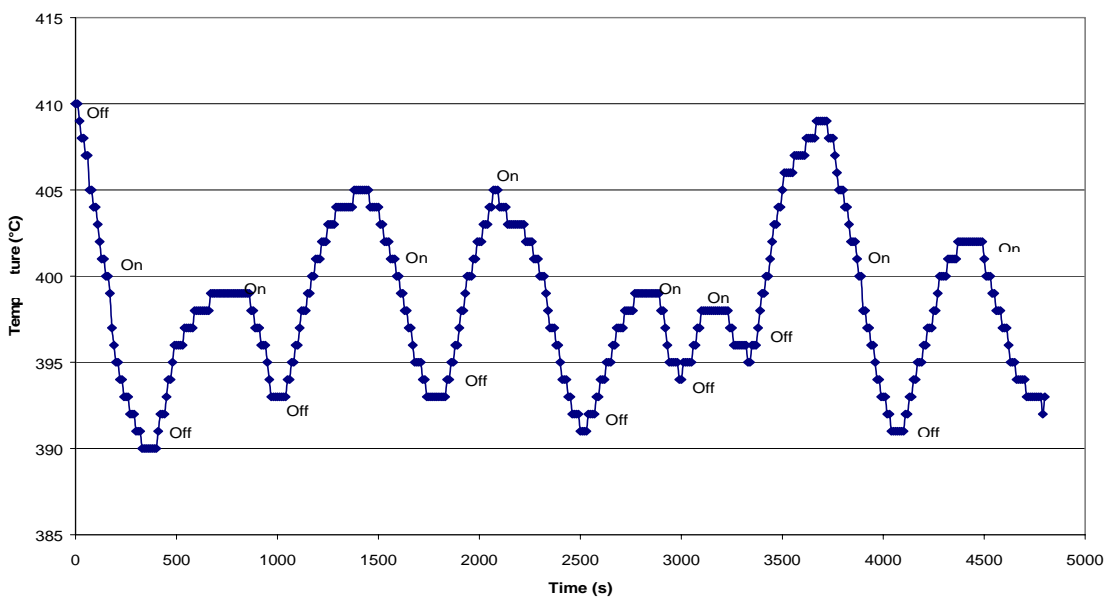


Figure A.3. Control Temperature Profile of Reforming Reactor at 400°F.

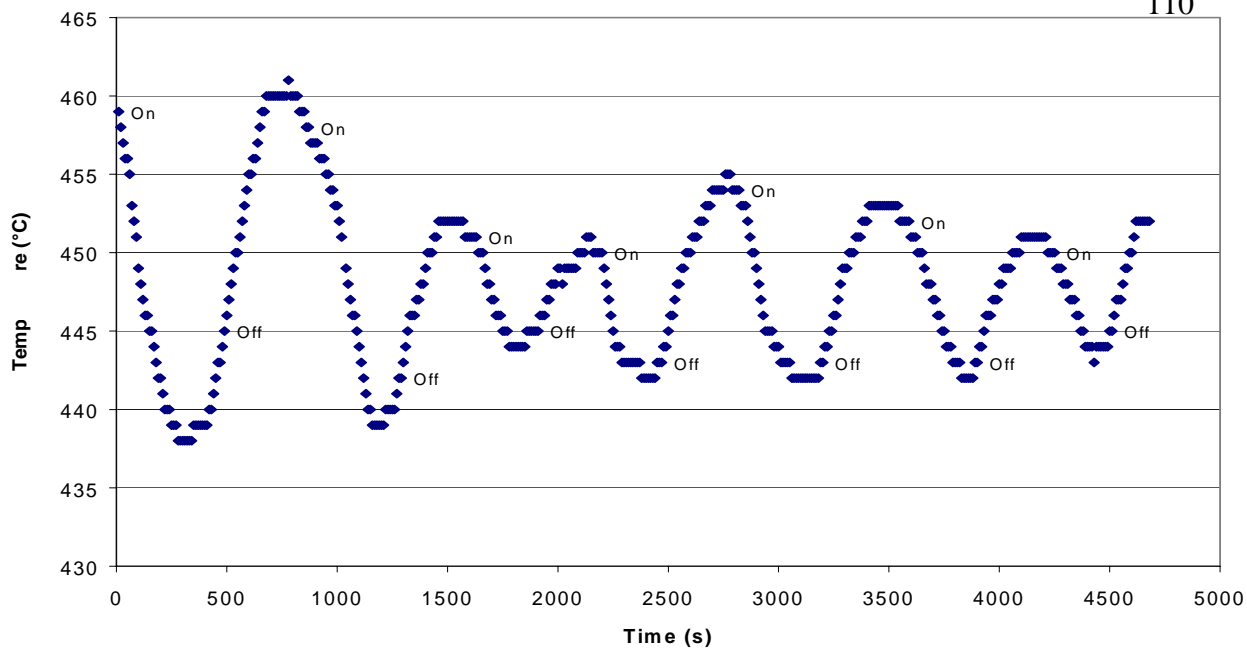


Figure A.4. Control Temperature Profile of Reforming Reactor at 450°F.

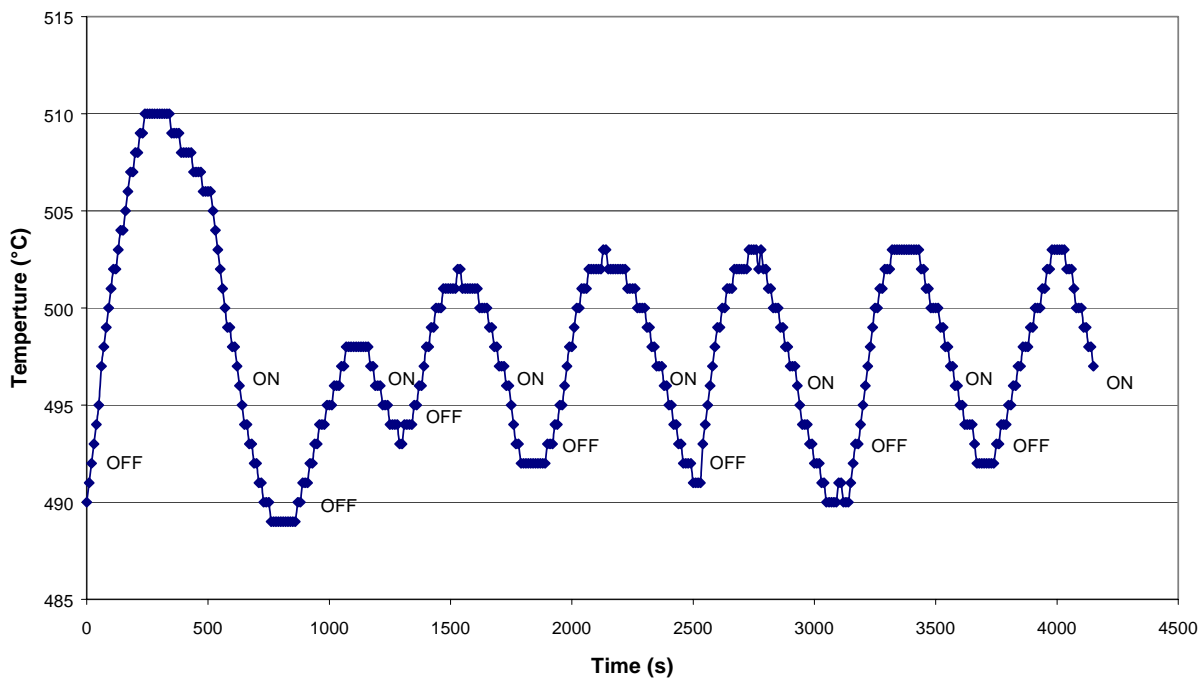


Figure A.5. Control Temperature Profile of Reforming Reactor at 500°F.

Preliminary experiments at different O_2 /fuel ratios were performed with the controller switch off. These experiments had the purpose to see how the temperature increased only with the heat of the oxygen reaction with methanol and control the heat in the reactor. It can be seen that the temperature increased more rapidly with an oxygen-to-fuel (x) ratio of 0.54. This is because at $x = 0.5$, the reaction is strongly exothermic. With no oxygen fed, the temperature increased due to the other reactants (fuel and water) were fed hot. Higher x ratios showed lower temperature rise.

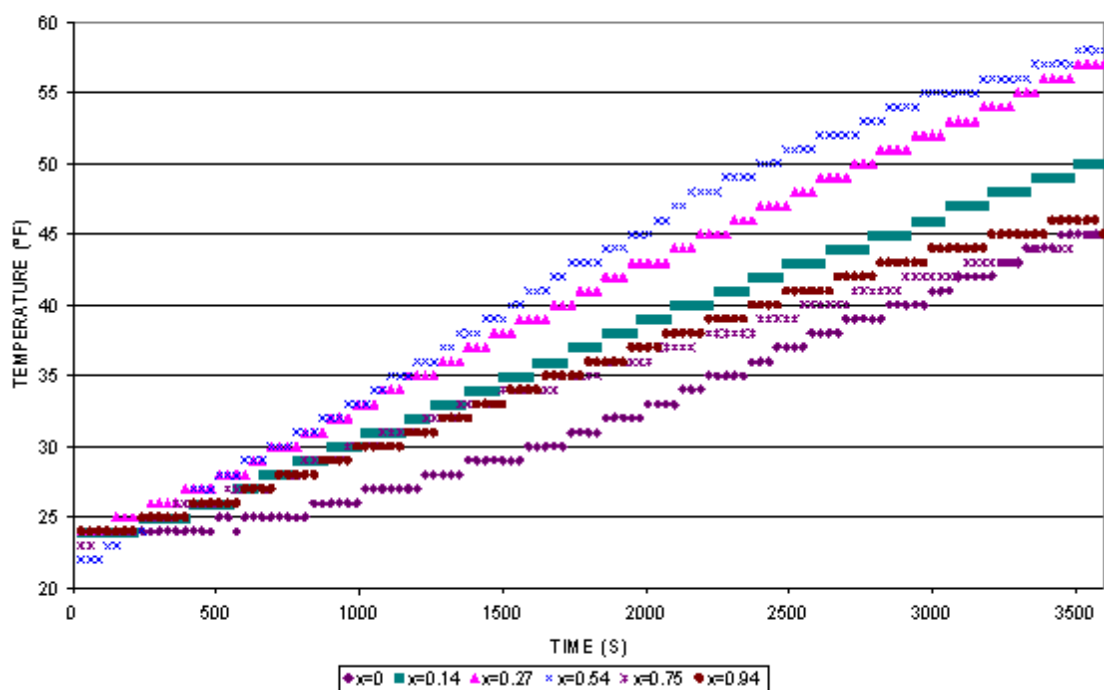


Figure A.6. Oxygen to methanol effect in the BSTR temperature.

APPENDIX B: CALIBRATION PLOTS

B.1 Calibration plots for GC-TCD analysis

The calibration plots obtained from GC-TCD analysis for hydrogen, oxygen, methane, carbon monoxide, and carbon dioxide are shown below. Also, the equation of the straight line and coefficient of linearity (R^2) are presented.

The plots were constructed at different volumes (0.02, 0.04, 0.06, 0.08, 0.10, 0.20, 0.30, 0.40, 0.50, 0.60, 0.70, 0.80, 0.90 and 1.0 mL) from each of the pure gases. Each gas had a purity of almost 99.999%. When the TCD detected the pure gas at a certain retention (see table B.1) it gave a peak signal, which was integrated by the HP 3396 Series II Integrator. This integration value was plotted versus its volume percent (i.e., $(0.10\text{mL}/1.0\text{mL}) \times 100$). Each injection volume was analyzed five times. Average values were reported. Hydrogen calibration curves were made separately, at low and high concentrations, in order to know with more accuracy the concentration of hydrogen in the reformat. This is done when the analytical equipment does not have enough sensitivity for certain compounds.

Table B.1. Standard pure gases and their average retention times.

Gas	Average Retention Time (min.)
Hydrogen	0.536
Oxygen	0.885
Methane	2.095
Carbon Monoxide	2.467
Carbon Dioxide	15.520

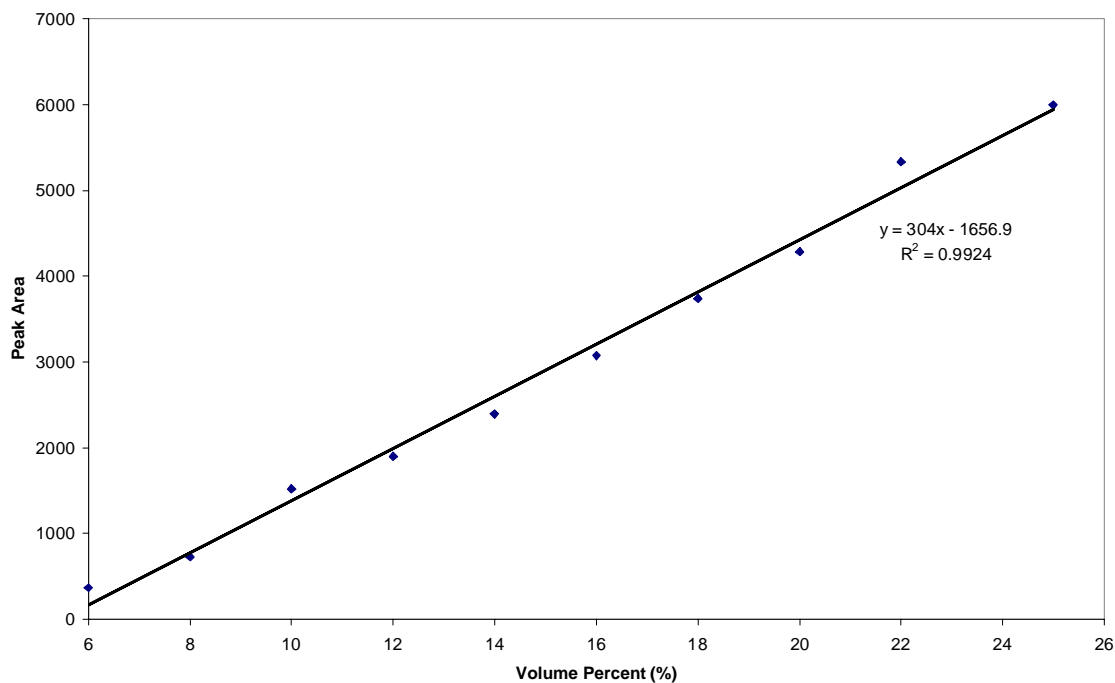


Figure B.1. Hydrogen Calibration Curve-Low Concentrations

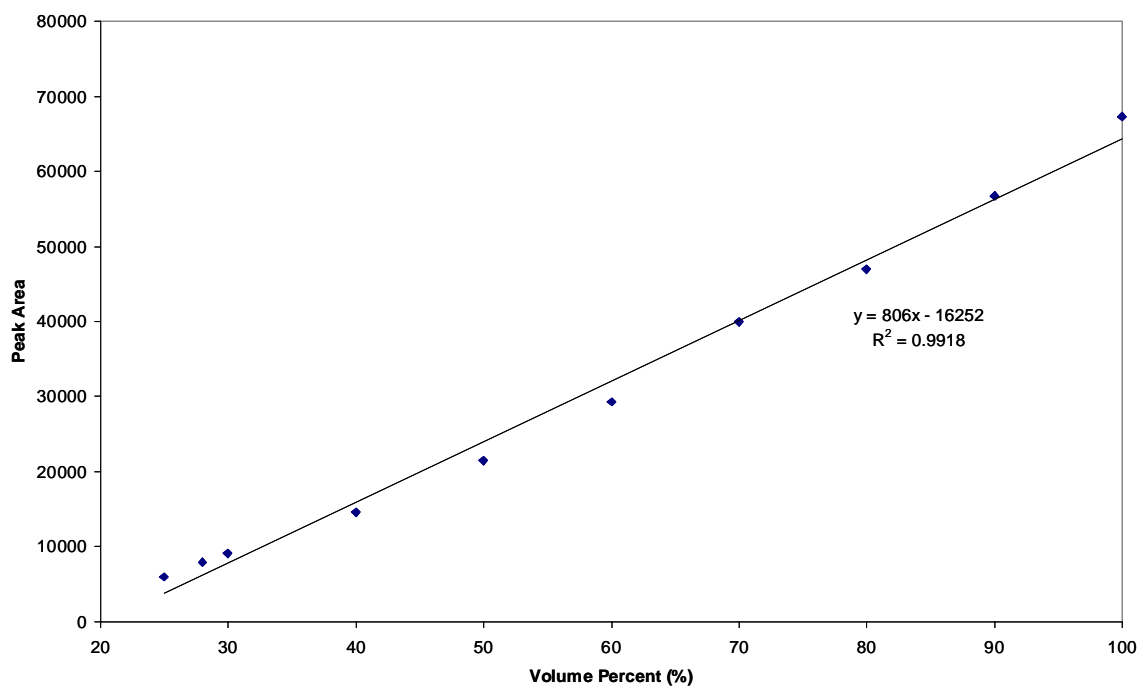


Figure B.2. Hydrogen Calibration Curve-High Concentrations

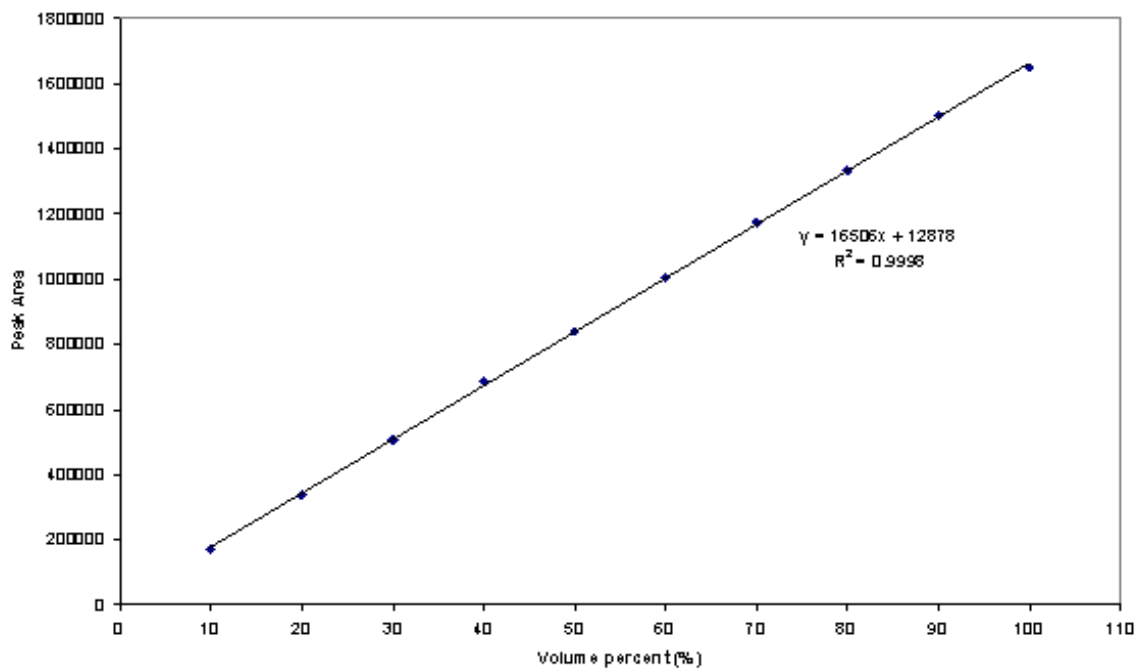


Figure B.3. Oxygen Calibration Curve

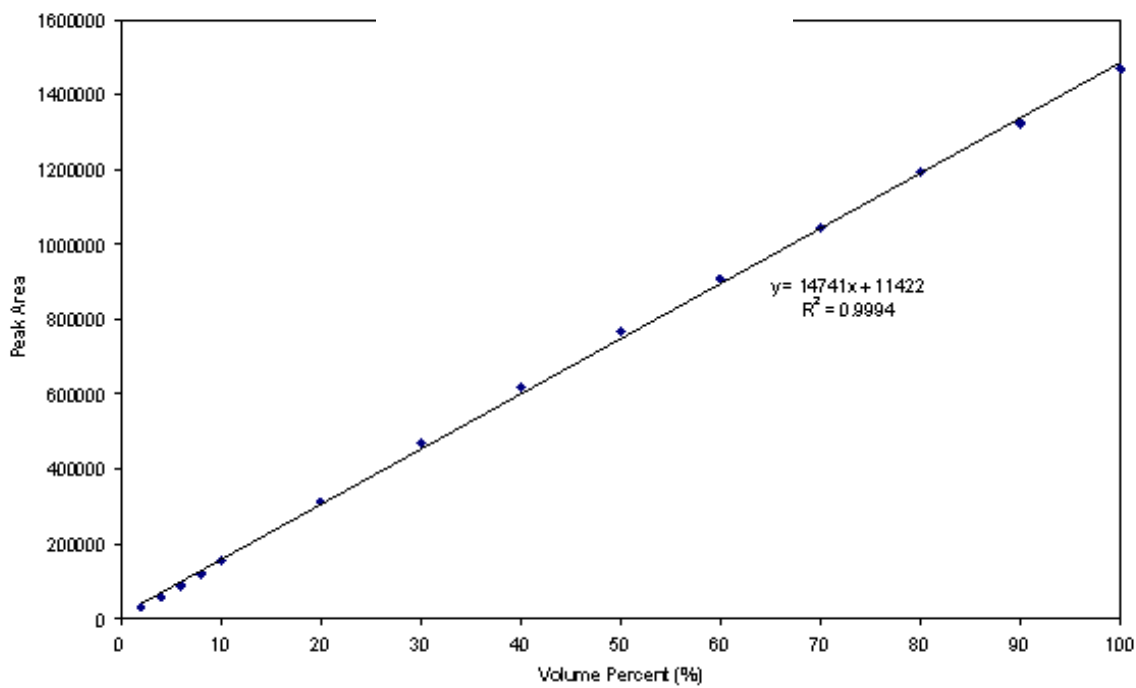


Figure B.4. Methane Calibration Curve

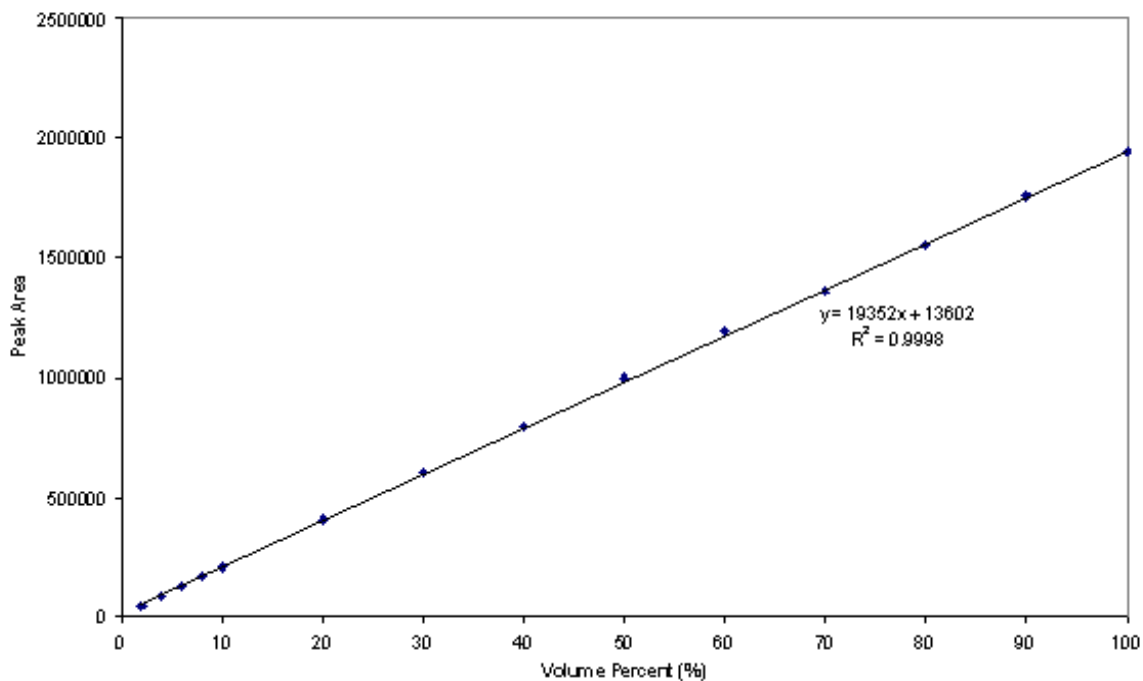


Figure B.5. Carbon Monoxide Calibration Curve

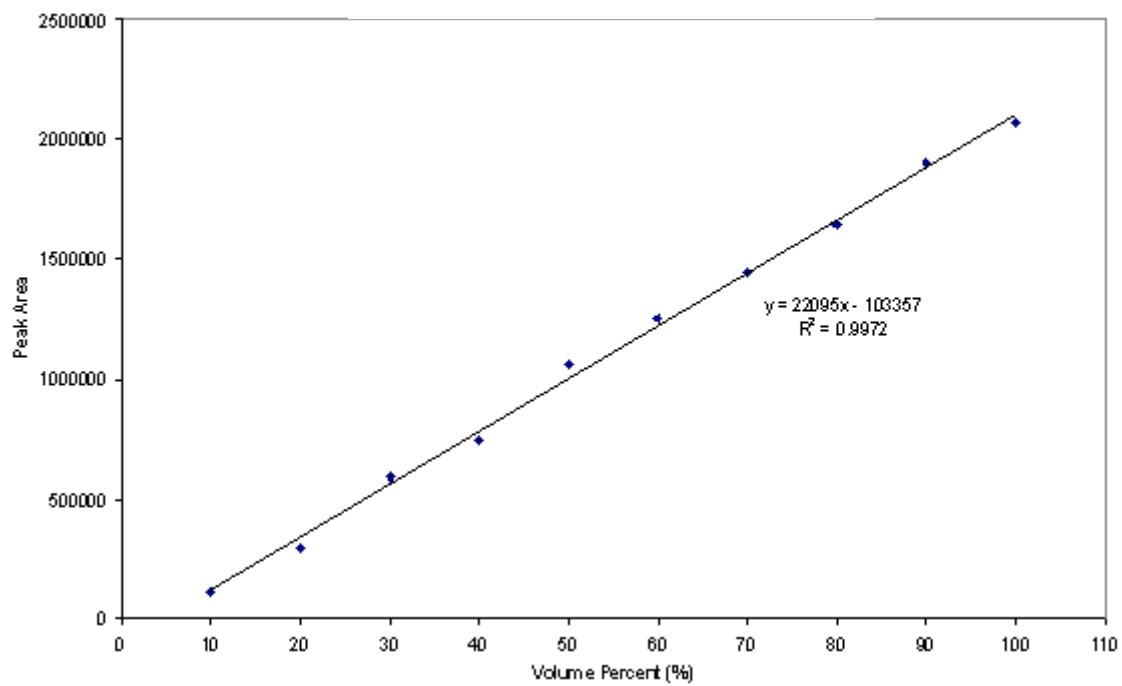


Figure B.6. Carbon Dioxide Calibration Curve

APPENDIX C: EXAMPLE RESULTS

C.1. Mass Balance for Methanol

In this section, a discussion of the how the mass balance was calculated for the autothermal reforming of methanol and for the system used to perform the experiments will be given. Figure C.1 shows a simplified diagram of the system used.

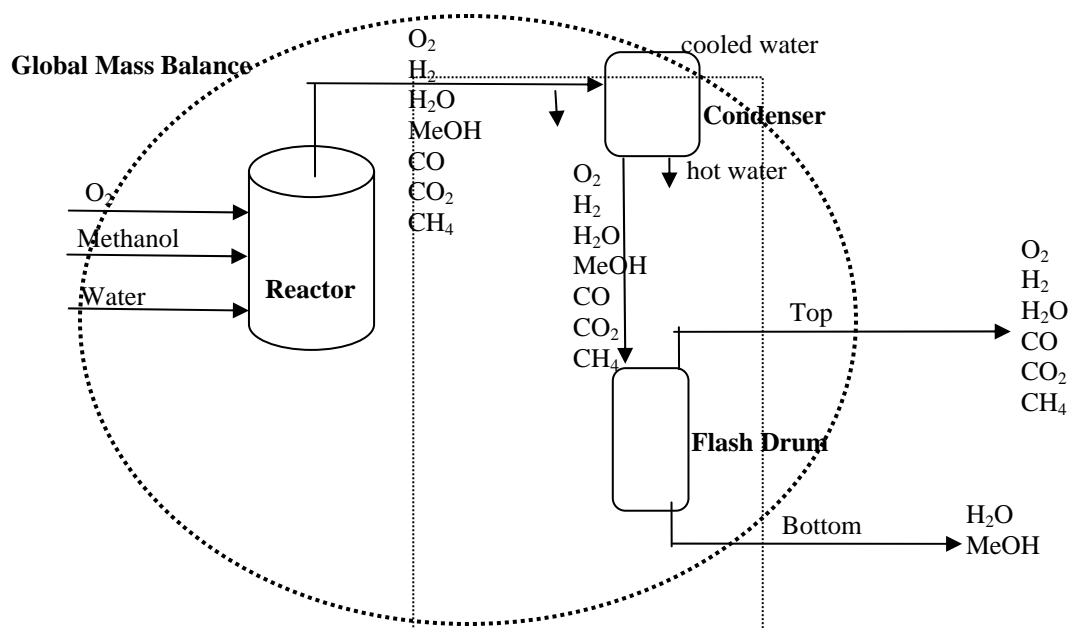


Figure C.1. Diagram of the system studied for the autothermal reforming of methanol.

The mass flowrate at the top exit gas of the flash drum was calculated by global mass balance in the whole system (see circle dashed-lines in the diagram). The sum of the three feeds (oxygen, methanol, and water) entering the reactor will be equal to the sum of the mass flowrates at the top and bottom of the flash drum.

The water molar fraction at the top of the flash drum can be calculated using the equation:

$$y_{\text{H}_2\text{O}} = \frac{P^{\text{sat}}(T)}{P_{\text{total}}} \quad (\text{C.1})$$

where $P^{\text{sat}}(T)$ is the saturation vapor pressure at the temperature of the flash drum exit gas. This temperature was assumed by adding the temperature of the condenser (11°C) to the ambient temperature (25°C) (2). For all the experiments run, the exit gas at the top of the flash drum was approximately 36°C .

Using Antoine equation for water (25):

$$\ln(P) = 18.3036 - \frac{3816.44}{-46.13 + T(\text{K})} \quad (\text{C.2})$$

$T = 36 + 273.15 = 309.15\text{K}$, and the saturation pressure was $44.41\text{mm Hg} = 0.058438\text{atm}$.

If the total pressure of the system was 1 atm, the molar fraction of water at the exit gas of the flash drum was

$$y_{\text{H}_2\text{O}} = \frac{0.058438\text{atm}}{1\text{atm}} = 0.058438$$

Then, the mass compositions for every gas at the top of the flash drum were calculated. The water content and methanol in the condensable at the bottom of the exit flash drum was measured by density (see section 3.3). Doing a mass balance around the condenser and the flash drum (see dashed-square in the diagram), it can be calculated the water concentration at the reactor exit gas. The condensable water molar quantity was added to the water molar quantity calculated at the top of the flash drum. The quantity of methanol measured by density at the bottom of the flash drum, was the same at the exit reactor gas because it was assumed that all the methanol that did not react was condensed.

C.2. GC-TCD chromatograms for the reformat analysis

An example of a chromatograph obtained from a GC-TCD of the exit gas sample of methanol taken every half hour during 4.5 hours is shown in figures C.2 and C.3. Example of isooctane chromatograms are shown in figure C.4. Every sample was taken around 36°C. The reactor temperature was 500°F and the oxygen-to-fuel and water-to-carbon ratios were 0.5 and 1.12, respectively. The order of appearance is hydrogen, oxygen, carbon monoxide and carbon dioxide. Methane was never observed in any of the chromatograms. Hydrogen was always injected in a separated sample because of its characteristic of showing its peak at a negative polarity with helium as a carrier gas. To analyze the hydrogen concentration, the polarity of the detector was changed from positive to negative in order to see the peak upward.

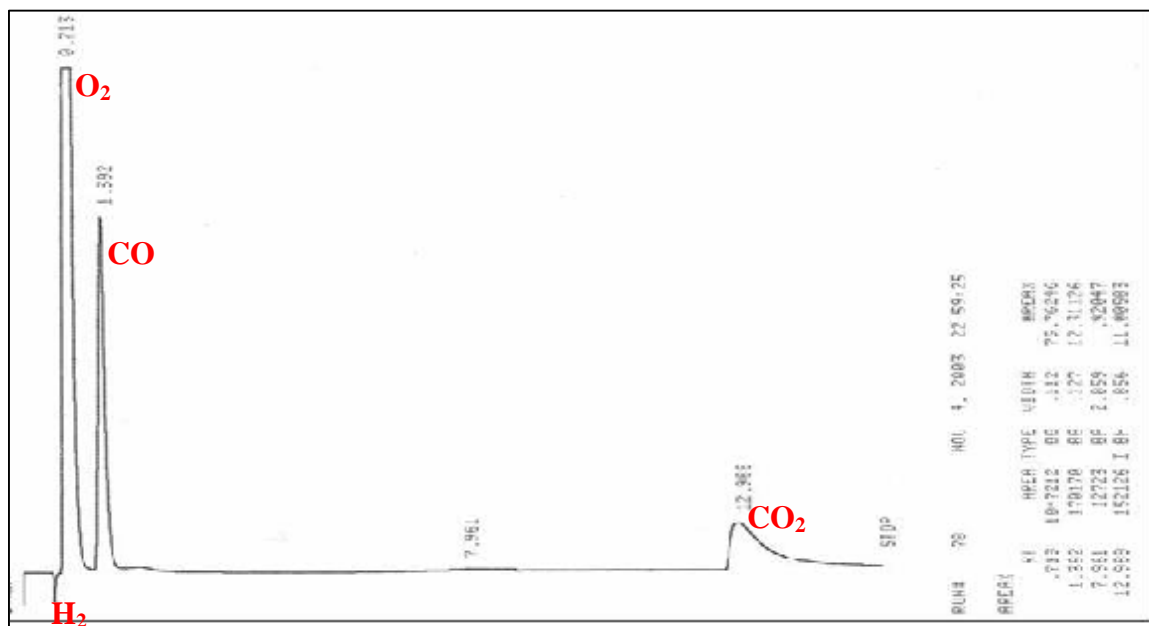


Figure C.2. GC-TCD chromatograph of the product gas composition of methanol at 500°F, $O_2/\text{fuel} = 0.5$; $H_2O/C = 1.12$.

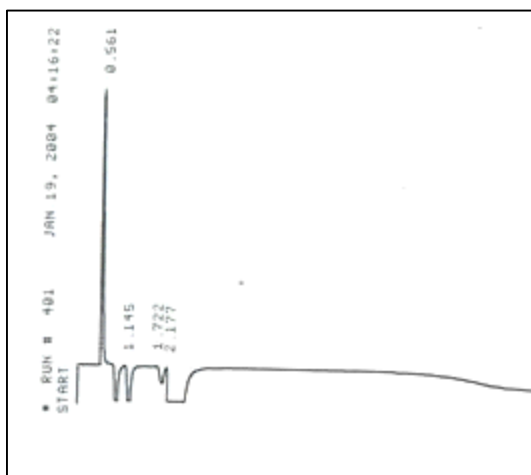


Figure C.3. GC-TCD chromatograph of the product gas composition of methanol at 500°F, $O_2/\text{fuel} = 0.5$; $H_2O/C = 1.12$ (injected with a negative polarity).

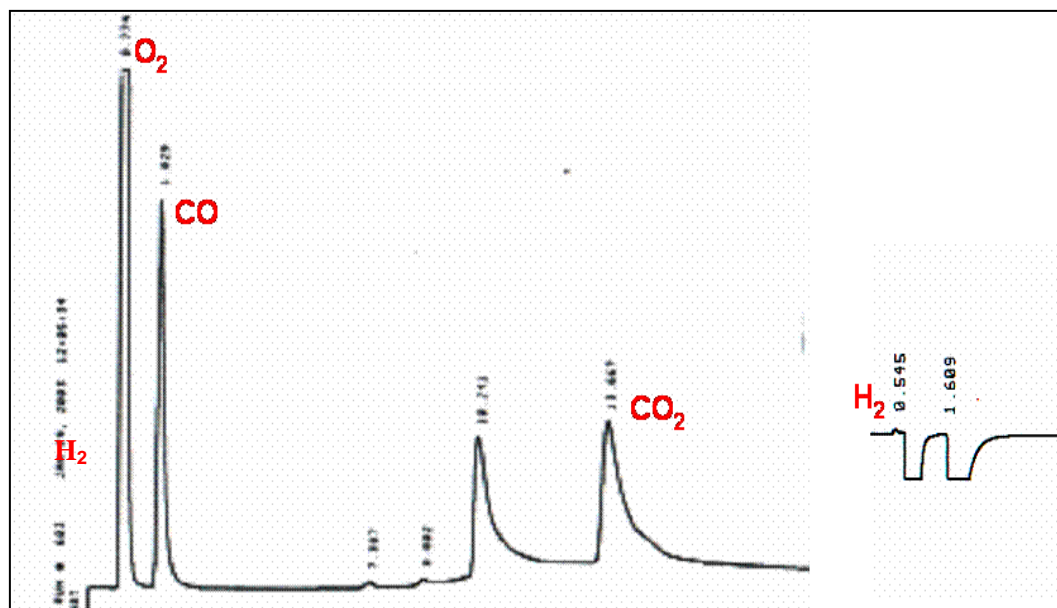


Figure C.4. GC-TCD chromatograph of the product gas composition of isooctane at 900°F, $O/C = 1.0$; $H_2O/C = 1.2$.

C.3. Hydrogen production in the exit gas reformat at different O_2 /fuel and H_2O/C ratios with methanol as a fuel

Figures C.5 - C.13 shows the hydrogen production at the flash drum exit (dry basis) at different levels and temperatures. Five samples were taken for each temperature every half hour, for 4.5 hours. The hydrogen concentration was reproducible, indicating that the catalyst was not deactivated and the reactor was operating at steady-state conditions.

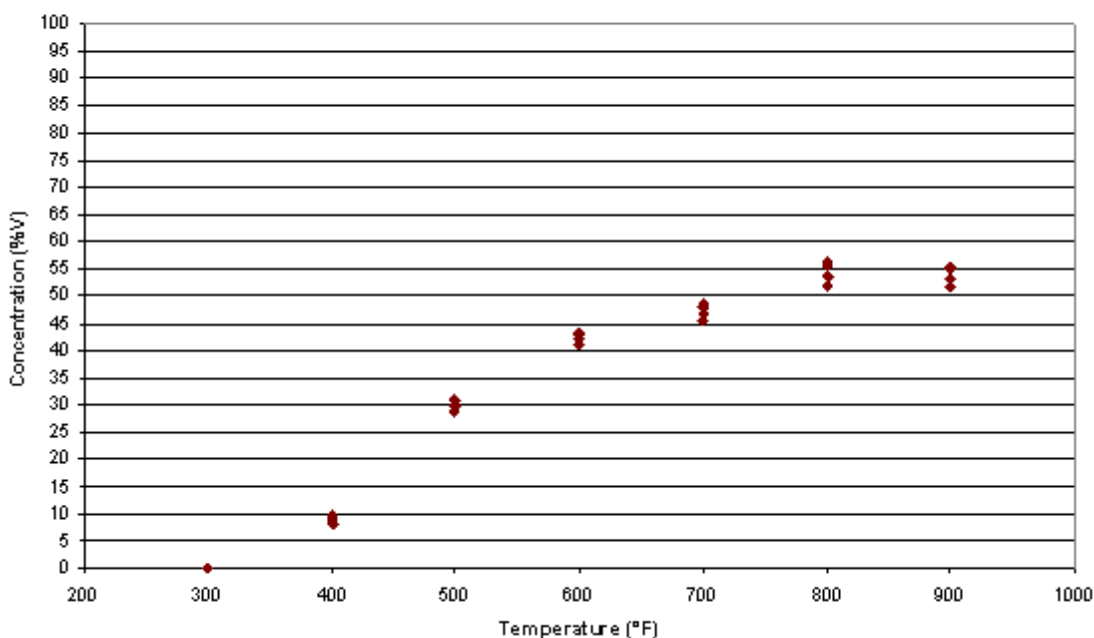


Figure C.5. Exit Hydrogen Concentration (O_2 /fuel = 0.27; H_2O/C = 0.46)

at 300, 400, 500, 600, 700, 800 and 900°F.

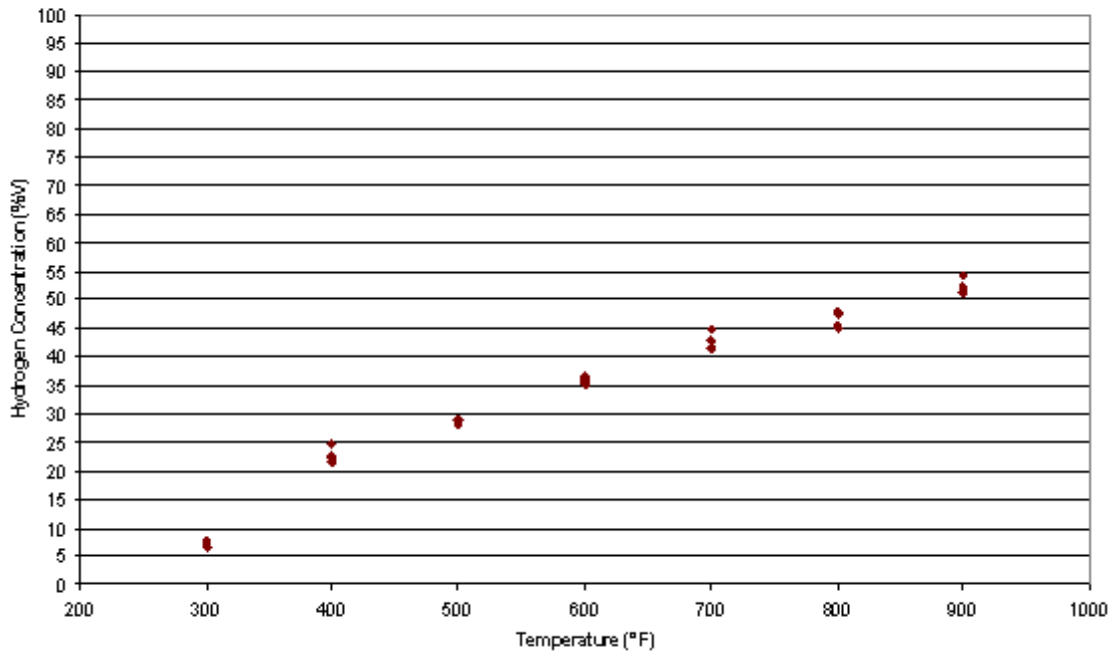


Figure C.6. Exit Hydrogen Concentration ($O_2/\text{fuel} = 0.39$; $H_2O/C = 0.46$)

... at 300, 400, 500, 600, 700, 800 and 900°F ...

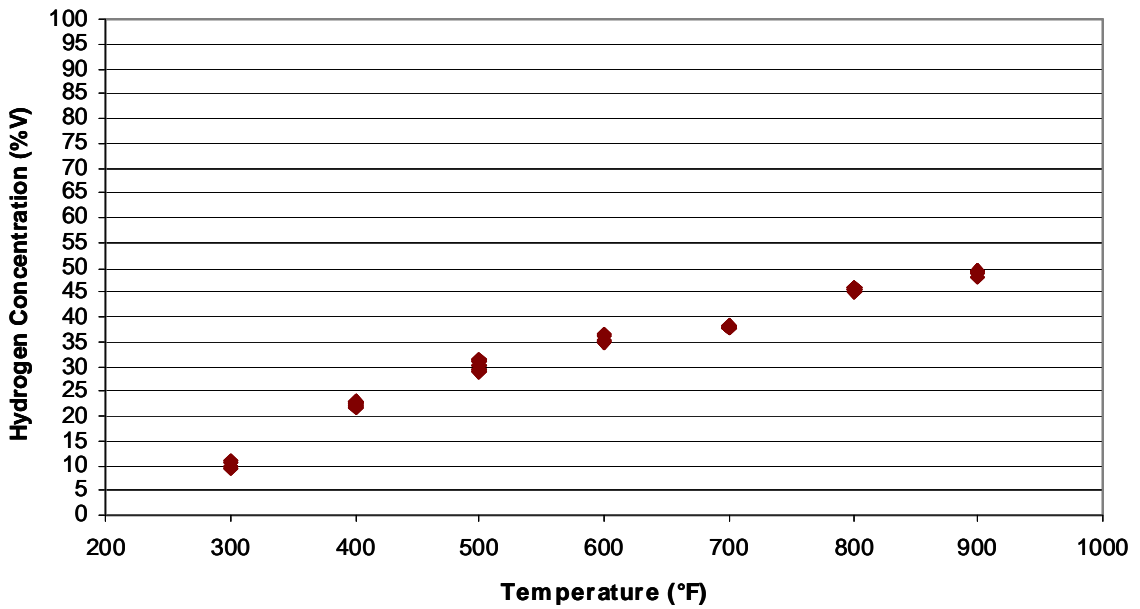


Figure C.7. Exit Hydrogen Concentration ($O_2/\text{fuel} = 0.50$; $H_2O/C = 0.46$)

at 300, 400, 500, 600, 700, 800 and 900°F.

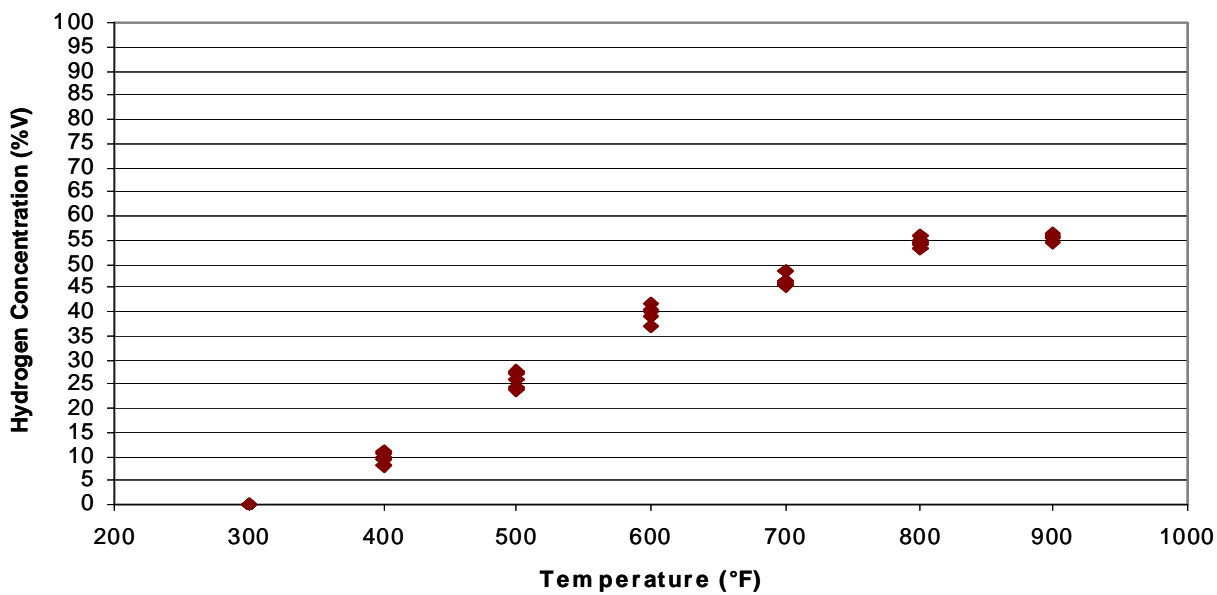


Figure C.8. Exit Hydrogen Concentration ($O_2/\text{fuel} = 0.27$; $H_2O/C = 0.76$)

at 300, 400, 500, 600, 700, 800 and 900°F.

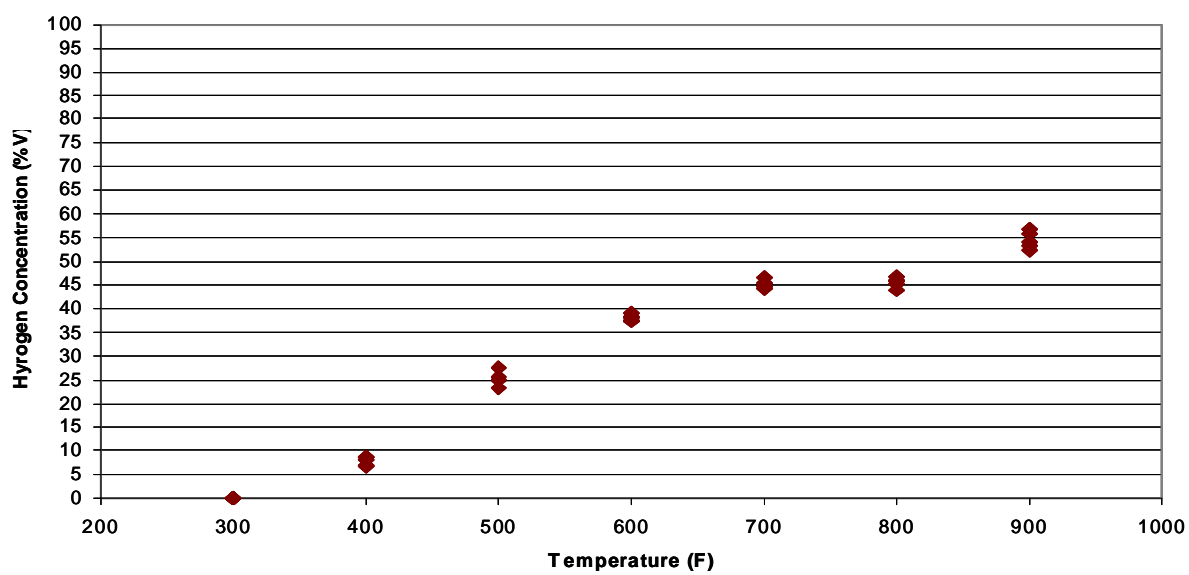


Figure C.9. Exit Hydrogen Concentration ($O_2/\text{fuel} = 0.27$; $H_2O/C = 1.12$)

at 300, 400, 500, 600, 700, 800 and 900°F.

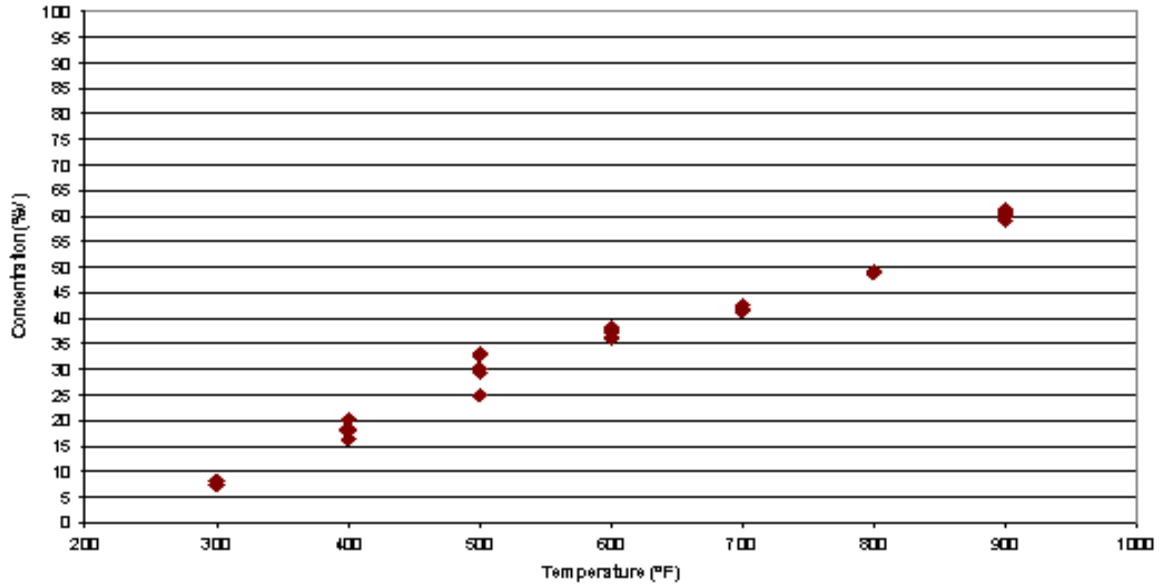


Figure C.10. Exit Oxygen Concentration ($O_2/fuel = 0.50$; $H_2O/C = 0.76$)
at 300, 400, 500, 600, 700, 800 and 900°F

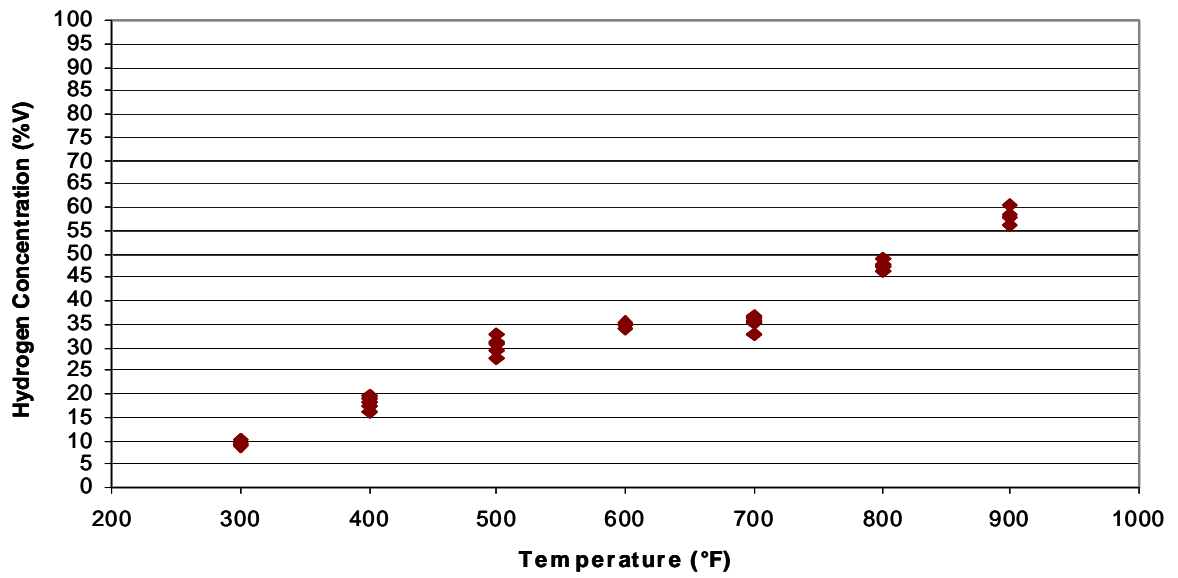


Figure C.11. Exit Hydrogen Concentration ($O_2/fuel = 0.50$; $H_2O/C = 0.76$)
at 300, 400, 500, 600, 700, 800 and 900°F.

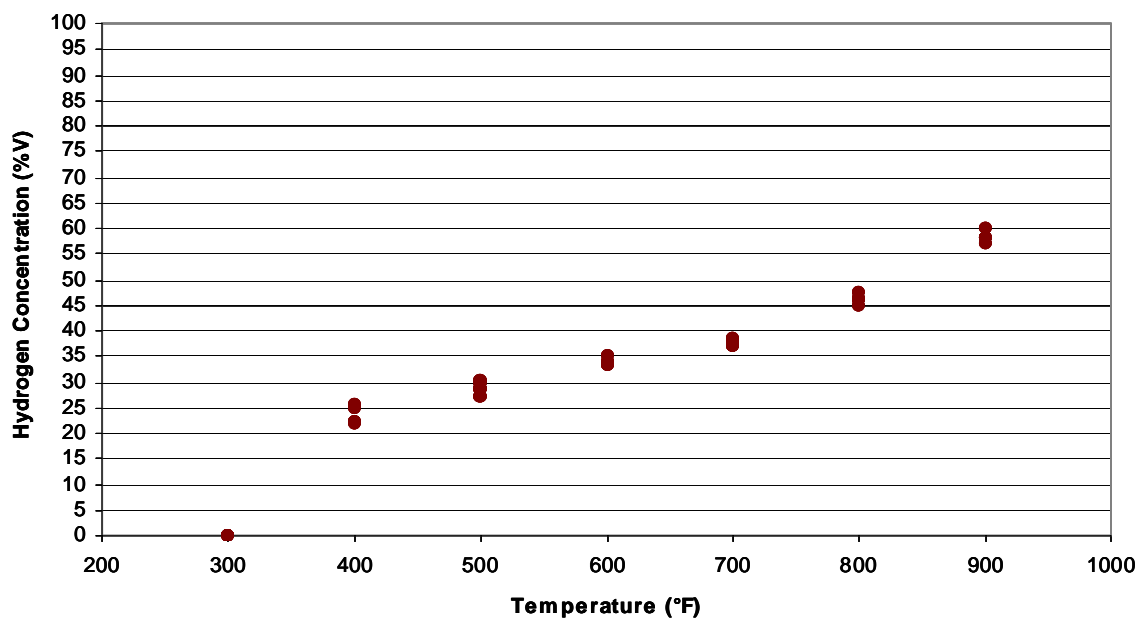


Figure C.12. Exit Hydrogen Concentration ($O_2/\text{fuel} = 0.50$; $H_2O/C = 1.12$)
at 300, 400, 500, 600, 700, 800 and 900F

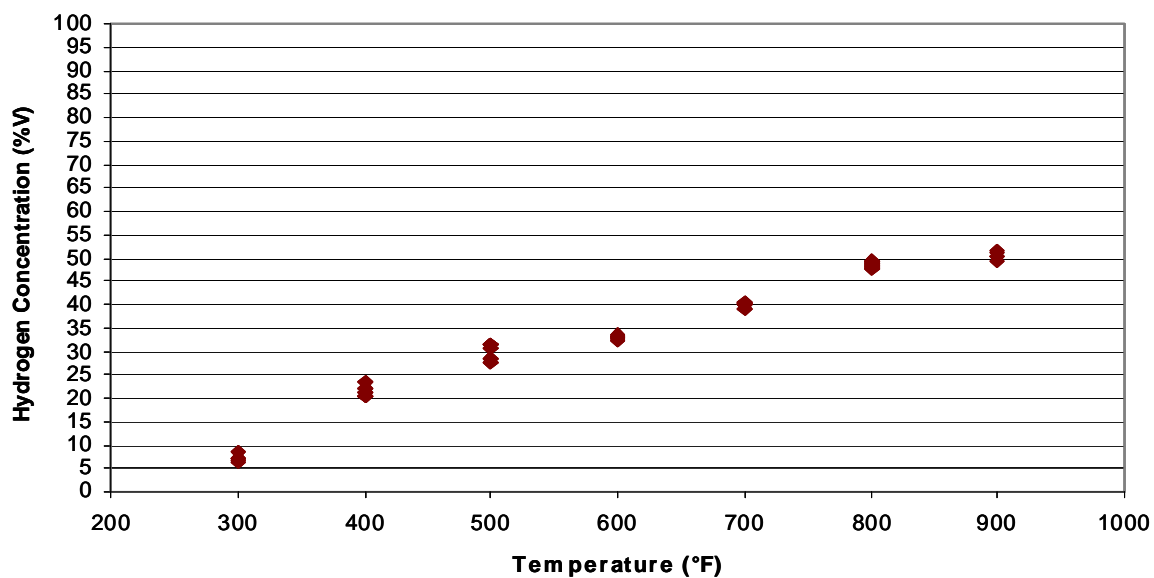


Figure C.13. Exit Hydrogen Concentration ($O_2/\text{fuel} = 0.39$; $H_2O/C = 1.12$)
at 300, 400, 500, 600, 700, 800 and 900F.

C.4. Chromatograms

These chromatograms (C.14–C.15) show the best condition ($O_2/fuel=0.27$; $H_2O/C=0.46$; $900^\circ F$) where maximum hydrogen production and minimum carbon monoxide and carbon dioxide was observed (59.8% H_2 , 14.6% CO and 12.6% CO_2).

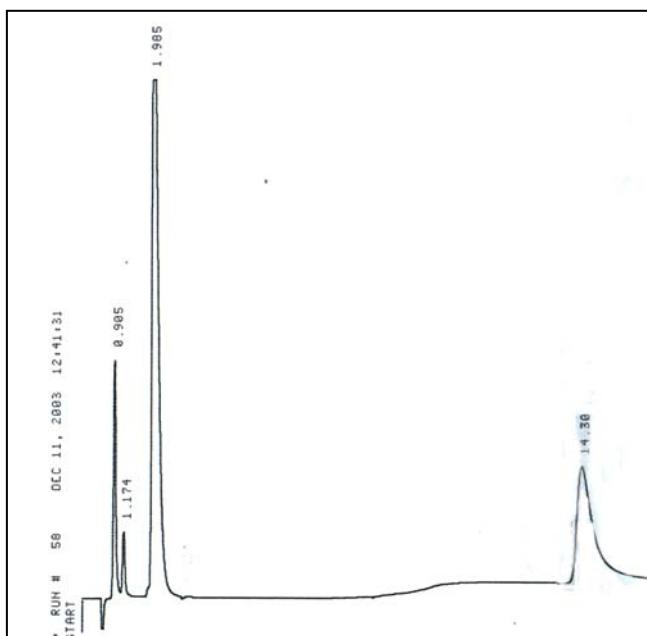


Figure C.14. Oxygen, carbon monoxide and carbon dioxide chromatograph ($O_2/fuel=0.27$; $H_2O/C=0.46$; $900^\circ F$).

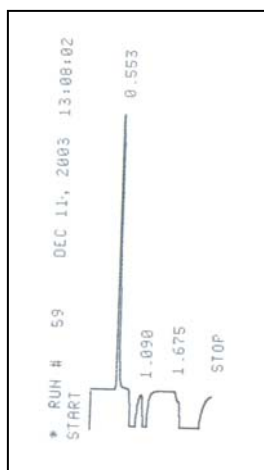


Figure C.15. Hydrogen chromatograph ($O_2/fuel=0.27$; $H_2O/C=0.46$; $900^\circ F$).

These chromatograms (C.16–C.17) show the condition ($O_2/\text{fuel}=0.5$; $H_2O/C=1.12$; 900°F) where hydrogen, carbon monoxide, and carbon dioxide production were nearly the same as in equilibrium (59% H_2 , 20% CO , and 18% CO_2).

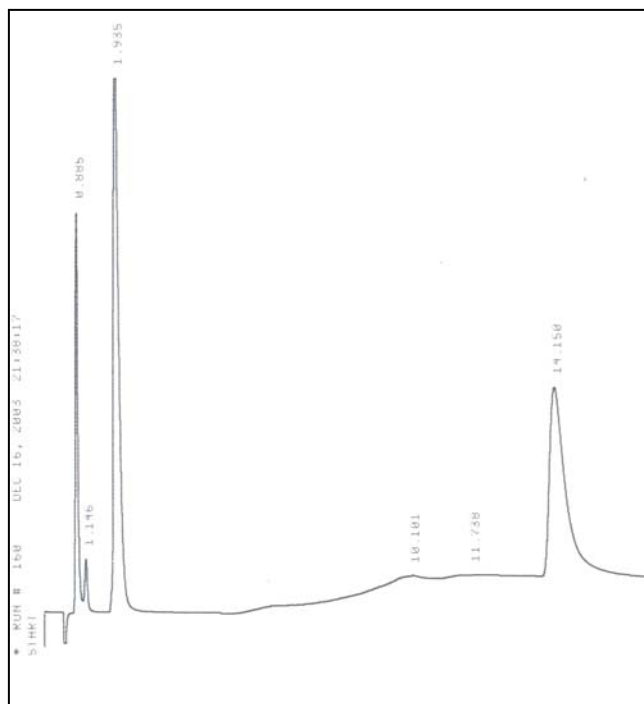


Figure C.16. Oxygen, carbon monoxide and carbon dioxide chromatograph ($O_2/\text{fuel}=0.5$; $H_2O/C=1.12$; 900°F).

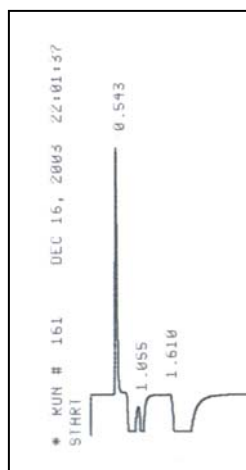


Figure C.17. Hydrogen chromatograph ($O_2/\text{fuel}=0.5$; $H_2O/C=1.12$; 900°F).

C.5. Product gas composition of methanol

This table is a summary of the methanol reformat products at different O₂/fuel and H₂O/C ratios and temperatures. Level 11 (O₂/fuel=0.39 and H₂O/C=0.76) was the best condition, where maximum hydrogen (59.8%) and minimal CO₂ (12.6%) and CO (14.6%) concentrations were found. Methane was not formed or was below the GC-TCD detection limit (2%).

Table C.1. Methanol products concentrations at different O₂/fuel and H₂O/C ratios and temperatures.

Level	Temperature (°F)	(%H ₂)	(%O ₂)	(%CO)	(%CH ₄)	(%CO ₂)	TOTAL (%)
00	300	0.00	84.78	5.76	<2	9.46	~100
	400	8.93	72.98	7.63	<2	10.47	~100
	500	30.20	46.83	14.24	<2	8.77	~100
	600	42.08	22.66	18.16	<2	17.42	~100
	700	45.91	18.46	19.16	<2	16.65	~100
	800	53.18	10.41	20.36	<2	16.17	~100
	900	52.08	15.57	21.04	<2	11.31	~100
	11	300	7.33	78.53	5.69	<2	8.49
400		17.48	57.98	10.15	<2	14.39	~100
500		31.98	47.70	15.52	<2	5.09	~100
600		37.38	37.49	12.31	<2	12.85	~100
700		41.79	31.85	11.39	<2	15.18	~100
800		49.15	21.53	13.39	<2	16.32	~100
900		59.79	13.82	14.58	<2	12.57	~100
22	300	0.00	80.00	9.89	<2	10.50	~100
	400	24.25	55.22	9.83	<2	10.84	~100

Table C.1 (continued). Methanol products concentrations at different O₂/fuel and H₂O/C ratios and temperatures.

Level	Temperature (°F)	(%H ₂)	(%O ₂)	(%CO)	(%CH ₄)	(%CO ₂)	TOTAL (%)
	500	30.69	47.92	9.88	<2	11.51	~100
	600	33.36	43.97	8.30	<2	15.23	~100
	700	37.06	36.80	8.46	<2	17.69	~100
	800	45.57	19.89	14.50	<2	20.04	~100
	900	58.06	3.62	20.39	<2	18.74	~100
10	300	7.05	78.35	5.66	<2	9.02	~100
	400	25.61	48.46	15.96	<2	10.13	~100
	500	28.37	48.56	13.99	<2	8.29	~100
	600	36.20	38.21	14.31	<2	11.48	~100
	700	42.15	29.69	13.46	<2	15.11	~100
	800	46.58	18.47	19.94	<2	15.01	~100
	900	51.54	14.70	20.42	<2	13.34	~100
21	300	8.77	73.41	8.38	<2	9.43	~100
	400	17.02	66.49	7.79	<2	8.69	~100
	500	27.54	53.83	10.02	<2	8.60	~100
	600	34.89	44.19	9.37	<2	12.45	~100
	700	34.62	37.26	7.88	<2	20.37	~100
	800	47.30	15.24	17.02	<2	20.51	~100
	900	57.24	2.01	23.17	<2	18.10	~100
02	300	0.00	91.30	1.59	<2	7.35	~100
	400	7.24	81.07	3.70	<2	7.99	~100
	500	27.43	55.15	11.27	<2	6.76	~100

Table C.1 (continued). Methanol products concentrations at different O₂/fuel and H₂O/C ratios and temperatures.

Level	Temperature (°F)	(%H ₂)	(%O ₂)	(%CO)	(%CH ₄)	(%CO ₂)	TOTAL (%)
	600	38.23	36.62	10.11	<2	15.20	~100
	700	45.40	27.56	11.94	<2	15.47	~100
	800	45.09	17.83	7.36	<2	30.00	~100
	900	53.20	10.13	14.58	<2	22.21	~100
12	300	6.60	82.66	3.58	<2	7.21	~100
	400	20.61	59.24	11.04	<2	9.39	~100
	500	31.09	48.00	15.20	<2	6.59	~100
	600	32.82	44.59	4.87	<2	17.86	~100
	700	39.86	34.09	8.93	<2	17.93	~100
	800	48.76	16.94	11.26	<2	23.36	~100
	900	49.97	17.83	16.70	<2	15.51	~100
20	300	9.63	75.11	7.21	<2	8.24	~100
	400	22.95	55.77	12.15	<2	9.54	~100
	500	29.76	46.60	12.45	<2	11.93	~100
	600	35.90	39.92	9.93	<2	15.11	~100
	700	37.97	35.47	9.14	<2	17.76	~100
	800	45.85	16.84	14.31	<2	23.15	~100
	900	48.92	17.05	19.53	<2	14.51	~100
01	300	0.00	89.45	1.49	<2	9.76	~100
	400	10.09	74.21	7.00	<2	8.87	~100
	500	28.21	49.33	12.56	<2	10.20	~100
	600	39.42	38.35	9.71	<2	12.54	~100

Table C.1 (continued). Methanol products concentrations at different O₂/fuel and H₂O/C ratios and temperatures.

Level	Temperature (°F)	(%H ₂)	(%O ₂)	(%CO)	(%CH ₄)	(%CO ₂)	TOTAL (%)
	700	46.00	25.30	13.99	<2	15.59	~100
	800	54.20	9.06	16.80	<2	20.17	~100
	900	52.63	16.03	18.61	<2	12.73	~100

C.6. Exit gas composition in the reformat (O/C=1 and H₂O/C=1) at different temperatures with isooctane as a fuel.

Figures C.18 - C.21 show the gas production at the flash drum exit (dry basis) at a level where O/C=1 and H₂O/C=1 and different temperatures. Five samples were taken for each temperature every half hour, for 4.5 hours. The gas product concentrations were reproducible, indicating that the catalyst was not deactivated and the reactor was operated at steady-state conditions.

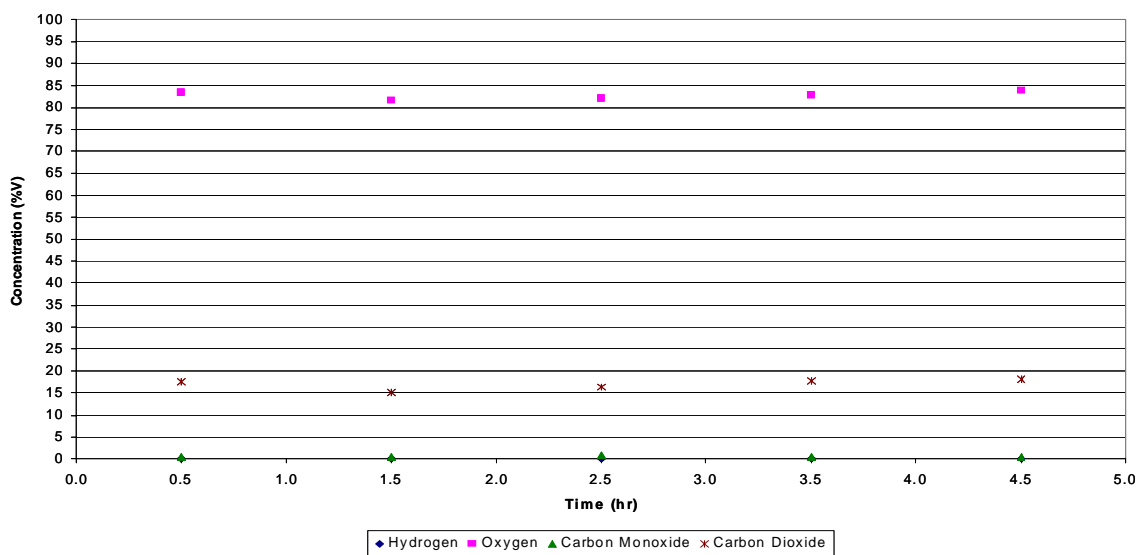


Figure C.18. Exit gas concentration with isooctane as a fuel at 600°F.

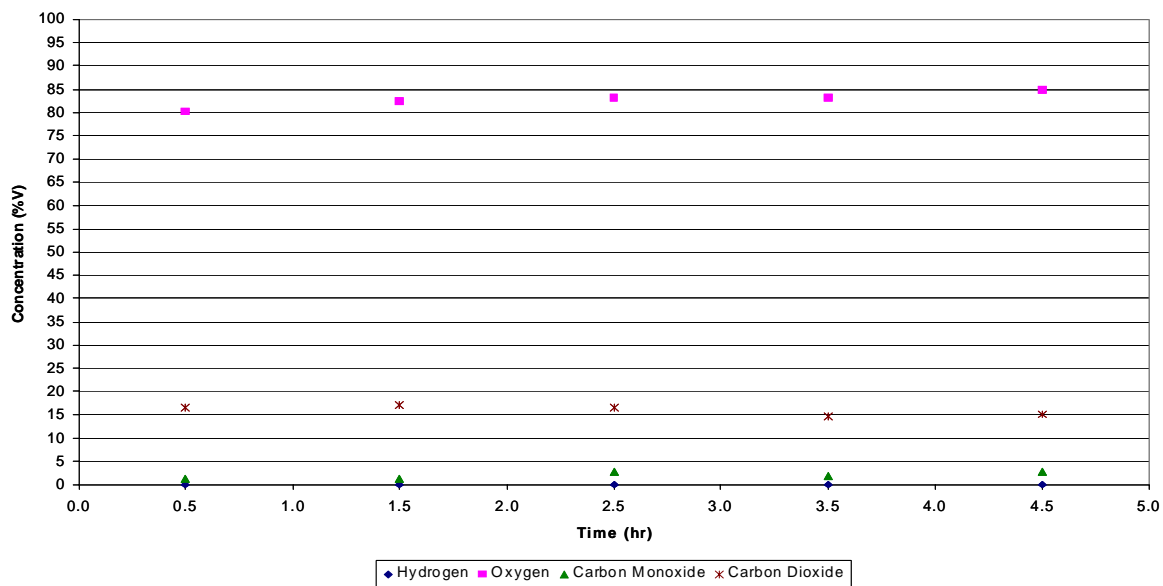


Figure C.19. Exit gas concentration with isooctane as a fuel at 700°F.

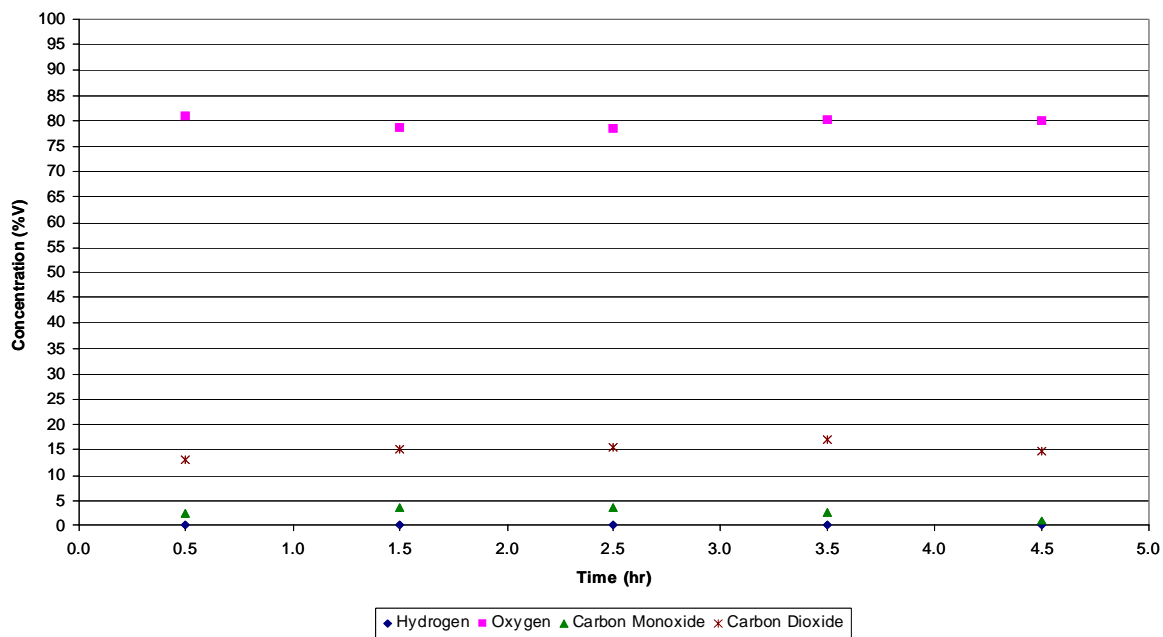


Figure C.20. Exit gas concentration with isooctane as a fuel at 800°F.

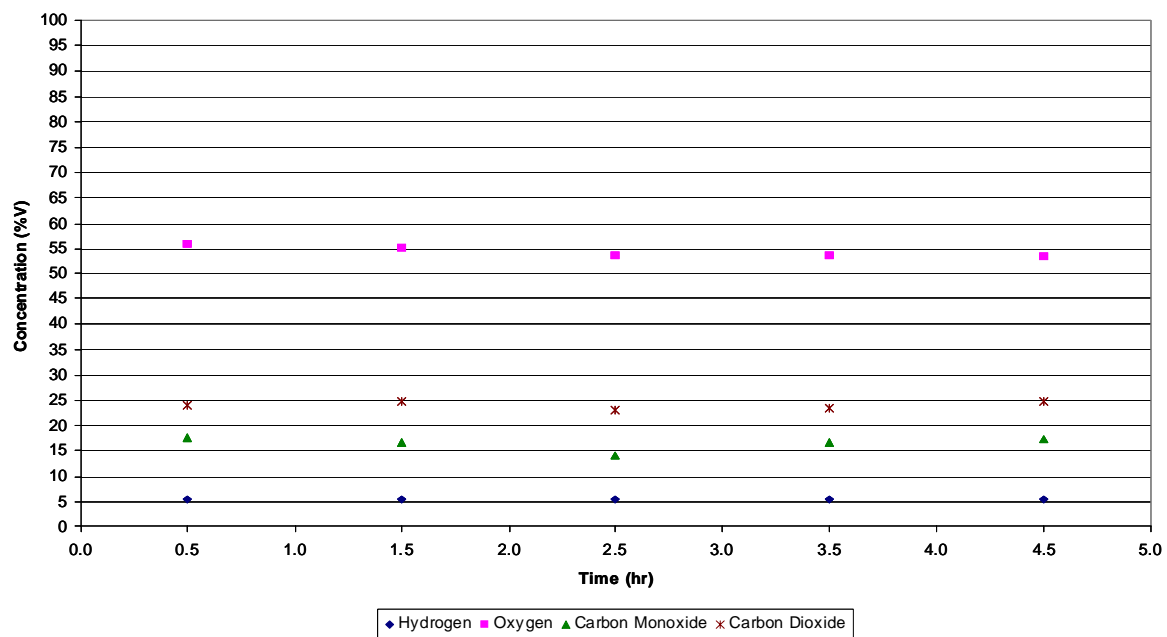


Figure C.21. Exit gas concentration with isooctane as a fuel at 900°F.

APPENDIX D: YIELD OF REACTION PRODUCTS AS A FUNCTION OF GHSV AT DIFFERENT TEMPERATURES

Figures D.1-D.6 are graphs of the product yield compositions (moles product/moles isooctane) as a function of gas hourly space velocity (GHSV). They show to have the same behavior as the literature presents, where the product gas composition decreases as the gas residence time decreases (higher GHSV) (33).

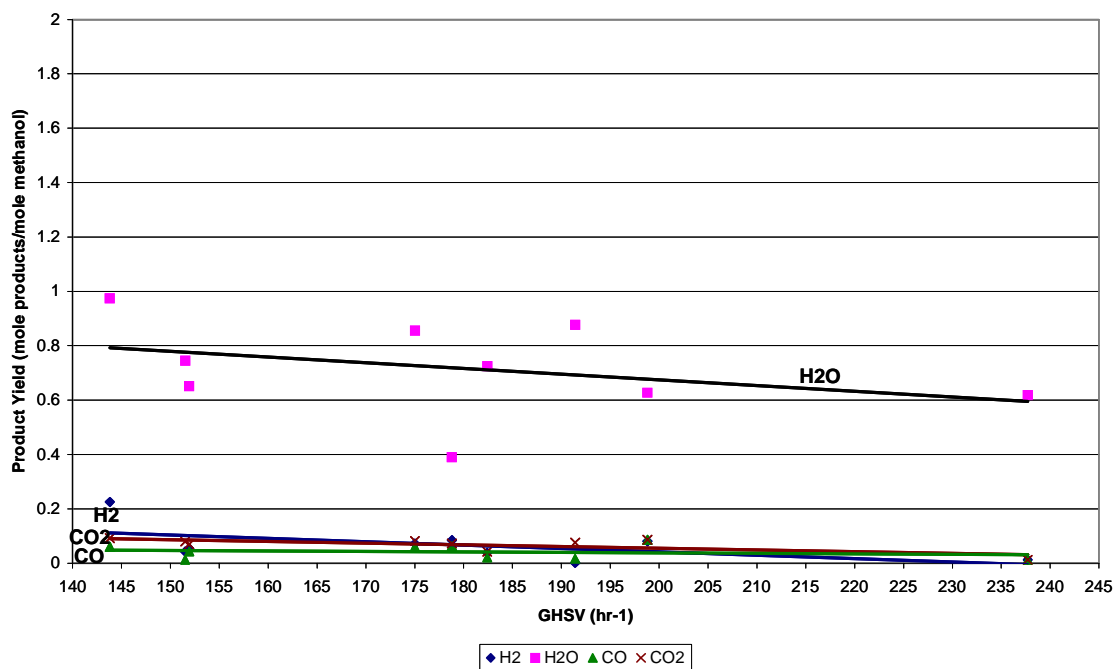


Figure D.1. Yield of reaction products as a function of GHSV for methanol at 300°F.

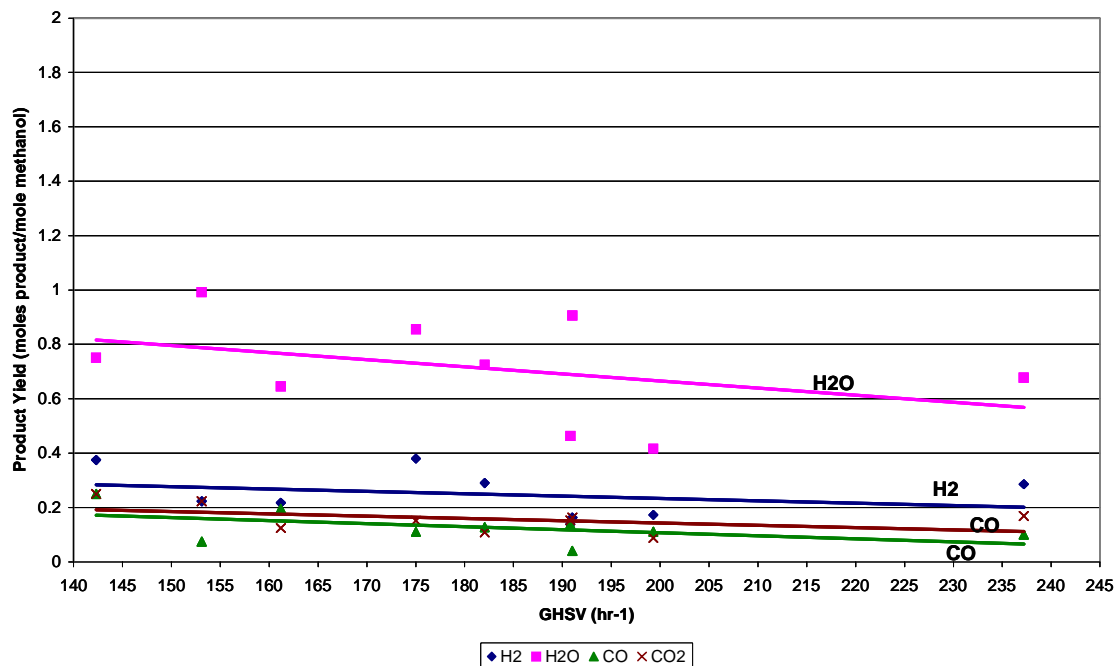


Figure D.2. Yield of reaction products as a function of GHSV for methanol at 400°F.

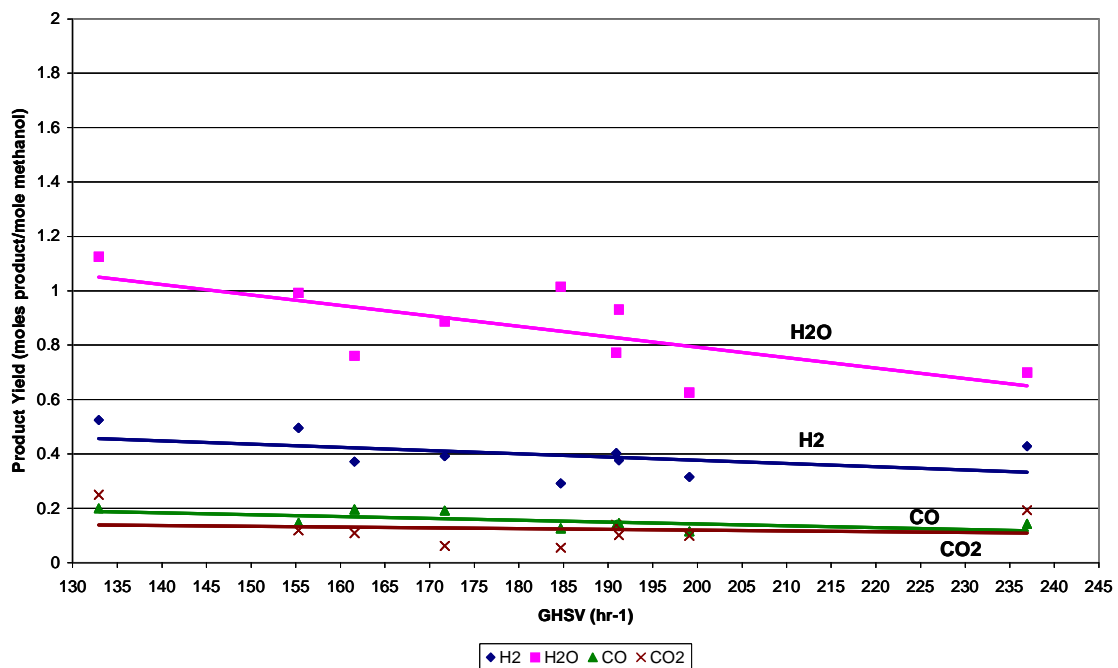


Figure D.3. Yield of reaction products as a function of GHSV for methanol at 500°F.

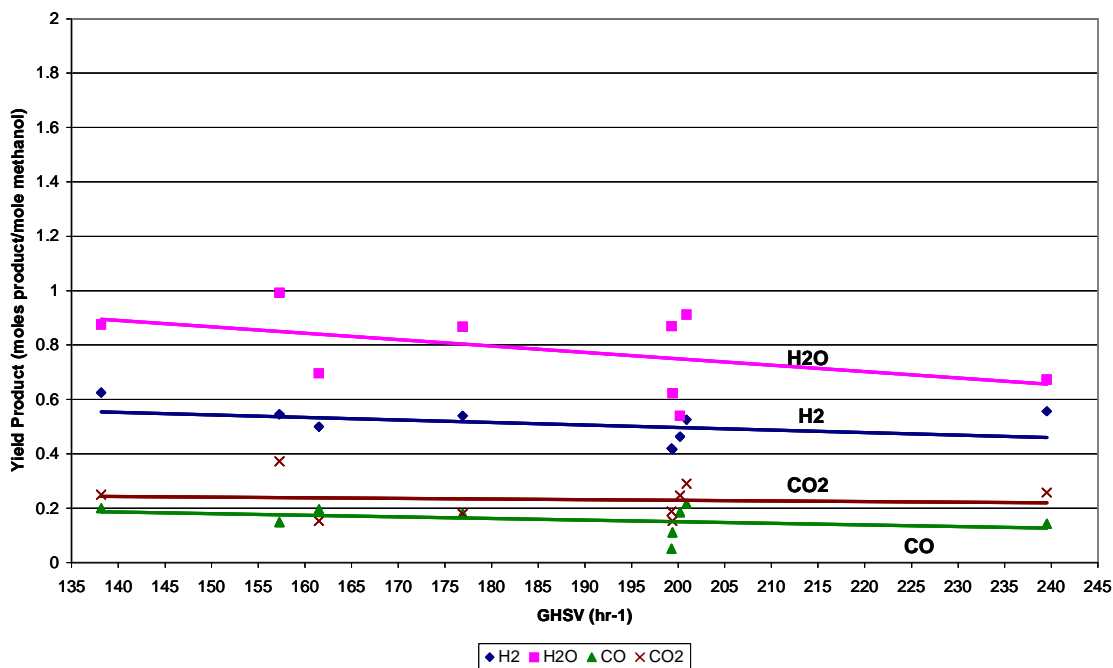


Figure D.4. Yield of reaction products as a function of GHSV for methanol at 600°F.

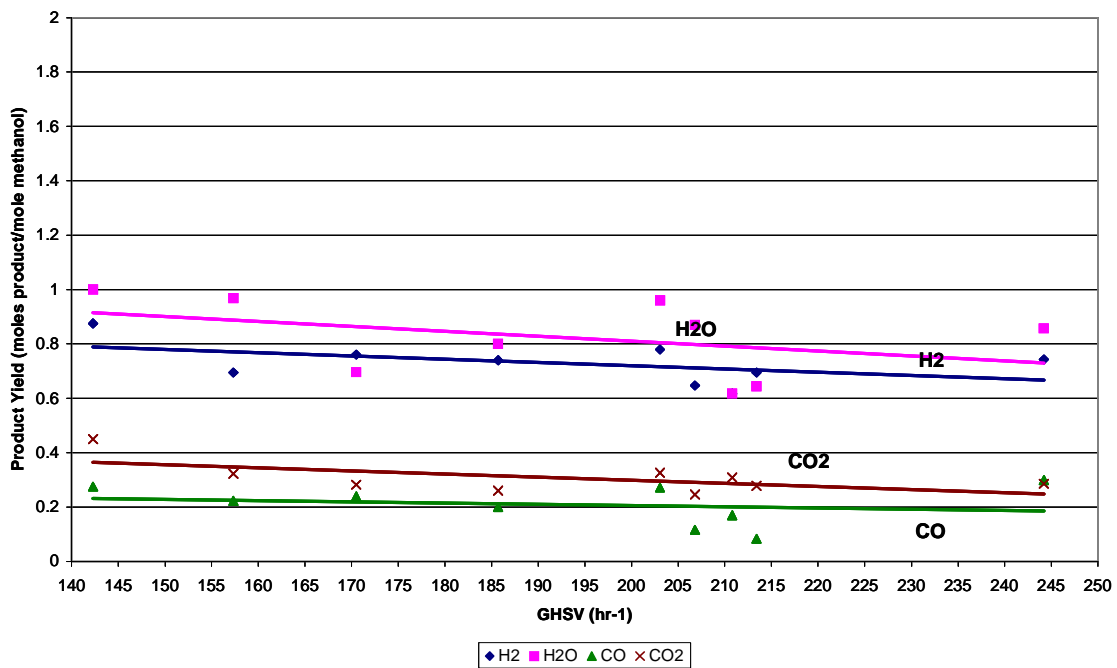


Figure D.5. Yield of reaction products as a function of GHSV for methanol at 700°F.

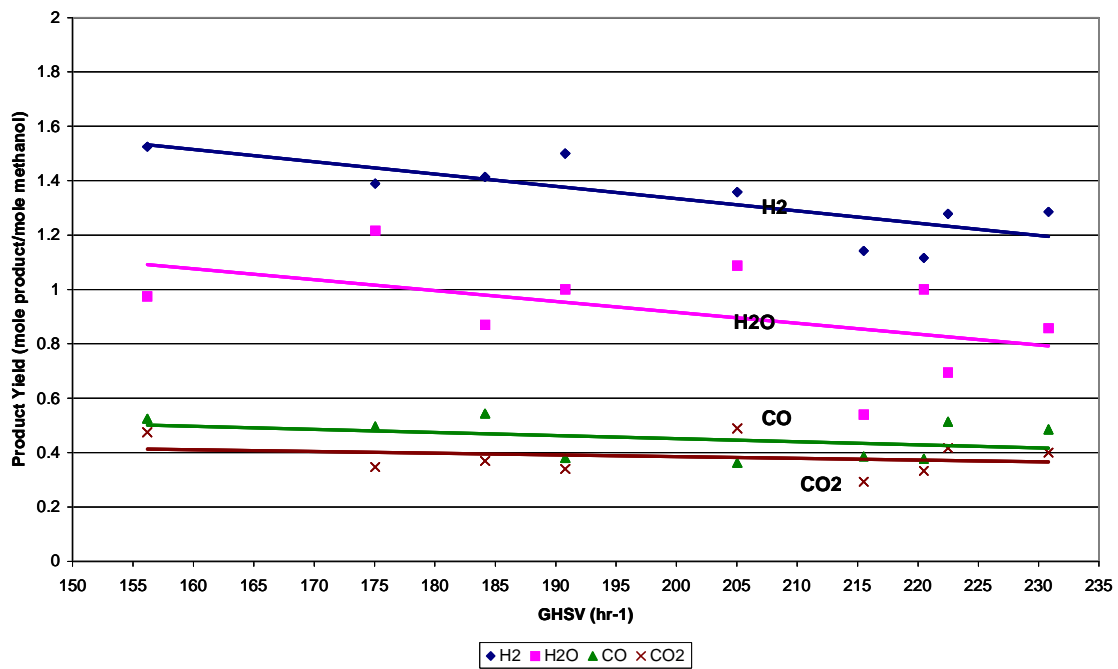


Figure D.6. Yield of reaction products as a function of GHSV for methanol at 900°F.

APPENDIX E: REFORMING PRODUCTS PERCENTS AT EQUILIBRIUM

These graphs (E.1-E.12) show the reforming products of both fuels (methanol and isooctane) at equilibrium. They were provided by Dr. Krause, ANL, using a thermodynamic simulation program at all the conditions performed in every experiments.

E.1. Methanol

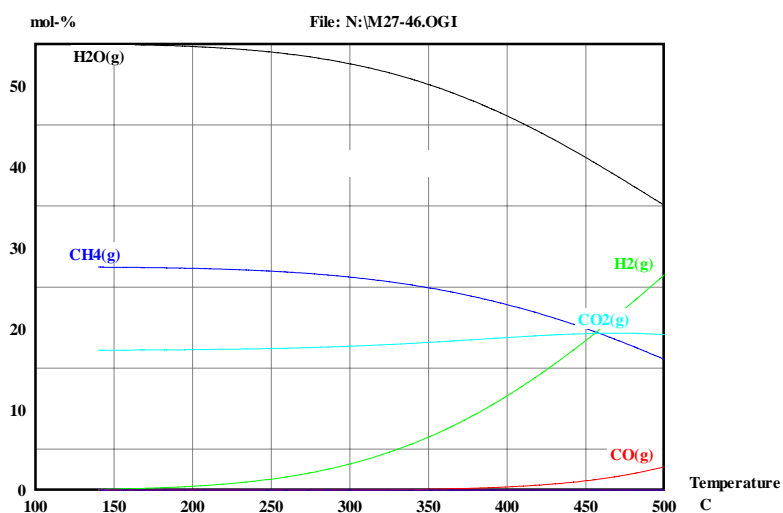


Figure E.1. Methanol exit product gas percents at equilibrium ($O_2/\text{fuel}=0.27$ and $H_2O/C=0.46$) at different temperatures.

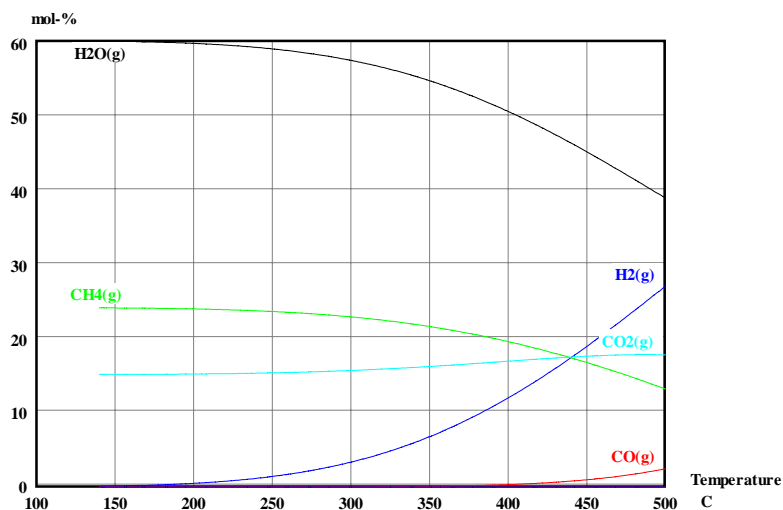


Figure E.2. Methanol exit product gas percents at equilibrium ($O_2/\text{fuel}=0.27$ and $H_2O/C=0.76$) at different temperatures.

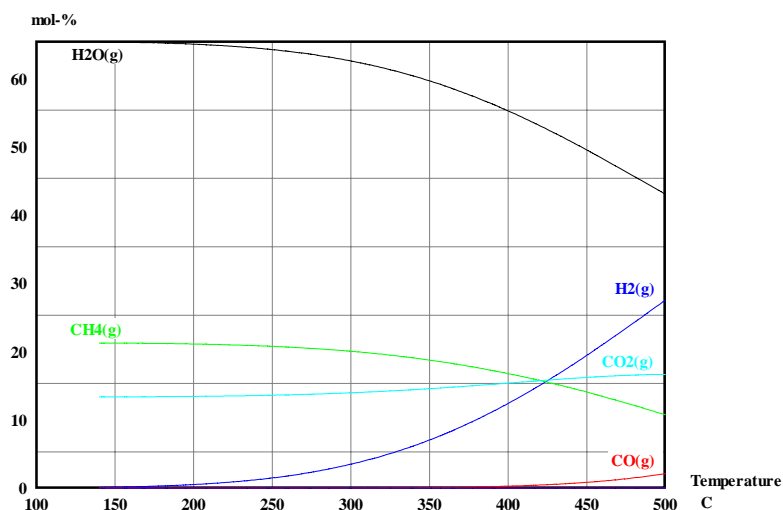


Figure E.3. Methanol exit product gas percents at equilibrium ($O_2/\text{fuel}=0.27$ and $H_2O/C=1.12$) at different temperatures.

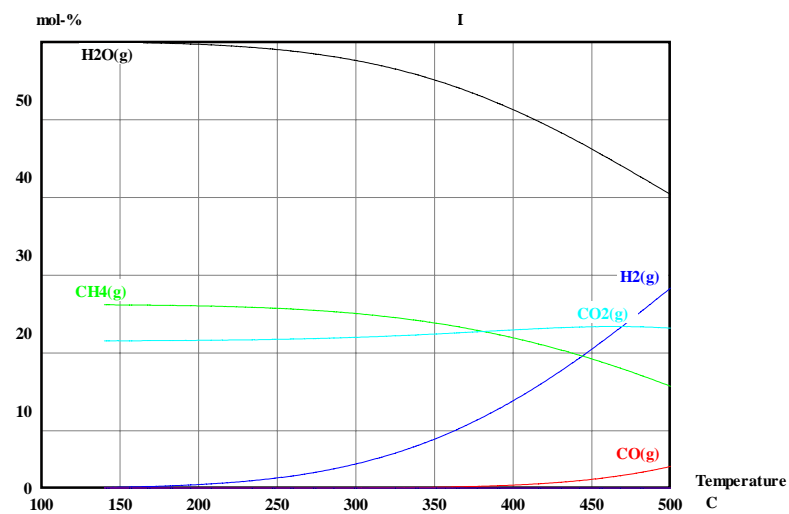


Figure E.4. Methanol exit product gas percents at equilibrium ($O_2/\text{fuel}=0.39$ and $H_2O/C=0.46$) at different temperatures.

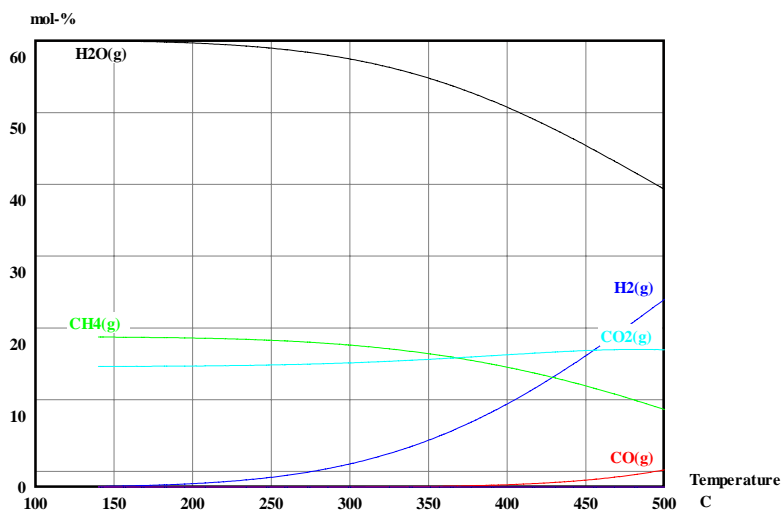


Figure E.5. Methanol exit product gas percents at equilibrium ($O_2/\text{fuel}=0.39$ and $H_2O/C=0.76$) at different temperatures.

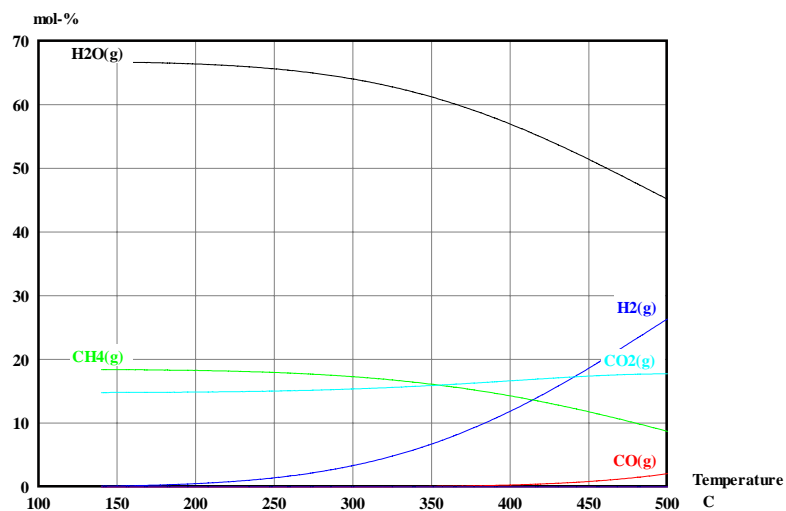


Figure E.6. Methanol exit product gas percents at equilibrium ($O_2/\text{fuel}=0.39$ and $H_2O/C=1.12$) at different temperatures.

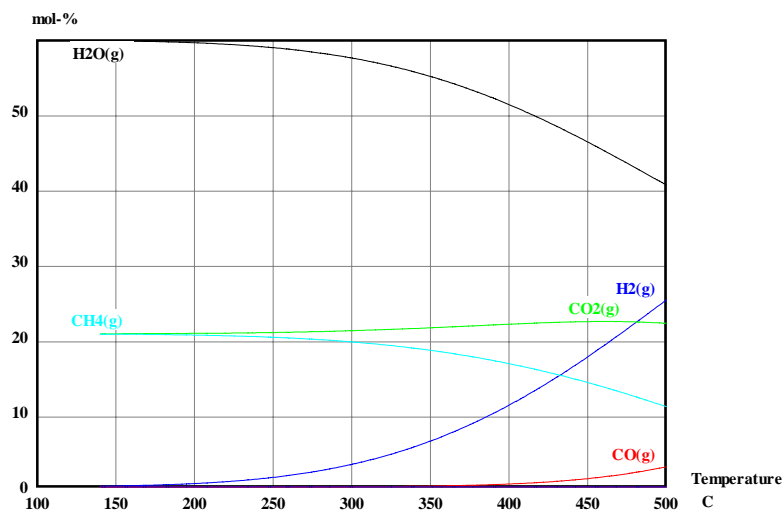


Figure E.7. Methanol exit product gas percents at equilibrium ($O_2/\text{fuel}=0.5$ and $H_2O/C=0.46$) at different temperatures.

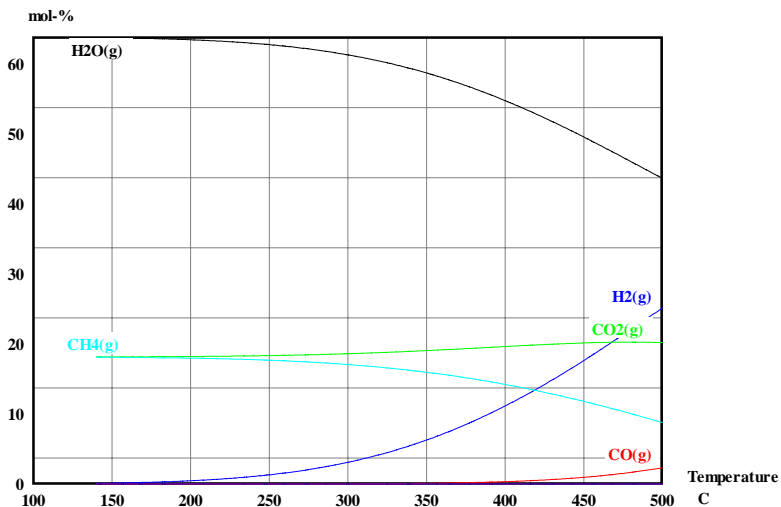


Figure E.8. Methanol exit product gas percents at equilibrium ($O_2/\text{fuel}=0.5$ and $H_2O/C=0.76$) at different temperatures.

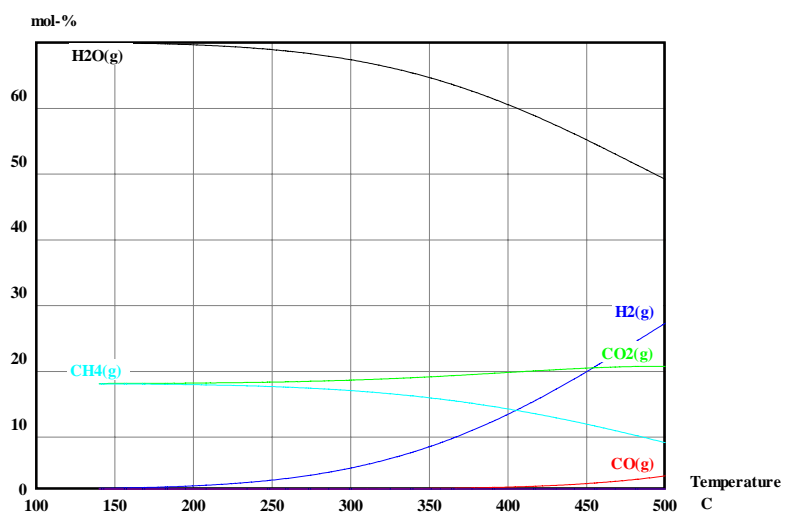


Figure E.9. Methanol exit product gas percents at equilibrium ($O_2/\text{fuel}=0.5$ and $H_2O/C=1.12$) at different temperatures.

E.2. Isooctane

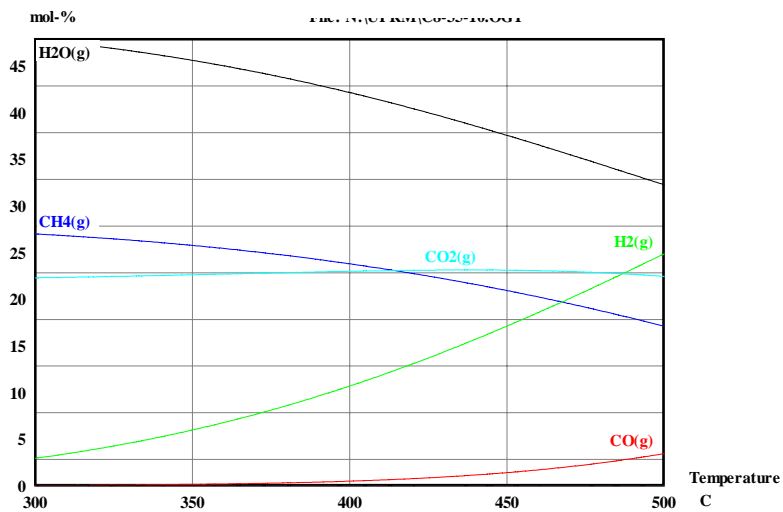


Figure E.10. Isooctane exit product gas percents at equilibrium ($O/C=1$ and $H_2O/C=1$) at different temperatures.

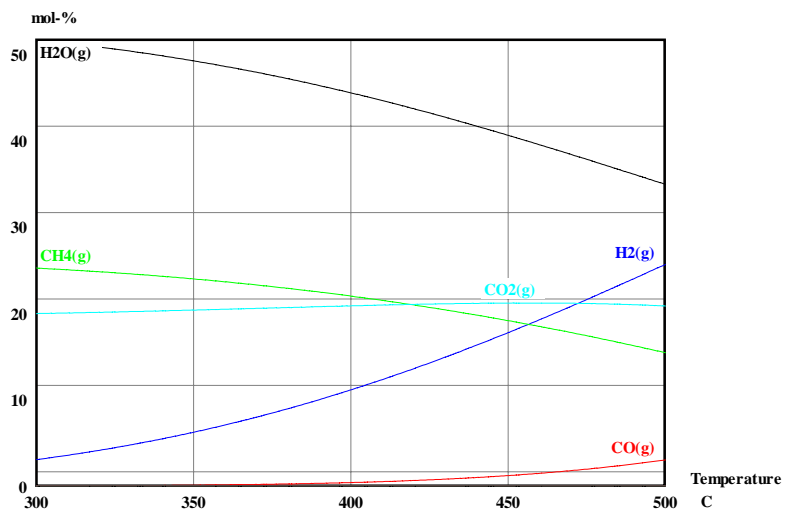


Figure E.11. Isooctane exit product gas percents at equilibrium ($O/C=1$ and $H_2O/C=1.2$) at different temperatures.

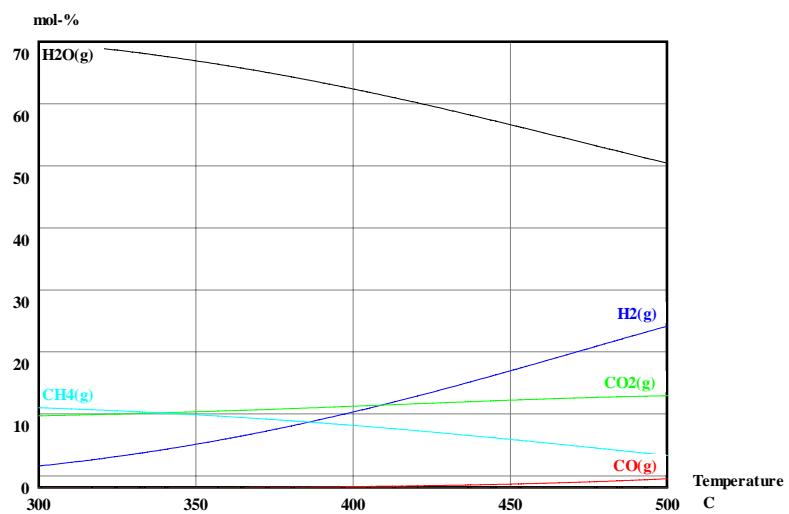


Figure E.12. Isooctane exit product gas percents at equilibrium ($O/C=1$ and $H_2O/C=3$) at different temperatures.